AD-A117 568 PURDUE UNIV LAFAYETTE IN SCHOOL OF ELECTRICAL ENGINEERING F/G 9/5
FAULT DIAGNOSIS OF NONLINEAR ANALOG CIRCUITS. VOLUME II. A MULT--ETC(U)
JUL 82 L RAPISARADA, R DECARLO N00014-81-K-0323
UNCLASSIFIED TR-EE-82-22 NL

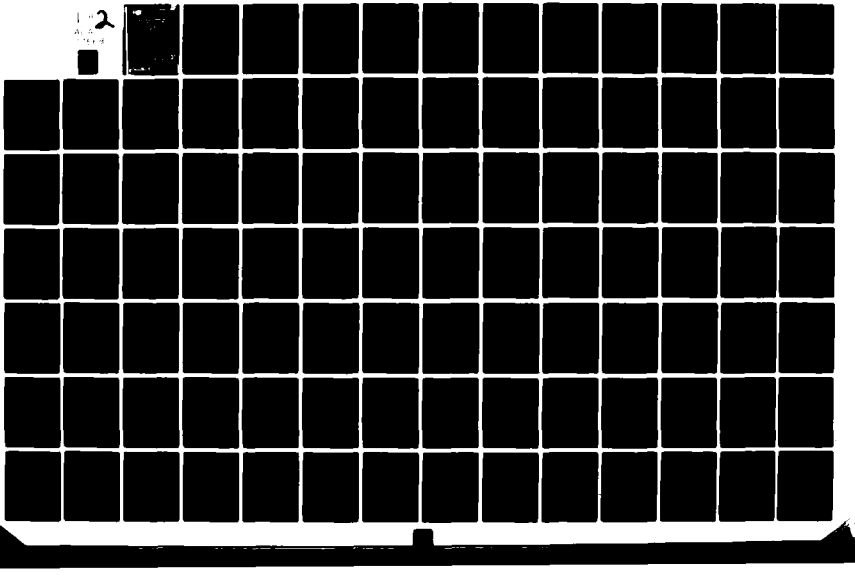


AD A
7568
1.0
1.1
1.25
1.4
1.6
1.8
2.0
2.2
2.5
2.8
3.2
3.6
4.0
MICROCOPY RESOLUTION TEST CHART
NATIONAL BUREAU OF STANDARDS-1963-A

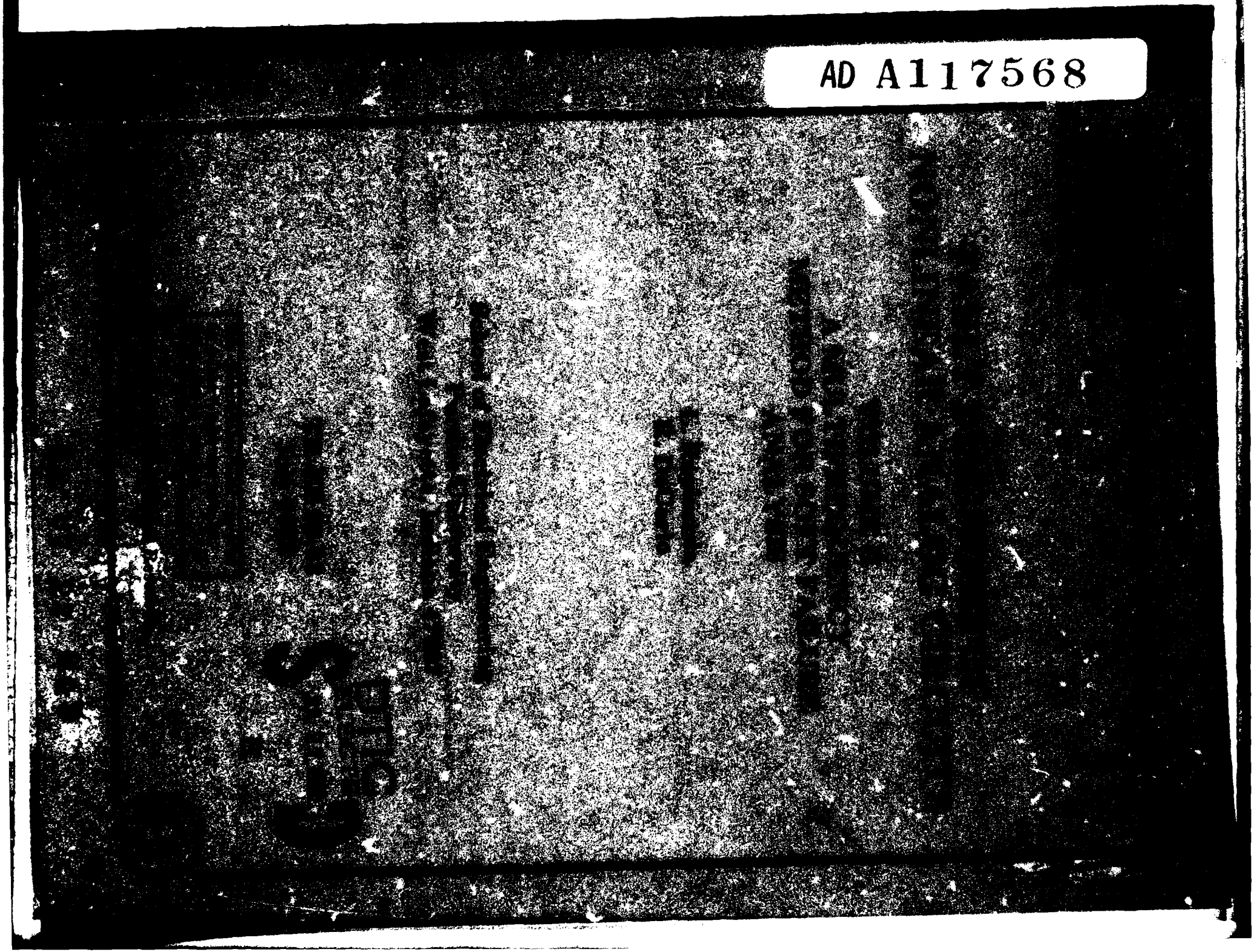

SECURITY CLASSIFICATION OF THIS PAGE (When Data Entered)

REPORT DOCUMENTATION PAGE		READ INSTRUCTIONS BEFORE COMPLETING FORM
1. REPORT NUMBER TR-EE-82-22	2. GOVT ACCESSION NO. AD-A117568	3. RECIPIENT'S CATALOG NUMBER
4. TITLE (and Subtitle) Fault Diagnosis of Nonlinear Analog Circuits: Volume II: A Multifrequency Method for Soft Failure Analysis		5. TYPE OF REPORT & PERIOD COVERED 6. PERFORMING ORG. REPORT NUMBER
7. AUTHOR(s) L. Rapisarada, R. DeCarlo		8. CONTRACT OR GRANT NUMBER(s) N00014-81-K-0323
9. PERFORMING ORGANIZATION NAME AND ADDRESS Purdue University School of Electrical Engineering West Lafayette, IN		10. PROGRAM ELEMENT, PROJECT, TASK AREA & WORK UNIT NUMBERS
11. CONTROLLING OFFICE NAME AND ADDRESS Office of Naval Research Arlington, VA		12. REPORT DATE July 1982 13. NUMBER OF PAGES
14. MONITORING AGENCY NAME & ADDRESS(if different from Controlling Office) Same		15. SECURITY CLASS. (of this report) Unclassified 15a. DECLASSIFICATION/DOWNGRADING SCHEDULE

16. DISTRIBUTION STATEMENT (of this Report)

Approved for Public Release, Distribution Unlimited

17. DISTRIBUTION STATEMENT (of the abstract entered in Block 20, if different from Report)

Same

18. SUPPLEMENTARY NOTES

None

19. KEY WORDS (Continue on reverse side if necessary and identify by block number)

Fault Diagnosis, Interconnected Circuits
Multifrequency, Tableau Equations

20. ABSTRACT (Continue on reverse side if necessary and identify by block number)

This report is a companion report (Volume II) of TR-EE-82-21. This volume describes multifrequency testing of interconnected analog circuits assuming soft failures. In particular the report details two approaches to soft failure multifrequency diagnosis: the composite system transfer function approach and the tableau approach. The two approaches are evaluated theoretically and numerically with the tableau approach shown to be far superior. In the context of the tableau approach a diagnosability set is

DD FORM 1 JAN 73 1473 EDITION OF 1 NOV 65 IS OBSOLETE
S/N 0102-LF-014-6601

SECURITY CLASSIFICATION OF THIS PAGE (When Data Entered)

developed and upper and lower bounds on the number of test frequencies necessary to conduct a diagnosis are given.

The report also includes investigations of various other aspects of the tableau fault diagnosis equations. In particular, a detailed investigation of the quadratic nature of the tableau equations is presented. By exploiting this quadratic structure superior numerical algorithms for the solution of the diagnosis equations arise. Examples of the above techniques, given throughout the report, serve to illustrate the utility of the tableau approach.

FAULT DIAGNOSIS OF NONLINEAR ANALOG CIRCUITS

VOLUME II

A MULTIFREQUENCY METHOD FOR SOFT FAILURE ANALYSIS

L. Rapisarda

R. DeCarlo

TR-EE-82-22

July 1982

School of Electrical Engineering

Purdue University

West Lafayette, Indiana 47907

This work was supported by Office of Naval Research,

Contract No. N00014-81-K-0323

ACKNOWLEDGMENT

The authors would like to thank the Office of Naval Research for the support of this work under ONR Contract No. N00014-81-K-0323. We would also like to thank the engineers of the Bendix Corporation Energy Controls Division, in particular Joe Peczkowski, Bob Raymond, and Dick Conrad, for their stimulating interaction with us while participating in the many activities of the Purdue Electrical Engineering Industrial Institute and for their cooperative support of the ONR contract.

TABLE OF CONTENTS

EXECUTIVE SUMMARY

The present development of fault diagnosis theory is in response to the proliferation of large circuits and systems whose complexity precludes the use of manual methods of trouble shooting. Although great success has been achieved in the automation of fault analysis for digital systems, the automated diagnosis of analog circuits and systems remains a difficult problem.

The fault diagnosis method discussed in this volume of the progress report is one part of a two phase automated test philosophy. The complete diagnosis process consists of D.C. testing (Volume I of the report) which considers the nonlinear aspects of the system (e.g. bias point determination and multifrequency testing applied to the system linearized about its operating point. The former is most suited to isolating hard faults (catastrophic changes in parameter values such as shorts and opens) while the latter is more suited to the determination of more subtle variations in component behavior. Although this volume discusses only the multifrequency testing, remember that both testing methods must be combined to make a viable approach to the analog fault analysis problem.

The various methods of fault analysis by "simulation after test" appearing in the recent literature have essentially two distinct orientations. The philosophy of the first approach, is to equate measurement data with a nonlinear function of ALL pertinent parameter values of the system. This is in contrast to the computationally simpler method of limiting the number of faults allowed, so that the resulting equations are linear. Our research focuses on the former approach for the following reasons. System component models are often generated by linearizing the

actual components behavior about an operating point. This linearization of an actual component often means replacing it with a network of idealized components, each characterized by a parameter value which depends on the operating point. A good example of this is a transistor whose linear model is generally a dependent source interconnected with several resistors and capacitors. If such an operating point is incorrect but is not identified conclusively by the D.C. analysis, it is possible for all the parameters in the model which are affected by that bias point to be faulty. In this case the a priori assumption that the number of faults is small is not appropriate. Also a focus on complete parameter identification is useful in the role of failure prediction. Periodic analysis which is capable of identifying all component values allows minor variations of each component's behavior to be tracked over time and its failure predicted.

With the above focus in mind this report introduces the CCM (component connection model) and describes two approaches to multifrequency diagnosis: the composite system transfer function approach and the tableau approach. The two approaches are evaluated theoretically and numerically with the tableau approach shown to be far superior. In the context of the tableau approach a diagnosability set is developed and upper and lower bounds on the number of test frequencies necessary to conduct a diagnosis are given.

The report also includes investigations of various other aspects of the tableau fault diagnosis equations. In particular, a detailed investigation of the quadratic nature of the tableau equations is presented. By exploiting this quadratic structure superior numerical algorithms for the solution of the diagnosis equations arise. Examples of the above techniques given throughout the report, serve to illustrate the utility of the tableau approach.

CHAPTER 1

THE COMPONENT CONNECTION MODEL

1. Introduction

Underlying the fault diagnosis investigations which follow in subsequent chapters is an interconnected system model called the component connection model, abbreviated CCM [1,2,3]. The purpose of this chapter is to introduce the notation and modelling philosophies of the CCM.

Two sets of equations characterize the CCM: (i) component characteristic equations and (ii) interconnection or topological equations. Basically all system models are equivalent. The differences lie in the way the system information is displayed. The philosophy behind the CCM is the separate descriptions of the component dynamics and system topology. Such descriptions result in large numbers of equations and unknowns. In matrix form the equations are very sparse and hence admit the use of sparse matrix storage and manipulation techniques [4]. For large systems, storage requirements are often lower than smaller non-sparse composite system representations. In some applications the use of the CCM has produced dramatic improvements in the use of computing resources. The most notable example is the MARSYAS program which used the CCM in a Space Shuttle engine model. The program performed the simulation 26 times faster than previous simulations used by NASA [5].

2. CCM Basics

Figure 1 shows a linear system consisting of N components. The components are shown explicitly as numbered blocks. The section labeled interconnections contains only the information describing how the components are connected to each other and to the outside world.

The system input is the vector u and the system output is the vector y. Each component of the system has an input and output vector a_i and b_i respectively (i=1,2,...,N). The component inputs and outputs will often be handled collectively so for convenience define:

$$a = \text{col}(a_1, a_2, \ldots, a_N) \tag{2.1a}$$

$$b = \text{col}(b_1, b_2, \ldots, b_N) \tag{2.1b}$$

The vectors a and b are called the composite component input and composite component output vectors. The composite component output, b, is related to the composite component input, a, via the component characteristics. The composite component input, a, is related to both b and u (the system input) through the interconnection or topological equations. Finally, the system output, y, depends on the composite component output, b, and the system input u.

3. The Component Equations

Since the components are linear they can be characterized by a transfer function in the frequency domain. Let the transfer function matrix for component i be $Z_i(s,r_i)$ where:

(i) s is the Laplace transform variable

(ii) r_i is a vector parameter which characterizes component i

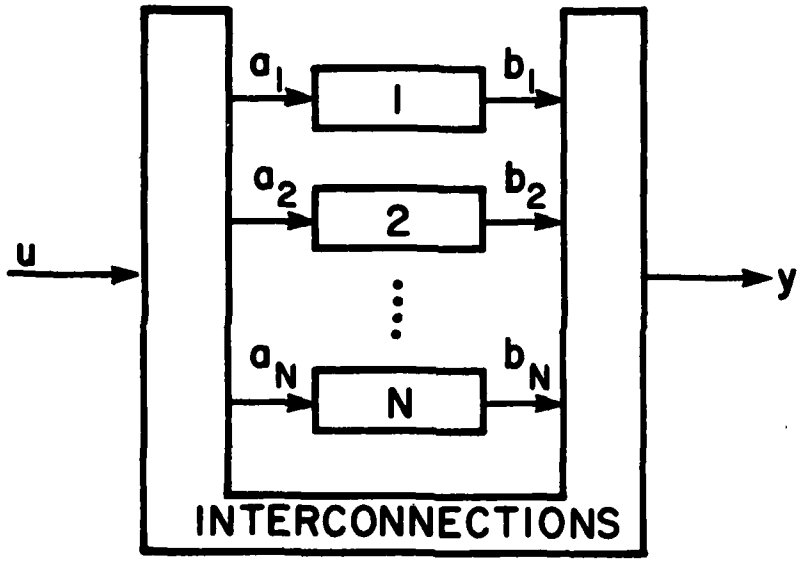

Figure 1. Linear system with N components.

The object of the fault diagnosis procedure developed in this paper will be to identify (diagnose) the value of r_i $(i=1,2,\ldots,N)$.

Let $a_i(s)$ and $b_i(s)$ be the Laplace transforms of the component input and output vectors. Then the component characteristic equation for component i is:

$$b_i(s) = Z_i(s,r_i)a_i(s) \tag{3.1}$$

Define:

$$r = \text{col}(r_1,r_2,\ldots,r_N) \tag{3.2}$$

$$Z(s,r) = \text{block-diag}\left[Z_1(s,r_1),Z_2(s,r_2),\ldots,Z_n(s,r_n)\right] \tag{3.3}$$

The characteristic relation for all the components can now be written compactly as

$$b(s) = Z(s,r)a(s) \tag{3.4}$$

where a(s) and b(s) are the Laplace transforms of the composite component input and composite component output vectors. The matrix Z(s,r) is called the composite component transfer function matrix. It is sparse due to its block diagonal structure.

Figure 2 illustrates the relationship of the composite component transfer function to the entire system.

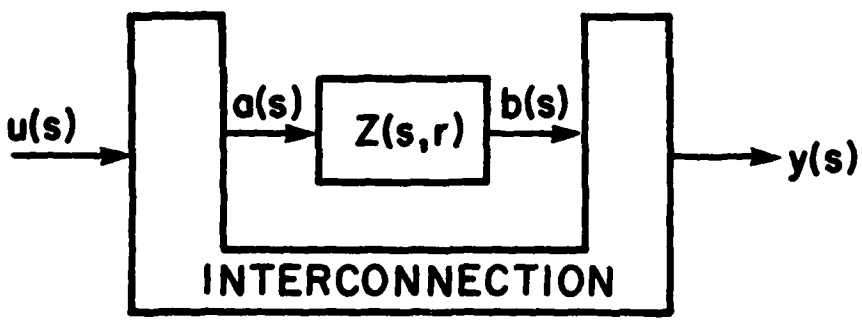

Figure 2. Illustration of the relationship of the composite transfer function to the entire system.

4. The Connection Equations

The connection equations model the constraints which result when the components are interconnected. These constraints are linear and algebraic representing conservation laws such as Kirchoff's current and voltage laws. Let u(s) be the Laplace transform of the system input vector and y(s) the Laplace transform for the system output vector. From Figure 2 note that the inputs to the interconnections are u(s) and b(s) and the outputs from the interconnections are a(s) and y(s). This leads naturally to the following form for the connection equations:

$$a(s) = L_{11}b(s) + L_{12}u(s) \tag{4.1a}$$

$$y(s) = L_{21}b(s) + L_{22}u(s) \tag{4.1b}$$

where the L_{ij} are matrices whose dimensions conform to the given vector quantities. The L_{ij} are called the connection matrices and they are generally very sparse. This occurs because most circuit elements and/or subsystem blocks have physical connections to only a few "neighbors". Figure 3 shows the system schematic further updated to portray the role of the connection matrices.

A small example described in the next section best summarizes the above development.

5. A CCM Example

Figure 4 is a circuit consisting of three components, two resisters and a capacitor. The components are shown separated from their positions in the circuit to emphasize the difference between the connection equations and the component equations. The circuit input is

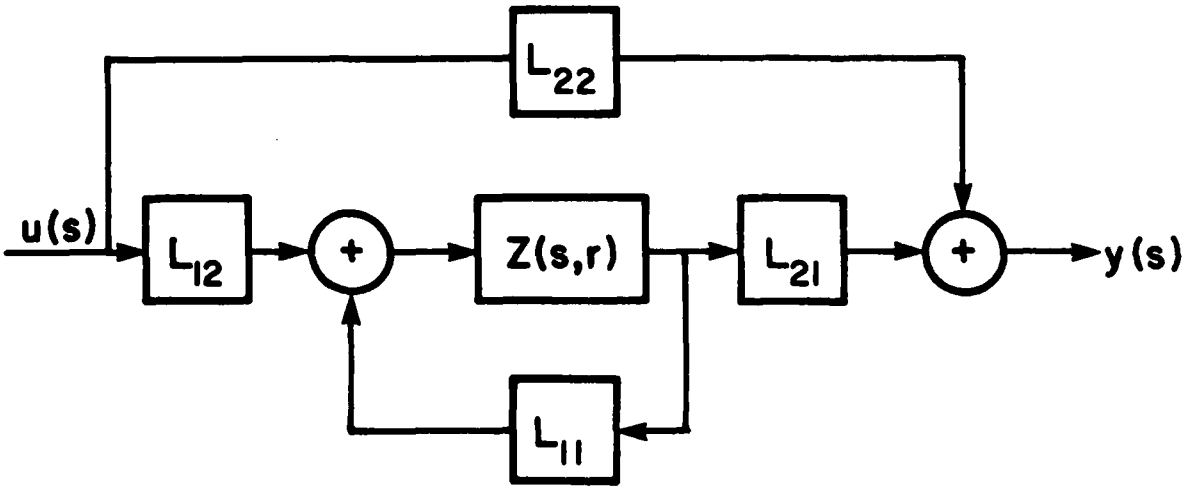

Figure 3. Block diagram representation of the CCM equations.

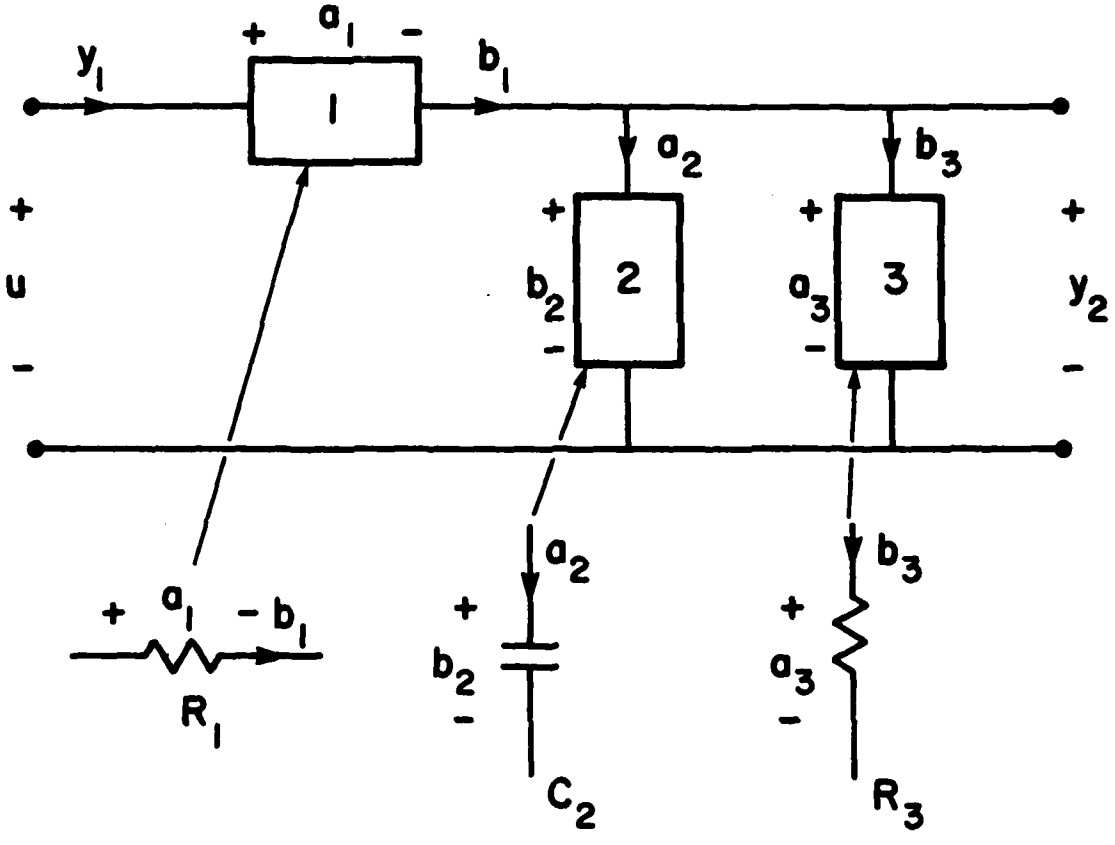

Figure 4. CCM example circuit.

u and the output is $y = [y_1, y_2]^t$. Using the usual resistor, capacitor equations as component models produces the following composite component transfer function matrix equation:

$$\begin{bmatrix} b_1(s) \\ b_2(s) \\ b_3(s) \end{bmatrix} = \begin{bmatrix} 1/R_1 & 0 & 0 \\ 0 & 1/sC_2 & 0 \\ 0 & 0 & 1/R_3 \end{bmatrix} \begin{bmatrix} a_1(s) \\ a_2(s) \\ a_3(s) \end{bmatrix} \tag{5.1}$$

Note that this equation is independent of the connections. It was derived by relating the component outputs and inputs through the components dynamics.

Next consider the connections. By using KVL and KCL on the circuit, the following equations result:

$$\begin{bmatrix} a_1(s) \\ a_2(s) \\ a_3(s) \end{bmatrix} = \begin{bmatrix} 0 & -1 & 0 \\ 1 & 0 & -1 \\ 0 & 1 & 0 \end{bmatrix} \begin{bmatrix} b_1(s) \\ b_2(s) \\ b_3(s) \end{bmatrix} + \begin{bmatrix} 1 \\ 0 \\ 0 \end{bmatrix} u(s) \tag{5.2a}$$

$$\begin{bmatrix} y_1(s) \\ y_2(s) \end{bmatrix} = \begin{bmatrix} 1 & 0 & 0 \\ 0 & 1 & 0 \end{bmatrix} \begin{bmatrix} b_1(s) \\ b_2(s) \\ b_3(s) \end{bmatrix} + \begin{bmatrix} 0 \\ 0 \end{bmatrix} u(s) \tag{5.2b}$$

Note that the interconnection equations did not require any knowledge of the actual components dynamics.

Most notable in the example is the large number of zero entries in the $Z(s,r)$ and L_{ij} matrices. In fact the number of non-zero entries in the system matrices usually increases as the order of the number of

components, (ie linearly) resulting in extremely sparse matrices for large systems.

6. *Simulation in the Frequency Domain*

As will be seen the objective of fault diagnosis is to identify the parameters of a system by observing the systems response (outputs) to a given stimuli (system input). Essentially this process is the inverse of the system simulation problem wherein system parameters and inputs are given with the goal of numerically computing system outputs. Since the CCM leads to a highly efficient method for system simulation, it appears reasonable to suppose that its use in the fault diagnosis problem may share some of the same advantages. Thus we present a brief description of the frequency domain simulation problem as an aid to understanding the fault diagnosis discussions to follow.

Often, frequency domain simulations proceed by first constructing a composite system transfer function matrix S(s) and then solving directly for the system output y(s) according to

$$y(s) = S(s)u(s) \tag{6.1}$$

It is possible to compute the composite system transfer function matrix explicitly in terms of the CCM matrices as follows:

$$S(s) = L_{22} + L_{21}(I-Z(s,r)L_{11})^{-1}Z(s,r)L_{12} \tag{6.2}$$

where the inverse is taken as an element in the field of rational matrices [1,9]. But this is not the most efficient way to compute y(s) using the CCM. Instead equations 3.4 and 4.1 are combined to form a sparse tableau given in equation 6.3

$$\begin{bmatrix} Z(s,r) & -I \\ -I & L_{11} \end{bmatrix} \begin{bmatrix} a(s) \\ b(s) \end{bmatrix} = \begin{bmatrix} 0 \\ -L_{12}u(s) \end{bmatrix} \tag{6.3a}$$

$$y(s) = L_{21}b(s) + L_{22}u(s) \tag{6.3b}$$

The solution of the sparse tableau equations of 6.3a are substituted into 6.3b to obtain the system output. The advantage of this method for system simulation comes from the fact that the tableau can be solved using sparse matrix technique. The tableau matrix

$$M(s,r) = \begin{bmatrix} Z(s,r) & -I \\ -I & L_{11} \end{bmatrix}$$

is very sparse since all its component matrices are highly sparse. Therefore only the information on the nonzero entries need be stored. The solution proceeds by using an LU-decomposition algorithm which factors M(s,r) as L(s,r)U(s,r) where L(s,r) is lower triangular and U(s,r) is upper triangular. In general the matrices L(s,r) and U(s,r) are both sparse and can be stored in the same space allocated to the storage of M(s,r).

Solution of 6.3 at a single frequency is most efficiently done by solving

$$L(s,r)X = \begin{bmatrix} 0 \\ -L_{12}u(s) \end{bmatrix}$$

by forward substitution and

$$U(s,r) \begin{bmatrix} a(s) \\ b(s) \end{bmatrix} = X$$

by back substitution. All operations are efficiently executed using sparse matrix techniques [4]. Computations over a range of frequencies, $s = j\omega$, $\omega_1 \leq \omega \leq \omega_2$, can also proceed efficiently via a continuation algorithm [9].

As an example equation 6.4 presents the tableau equations for the circuit of figure 4, where $G_1 = \frac{1}{R_1}$ and $G_3 = \frac{1}{R_3}$:

$$\begin{bmatrix} G_1 & 0 & 0 & -1 & 0 & 0 \\ 0 & \frac{1}{sC_2} & 0 & 0 & -1 & 0 \\ 0 & 0 & G_3 & 0 & 0 & -1 \\ -1 & 0 & 0 & 0 & -1 & 0 \\ 0 & -1 & 0 & 1 & 0 & -1 \\ 0 & 0 & -1 & 0 & 1 & 0 \end{bmatrix} \begin{bmatrix} a_1(s) \\ a_2(s) \\ a_3(s) \\ b_1(s) \\ b_2(s) \\ b_3(s) \end{bmatrix} = \begin{bmatrix} 0 \\ 0 \\ 0 \\ -u(s) \\ 0 \\ 0 \end{bmatrix} \qquad (6.4)$$

7. Summary

In the CCM context the equations describing the components and the equations describing their interconnections remain separate and distinct. It is therefore possible to distinguish the effect of the component dynamics from the effect of their topology. This will prove to be an extremely desirable feature of the CCM when applied to the fault diagrams problem.

The use of the CCM for system simulation has resulted in fast and numerically well conditioned computations when sparse matrix techniques

are employed [4,5]. It is not unreasonable to believe that similar advantages are waiting to be achieved by the use of the CCM in the fault diagnosis problem.

CHAPTER 2

MULTIFREQUENCY FAULT DIAGNOSIS (THE COMPOSITE TRANSFER FUNCTION APPROACH)

1. Introduction

This chapter has two objectives:

(i) Introduce the Multifrequency Fault Diagnosis problem; and

(ii) Highlight one of the two major methods for dealing with the diagnosis problem, namely the Composite Transfer Function Approach.

The following example illustrates the idea of multifrequency fault diagnosis and motivates a formal definition of the problem:

Suppose one desires to determine the values of R and L in the circuit in figure 5, but direct measurements of the components are prohibited.

Let the available data be the measurement of the voltage across the series RL impedance, y(s), and the known input current, u(s). The composite system transfer function of the circuit is:

$$y(s) = (R + sL)u(s) \tag{1.1}$$

Suppose (i) s_1 is a real test frequency; (ii) $u(s_1) = 1$; and (iii) the measured output is $y_1^M = y(s_1)$; where the superscript M means "measured". The evaluation of equation (1.1) at $s = s_1$ with the measured output y_1^M produces

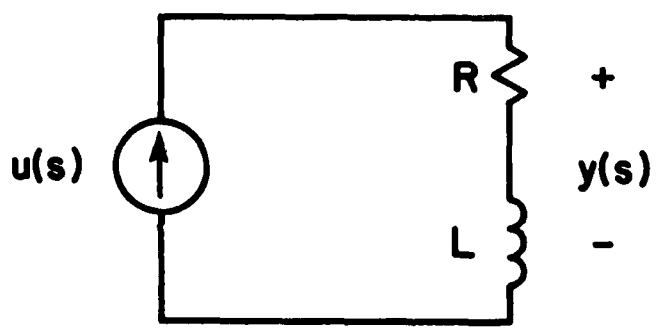

Figure 5. Circuit used for motivation of multifrequency measurements.

$$y_1^M = R + s_1 L \tag{1.2}$$

where R and L are the unknowns. Clearly the data at s_1 is insufficient to determine the values of R and L; however performing a second measurement at test frequency $s_2 \neq s_1$ yields the matrix equation

$$\begin{bmatrix} y_1^M \\ y_2^M \end{bmatrix} = \begin{bmatrix} 1 & s_1 \\ 1 & s_2 \end{bmatrix} \begin{bmatrix} R \\ L \end{bmatrix} \tag{1.3}$$

Equation (1.3) uniquely determines R and L provided s_1 and s_2 are distinct. This simple example illustrates the use of multifrequency testing to identify circuit parameters. With this example in mind the general fault diagnosis problem can be formulated as follows.

Given the following information:

(i) a linear network appropriately modeled containing N components, each component characterized by a parameter, r_i, $i=1,2,\ldots,N$;

(ii) a set of test inputs; and

(iii) a set of test outputs

determine the parameters, r_i, $i=1,2,\ldots,N$. As the simple example illustrated measurements at a single test frequency may be insufficient to determine all the parameters. Thus it is necessary to make a series of measurements at enough different test frequencies to provide sufficient data to uniquely specify all parameters.

There are two major approaches to multifrequency fault diagnosis for linear systems based on the use of the CCM:

(i) The Composite Transfer Function Approach developed by Sen and Saeks [6] and

(ii) The Tableau Approach developed by Decarlo and Gordan [7].

The purpose of this report is to continue the development of the multifrequency fault diagnosis theory in the context of the tableau approach. A comparison of the two approaches will best illustrate the motivation for this choice. For this reason the next four sections present a summary of the composite transfer function approach as well as an example of its use.

2. The Fault Diagnosis Equations (Composite Transfer Function Approach)

Suppose a linear system has the transfer function matrix representation $S(s,r)$ where r is the circuit/system parameter vector, i.e. $r = \text{col}(r_1, r_2, \ldots, r_n)$. The diagnosis of a linear circuit/system begins by measuring $S(s,r)$ at a set of q distinct real test frequencies, $s = s_i$, $i=1,2,\ldots,q$. The measured data has the form [6]:

$$\text{col}\left[S(s_1,r), S(s_2,r), \ldots, S(s_q,r)\right]$$

The measurement in this form is a matrix valued function of the parameter vector, r. It is much more convenient to convert it to a vector valued function through the use of the "vec" function [8] of a matrix defined as:

$$\text{vec}(A) = \begin{bmatrix} A_1 \\ A_2 \\ \vdots \\ A_p \end{bmatrix} \tag{2.1}$$

where (i) A is an mxp matrix

(ii) A_i is the ith column of A

(iii) vec(A) has dimensions mpx1

The composite transfer function matrix $S(s_i,r)$ [9] can be expressed explicitly in terms of the CCM matrix as:

$$S(s_i,r) = L_{22} + L_{21}(I-Z(s_i,r)L_{11})^{-1} Z(s_i,r)L_{12} \tag{2.2}$$

$i = 1,2,\ldots,q$. Let M be the vector of all the measured data defined precisely by:

$$M \triangleq \begin{bmatrix} \text{vec}[S(s_1,r)] \\ \text{vec}[S(s_2,r)] \\ \vdots \\ \text{vec}[S(s_q,r)] \end{bmatrix} \tag{2.3}$$

The measurement M can also be expressed in terms the CCM matrices directly using equation 2.2 and the following identity [8,10]:

$$\text{vec}[X\ Y\ Z] = [Z^t \otimes X]\ \text{vec}[Y] \tag{2.4}$$

where (i) X, Y and Z are any appropriately dimensional matrices;

(ii) the superscript t denotes matrix transpose; and

(iii) $\otimes$ is the "Kronecker product," i.e. given a pxk matrix A and a mxq matrix B their Kronecker product is the pmxkq matrix [11]:

$$A \otimes B \triangleq \begin{bmatrix} a_{11}B & \cdots & a_{1k}B \\ a_{21}B & & \vdots \\ \vdots & & \vdots \\ a_{p1}B & \cdots & a_{pk}B \end{bmatrix} \tag{2.5}$$

Using equation 2.2 and 2.4 in equation 2.3 produces the fault diagnosis equations:

$$M \triangleq \begin{bmatrix} \text{vec}\,[S(s_1,r)] \\ \text{vec}\,[S(s_2,r)] \\ \vdots \\ \text{vec}\,[S(s_q,r)] \end{bmatrix} = \begin{bmatrix} \text{vec}\,[L_{22}] + [L_{12}^t \otimes L_{21}(I-Z(s_1,r)L_{11})^{-1}]\text{vec}\,[Z(s_1,r)] \\ \text{vec}\,[L_{22}] + [L_{21}^t \otimes L_{21}(I-Z(s_2,r)L_{11})^{-1}]\text{vec}\,[Z(s_2,r)] \\ \vdots \\ \text{vec}\,[L_{22}] + [L_{12}^t \otimes L_{21}(I-Z(s_k r)L_{11})^{-1}]\text{vec}\,[Z(s_q,r)] \end{bmatrix} \triangleq f(r) \tag{2.6}$$

where M is the measurement vector and f(r) is an explicit nonlinear vector valued function of r. The fault diagnosis problem amounts to solving:

$$F(r) \triangleq M - f(r) = \theta \tag{2.7}$$

where θ denotes the "zero" vector.

As mentioned earlier the use of multiple test frequencies is necessary since for most practical cases a measurement of $S(s,r)$ at one test frequency will not provide sufficient information to determine r. Notice also that the composite transfer function approach requires the computation of the composite transfer function matrix explicitly (as in equation 2.2). For large systems this is no easy matter. Finally note that the fault diagnosis equations are nonlinear. Furthermore, although it is not readily apparent from equation 2.6, the polynomial order of $f(r)$ increases in proportion to the size of the system. A small example at the end of this chapter will illustrate these points.

3. Measure of Solvability

Two key questions concerning the fault diagnosis equations $F(r) = 0$ are:

i) Does a solution exist?

ii) If a solution exists to what extent is it specified by M?

First consider the question of existence. Recall that M represents measurements made on an actual system under test. If the model used to derive the function $F(r)$ is assumed to be precise it should be possible to simulate the actual system mathematically by using $y = f(r)$. Since any behavior of the actual system can be simulated by $f(\cdot)$, there must be some value r^* for which $f(r^*) - M = F(r) = 0$, provided M has no measurement error. The parameter value r^* represents at least one possible solution to the equation $F(r) = 0$. This discussion of the existence of a solution to the fault diagnosis equation points out possible pitfalls which should be considered in the actual computation of a solution. In general there will be some error associated with the

measurement M. Furthermore the model used to derive the function $f(\cdot)$ used for system simulation may not be exact. It is therefore possible for the fault diagnosis equations to be inconsistent. For the subsequent discussion, however, the existence of a solution to $F(r) = \theta$ is assumed.

Now that $F(r) = \theta$ has a solution, to what extent is that solution specified by the measurement, M? Under ideal circumstances r is uniquely specified but because the fault diagnosis equations are nonlinear multiple solution may exist. In spite of this it is still possible for M to completely specify the desired solution if the region of consideration is restricted so that the desired root is an isolated solution. The solution, r^*, is an isolated solution if there is a neighborhood of r^* which contains no other solution of $M-F(r) = \theta$ [19]. By a neighborhood of r^* we mean a set of points $\{r| \ ||r^*-r||_2 < \varepsilon\}$ for some $\varepsilon > 0$, where $||\cdot||_2$ denotes the usual Euclidean norm.

When is the desired solution "isolated" and if it is not isolated how much information does the measurement, M, provide about the solution? Saeks and Sen [6] answer these questions by defining a parameter called the "measure of solvability". The reasoning behind the measure of solvability is based on the inverse function theorem which requires the following three definitions [19]:

Definition 1

The mapping $F:D \subset R^n \to R^m$ is Frechet differentiable at $x \in \text{int}(D)$ (interior of D) if there is a linear operator $A: R^n \to R^m$ such that

$$\lim_{h \to \theta} (1/||h||_2)||F(x+h) - F(x) - Ah||_2 = 0 \qquad (3.1)$$

Note: The usual representation of this derivative is the Jacobian matrix. The derivative of $F(\cdot)$ will therefore be denoted by the matrix $J_F(\cdot)$.

Definition 2

A mapping $F: D \subset R^n \to R^n$ is a homeomorphism of D onto F(D) if F is one-to-one on D and F and F^{-1} are continuous on D and F(D) respectively.

Definition 3

The mapping $F: D \subset R^n \to R^n$ is a local homeomorphism at $x \in \text{int}(D)$ if there exist open neighborhoods U and V of x and F(x) respectively, such that the restriction of F to V is a homeomorphism between U and V.

Clearly the solution, r^* to the equation $F(r) = \theta$ will be isolated if F(r) is a local homeomorphism at r^*. This is determined using the following [19]:

Inverse Function Theorem: Suppose that $F: D \subset R^n \to R^n$ has a Frechet derivative, $J_F(.)$, in a neighborhood of $x^o \in \text{int}(D)$ which is continuous at x_o and that $J_F(x_o)$ is non-singular. Then F is a local homeomorphism at x_o.

With the inverse function theorem in mind define the measure of solvability [6] of the fault diagnosis equation $F(r) = \theta$ by

$$\delta(r_o) \triangleq N - \text{rank}\,[J_F(r_o)] \qquad (3.2)$$

where (i) N is the number of unknown parameters,

(ii) $F: D \subset R^N \to R^N$,

(iii) $J_F(\cdot)$ is the NxN Jacobian Matrix of F, and

(iv) r_o is a solution point.

In other words $\delta(r_o)$ is the dimension of the nullspace of $J_F(r_o)$. The Inverse Function Theorem guarantees that when $\delta(r_o) = 0$ ($J_F(r_o)$ is non-singular) then r_o is an isolated solution. If $\delta(r_o) \neq 0$ then the fault diagnosis equations must be augmented with $\delta(r_o)$ additional independent constraints to guarantee that r_o is an isolated solution of the augmented equations.

Given the form of the fault diagnosis equations in equation 2.6 the Jacobian $J_F(r)$ is the following [6]:

$$J_F(r) = \begin{bmatrix} \{([I+L_{11}(I-Z(s_1,r)L_{11})^{-1}Z(s_1,r)]L_{12})^t \otimes (L_{21}(I-Z(s_1,r)L_{11})^{-1})\}[(\text{dvec } Z(s_1,r)]/dr \\ \{([I+L_{11}(I-Z(s_2,r)L_{11})^{-1}Z(s_2,r)]L_{12})^t \otimes (L_{21}(I-Z(s_2,r)L_{11})^{-1})\}[(\text{dvec } Z(s_2,r)]/dr \\ \vdots \\ \{([I+L_{11}(I-Z(s_q,r)L_{11})^{-1}Z(s_q,r)]L_{12})^t \otimes (L_{21}(I-Z(s_q,r)L_{11})^{-1})\}[(\text{devc } Z(s_q,r)]/dr \end{bmatrix}$$

(3.3)

It would appear from its definition that the measure of solvability is a local property, that is it varies as the parameter values of a given system vary. Saeks and Sen [6] show however that when $Z(s,r)$ is a rational function of r, $\delta(r)$ is "almost constant" and can be characterized by its generic value, δ. "Almost constant" means that $\delta(r) = \delta$ (a constant) everywhere in R^n except possibly for some values of r lying in an algebraic variety [6]. An algebraic variety in R^n is the intersection of the zero sets of a finite set of non constant

polynomials n variables [9]. For example in R^2 the solution of $y-x^2=0$ is an algebraic variety. Imagine a function $f(x,y)$ that is constant every where except along the locus of points described by $y-x^2=0$. Such a locus occupies "zero area" in the x-y-plane and it is therefore appropriate to consider $f(x,y)$ to be "almost" constant. Consider Figure 6 which displays the locus of the curve $y-x^2=0$ in the x-y-plane. If the intuitive idea of "area" (width x length) is used the curved line of figure 6 has zero thickness and consequently occupies zero area in the plane.

4. Solution of the Fault Diagnosis Equations

Although many methods exist for the solution of nonlinear equations the fact that an explicit form of the Jacobian of $F(r)$ is known suggests that the Taylor series expansion for $F(r)$ might be useful for finding an approximation to the solution point of $F(r) = \theta$. Let $F: D \subset R^N \rightarrow R^N$ and suppose $r = r^*$ is a solution point of $F(r) = \theta$ and r_o is some known value close to r^*. Express $F(r^*)$ as a Taylor series about the point r_o.

$$F(r^*) = F(r_o) + J_F(r_o)(r^* - r_o) + \text{higher order terms} \qquad (4.1)$$

Since r^* is a solution point, $F(r^*) = \theta$. Ignoring the higher order terms because of the closeness of r_o to r^* produces the following approximation:

$$\theta \approx F(r_o) + J_F(r_o)(r^* - r_o) \qquad (4.2)$$

This equation provides a means to estimate the value of r^*. That estimate is a natural choice for a new expansion point which suggests the following iteration procedure:

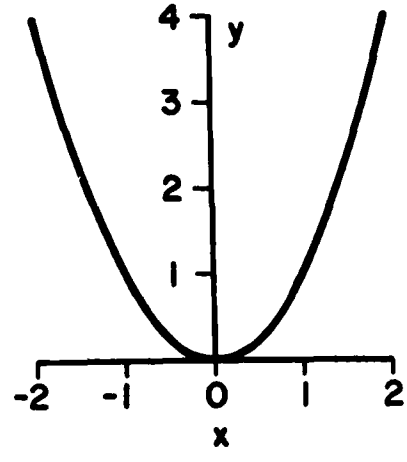

Figure 6. Locus of the curve $y - x^2 = 0$.

$$J_F(r^{(k)})\ (r^{(k+1)} - r^{(k)}) \approx - F(r^{(k)}) \qquad (4.3)$$

where $r^{(k)}$ is the "kth" estimate determined in the previous iteration and $r^{(k+1)}$ is the current estimate to be calculated. This method is called the Newton-Raphson iteration scheme and it converges reasonably fast when $r^{(0)} = r_o$ (the initial guess) is close to r^* [12]. If r_o is not sufficiently close to the solution point it is possible for the sequence of estimates to diverge. Navid and Willson propose an algorithm based on the following theorem which alleviates this divergence problem [13]:

Global Convergence Theorem:

Let $F: D \subset R^n \to R^n$ be continuously differentiable and have a nonsingular derivative $F'(x) = J_F(x)$ on the open set D, and assume there exists $x^* \in D$ for which $F(x^*) = 0$. Then, given any $x^o \in D$, there exist a sequence $\{\lambda_k\}$ such that the iterates

$$x^{k+1} = x^k - \lambda_k\ J_F(x^k)^{-1}\ F(x^k), \quad k = 0,1,... \qquad (4.4)$$

converges to the point x^*. Moreover, there exist m, depending on x^o, such that for $k \geq m$ we may take $\lambda_k = 1$; and hence achieve a faster rate of convergence to x^*.

The λ_k in this theorem diminishes the change between estimates and stablizes the sequence of estimates. When the estimates are sufficiently close to the solution then λ_k becomes unity and equation 4.4 becomes the Newton-Raphson iteration step.

5. Example

To illustrate the use of the Fault Diagnosis equations, apply them to the following circuit: The input is $u = V_{in}$ and the output is $y = [I, V_o]^t$. The circuit CCM equations are

$$\begin{bmatrix} b_1(s) \\ b_2(s) \\ b_3(s) \\ b_4(s) \end{bmatrix} = \begin{bmatrix} G_1 & & & \\ & \frac{1}{sC_2} & 0 & \\ & 0 & G_3 & \\ & & & G_4 \end{bmatrix} \begin{bmatrix} a_1(s) \\ a_2(s) \\ a_3(s) \\ a_4(s) \end{bmatrix} \tag{5.1}$$

$$\begin{bmatrix} a_1(s) \\ a_2(s) \\ a_3(s) \\ a_4(s) \end{bmatrix} = \begin{bmatrix} 0 & -1 & 0 & 0 \\ 1 & 0 & -1 & 0 \\ 0 & 1 & 0 & 0 \\ 0 & 0 & 0 & 0 \end{bmatrix} \begin{bmatrix} b_1(s) \\ b_2(s) \\ b_3(s) \\ b_4(s) \end{bmatrix} + \begin{bmatrix} 1 \\ 0 \\ 0 \\ 1 \end{bmatrix} V_{in} \tag{5.2}$$

$$\begin{bmatrix} I \\ V_o \end{bmatrix} = \begin{bmatrix} 1 & 0 & 0 & 1 \\ 0 & 1 & 0 & 0 \end{bmatrix} \begin{bmatrix} b_1(s) \\ b_2(s) \\ b_3(s) \\ b_4(s) \end{bmatrix} + \begin{bmatrix} 0 \\ 0 \end{bmatrix} V_{in} \tag{5.3}$$

The transfer function is

$$S(s,r) = L_{22} + L_{21}(I - Z(s,r)L_{11})^{-1}Z(s,r)L_{12} \tag{5.4}$$

$$= \begin{bmatrix} 0 \\ 0 \end{bmatrix} + \begin{bmatrix} 1 & 0 & 0 & 1 \\ 0 & 1 & 0 & 0 \end{bmatrix} \begin{bmatrix} 1 & G_1 & 0 & 0 \\ -\frac{1}{sC_2} & 1 & \frac{1}{sC_2} & 0 \\ 0 & -G_3 & 1 & 0 \\ 0 & 0 & 0 & 1 \end{bmatrix}^{-1} \begin{bmatrix} G_1 & \frac{1}{sC_2} & 0 & \\ & 0 & G_3 & \\ & & & G_4 \end{bmatrix} \begin{bmatrix} 1 \\ 0 \\ 0 \\ 1 \end{bmatrix}$$

$$S(s,r) = \frac{1}{sC_2+G_3+G_1} \begin{bmatrix} sC_2(G_1+G_4) + G_3G_1 + G_3G_4 + G_1G_4 \\ \\ G_1 \end{bmatrix}$$

where $r = (G_1, C_2, G_3, G_4)^t$. Notice that the calculation of $S(s,r)$ using the CCM matrix required the inversion of $(I-Z(s,r)L_{11})$.

For each test frequency, $s = s_i$, equating the transfer function equation to its measurement yields two independent equations in four unknowns. Hence two real test frequencies are both necessary and sufficient to uniquely specify the four unknown parameters. A discussion of the problem of test frequency selection will appear in a later chapter in the context of the tableau approach to fault diagnosis.

To solve for the unknown parameters choose two real test frequencies $s_1 = 1$ and $s_2 = 2$. Suppose that the measured transfer function values are:

$$S(1,r) = \begin{bmatrix} \frac{5}{3} \\ \\ \frac{1}{3} \end{bmatrix} \qquad S(2,r) = \begin{bmatrix} \frac{7}{4} \\ \\ \frac{1}{4} \end{bmatrix} \tag{5.5}$$

This produces the following nonlinear vector fault diagnosis equation:

$$M - F(r) \triangleq \begin{bmatrix} \frac{5}{3} \\ \frac{1}{3} \\ \frac{7}{4} \\ \frac{1}{4} \end{bmatrix} - \begin{bmatrix} \frac{C_2(G_1+G_4) + G_1G_3 + G_3G_4 + G_1G_4}{C_2 + G_1 + G_3} \\ \frac{G_1}{C_2 + G_1 + G_3} \\ \frac{2C_2(G_1+G_4) + G_1G_3 + G_3G_4 + G_1G_4}{2C_2 + G_1 + G_3} \\ \frac{G_1}{2C_2 + G_1 + G_3} \end{bmatrix} = 0 \qquad (5.6)$$

In this example the equations are quadratic but the order of the equations increases in proportion to the size of the system.

To solve the above equation set up the Newton-Raphson iteration scheme using the explicit form of the Jacobian.

$$\begin{bmatrix} \frac{(C_2^{(n)}+G_3^{(n)})^2}{(C_2^{(n)}+G_1^{(n)}+G_3^{(n)})^2} & \frac{G_1^{(n)2}}{(C_2^{(n)}+G_1^{(n)}+G_3^{(n)})^2} & \frac{G_1^{(n)2}}{(C_2^{(n)}+G_1^{(n)}+G_3^{(n)})^2} & 1 \\ \frac{C_2^{(n)}+G_3^{(n)}}{(C_2^{(n)}+G_1^{(n)}+G_3^{(n)})^2} & \frac{-G_1^{(n)}}{(C_2^{(n)}+G_1^{(n)}+G_3^{(n)})^2} & \frac{-G_1^{(n)}}{(C_2^{(n)}+G_1^{(n)}+G_3^{(n)})^2} & 0 \\ \frac{(2C_2^{(n)}+G_3^{(n)})^2}{(2C_2^{(n)}+G_1^{(n)}+G_3^{(n)})^2} & \frac{2G_1^{(n)2}}{(2C_2^{(n)}+G_1^{(n)}+G_3^{(n)})^2} & \frac{G_1^{(n)2}}{(2C_2^{(n)}+G_1^{(n)}+G_3^{(n)})^2} & 1 \\ \frac{2C_2^{(n)}+G_3^{(n)}}{(2C_2^{(n)}+G_1^{(n)}+G_3^{(n)})^2} & \frac{-2G_1^{(n)}}{(2C_2^{(n)}+G_1^{(n)}+G_3^{(n)})^2} & \frac{-G_1^{(n)}}{(2C_2^{(n)}+G_1^{(n)}+G_3^{(n)})^2} & 0 \end{bmatrix} \times$$

$$\begin{bmatrix} G_1^{(n+1)} - G_1^{(n)} \\ C_2^{(n+1)} - C_2^{(n)} \\ C_3^{(n+1)} - G_3^{(n)} \\ G_4^{(n+1)} - G_3^{(n)} \end{bmatrix} = \lambda_n [M - F(r^{(n)})] \tag{5.7a}$$

where

$$M - F(r^{(n)}) = \begin{bmatrix} 1.60 \\ .40 \\ 1.75 \\ .25 \end{bmatrix} - \begin{bmatrix} \dfrac{C_2^{(n)}(G_1^{(n)} + G_4^{(n)}) + G_1^{(n)} G_3^{(n)} + G_3^{(n)} G_4^{(n)} + G_1^{(n)} G_4^{(n)}}{C_2^{(n)} + G_1^{(n)} + G_3^{(n)}} \\ \dfrac{G_1^{(n)}}{C_2^{(n)} + G_1^{(n)} + G_3^{(n)}} \\ \dfrac{2C_2^{(n)}(G_1^{(n)} + G_4^{(n)}) + G_1^{(n)} G_3^{(n)} + G_3^{(n} G_4^{(n)} + G_1^{(n} G_4^{(n)}}{2C_2^{(n)} + G_1^{(n)} G_3^{(n)}} \\ \dfrac{G_2^{(n)}}{2C_2^{(n)} + G_1^{(n)} + G_3^{(n)}} \end{bmatrix} \tag{5.7b}$$

To start the iteration process choose an initial guess for r. Normally the nominal (or design) values for the components will suffice. The first choice for λ_n should be unity unless it causes the estimates to diverge. A straightforward check for this is to test the inequality $||M-F(r^{(n+1)})||_2 < ||M-F(r^{(n)})||_2$. Where $||\cdot||_2$ indicates the usual Euclidean norm. If it is true continue the iteration process but if false repeat the step with a new λ_n, calculating a new $r^{(n+1)}$. Navid and Willson [13] decrease λ_n by the factor $\frac{1}{2}$ until the $r^{(n+1)}$ estimate

satisfies the inequality test.

6. Disadvantages of the Transfer Function Matrix Approach

The example illustrates some shortcomings of the Composite Transfer Function Approach which become significant when it is applied to large systems. First the method requires the computation of the composite transfer function matrix. This involves the inversion of $(I-Z(s_i,r)L_{11})$ for $i=1,2,\ldots,q$. Next, if an explicit expression for $J_F(r)$ is used in a Newton Raphson iteration scheme then $(I-Z(s,r)L_{11})$ must be inverted symbolically. This is extremely cumbersome for even moderately sized networks. Finally since the CCM matrix (the L_{ij} and $Z(s,r)$) appear imbedded within the transfer function expression it is difficult to analyze the effect that each has on the fault diagnosis equations. For example test point selection is equivalent to choosing L_{21}. It is desirable to choose L_{21} to minimize δ for a given system but this is not an easy matter in the Composite Transfer Function context. The next chapter will introduce the Tableau Approach to the fault diagnosis problem. Although the Tableau Form of the Fault Diagnosis equations are equivalent to those of the Composite Transfer Approach they are formulated in a context which completely avoids the short comings listed above.

CHAPTER 3

TABLEAU APPROACH TO MULTIFREQUENCY FAULT DIAGNOSIS

1. Introduction

The Tableau Approach to multifrequency fault diagnosis is essentially the fault diagnosis problem developed in Chapter 2 recast in the context of the component connection model tableau introduced in Chapter 1. The rationale for this new approach is two fold. First, if the use of the CCM frequency domain tableau permits the development of highly efficient algorithms for simulating a systems behavior [9] it should offer comparable advantages in the fault diagnosis problem which *can be thought of as* simulation in reverse. In particular the tableau approach to fault diagnosis should prove to be superior to the composite transfer function approach discussed in Chapter 2.

Even more important than any computational advantages which the tableau approach might offer is the additional insight into the nature of the problem to be gained by this different perspective. The transfer function matrix approach for example has offered little insight into problems such as the selection of test points or choice of optimum test frequencies. Intuitively these issues center upon the individual characteristics of each component in relation to how the components are interconnected. In the CCM Tableau the component characteristic equations and the connection equations remain separate. It is therefore more reasonable to investigate the role each plays in the problem in

this context rather than through a transfer function matrix where both sets of equations are intermingled and hence indistinguishable. The purpose of this chapter is to detail the development of the tableau approach and to highlight its usefulness.

2. Development of the Fault Diagnosis Equations

The development of the fault diagnosis equations begin with the frequency domain tableau which was introduced in equation 6.3 of Chapter 1. For reader convenience the tableau is repeated here in equation 2.1:

$$\begin{bmatrix} Z(s,r) & -I \\ -I & L_{11} \end{bmatrix} \begin{bmatrix} a(s) \\ b(s) \end{bmatrix} = \begin{bmatrix} 0 \\ -L_{12}u(s) \end{bmatrix} \tag{2.1a}$$

$$y(s) = L_{21}b(s) + L_{22}u(s) \tag{2.1b}$$

Recall that y(s) is the composite system output, u(s) is the composite system input and b(s) and a(s) are the composite component outputs and inputs respectively. Also recall that the components are characterized by the parameter vector, r, via the composite component transfer function matrix, Z(s,r) and that the L_{ij} matrices describe the systems interconnections.

Suppose that a test input, u(s) is applied to a circuit/system characterized by equation 2.1 and that the output, $y^M(s)$ is observed. The superscript "M" emphasizes the fact that this is a test measurement. Apply the simulation procedure in reverse by putting $y^M(s)$ into the output equation (equation 2.1b) and gathering known quantities together to obtain:

$$L_{21}b(s) = y^{M}(s) - L_{22}u(s) \qquad (2.2)$$

The only unknown in equation 2.2 is the composite component output vector b(s). A closer look at the properties of L_{21} is necessary in order to determine the nature of the solution to equation 2.2.

In any practical situation the number of system outputs is less than the number of component outputs. (Measurements at essentially every point within a system makes the fault diagnosis problem trivial but it is unfortunately seldom practical.) To be consistent with this practical consideration, make the following assumption:

Assumption 1: For the $n_y x n_b$ matrix L_{21}, where n_y = number of outputs and n_b = dimension of b(s), $n_b > n_y$.

Furthermore it is reasonable to make a second assumption concerning L_{21}:

Assumption 2: The matrix L_{21} has full row rank.

The reasoning to support assumption 2 is that any dependent row of L_{21} corresponds to an output which can always be expressed as a linear combination of the inputs and the remaining outputs. As a diagnosis measurement such an output provides no additional information about the system under test and therefore can be discarded. Discarding all such outputs means eliminating all dependent rows of L_{21}. The resulting L_{21} matrix must have independent rows.

To solve equation 2.2 note that assumption 2 insures that L_{21} has a right inverse [14] and therefore a solution must exist. Unfortunately assumption 1 implies that L_{21} must have a non trivial null space and therefore there are infinitely many solutions to equation 2.2. The solution to equation 2.2 can be characterized in the following way [7]:

$$b(s) = L_{21}^{-R}\left[y^{M}(s) - L_{22}u(s)\right] + \sum_{k=1}^{p} \alpha_k(s)\, v_k \qquad (2.3)$$

where: i) L_{21}^{-R} is any right inverse of L_{21},

ii) p is the dimension of the null space of L_{21},

iii) The set $\{v_1, v_2, \ldots, v_p\}$ are basis vectors which span the null space of L_{21},

iv) The set $\{\alpha_1, \alpha_2, \ldots, \alpha_p\}$ are arbitrary (and possibly complex) functions of s.

With the aid of the following definitions:

$$V = [v_1 | v_2 | \ldots | v_p] \qquad (2.4)$$

$$\alpha(s) = \text{col}[\alpha_1(s), \alpha_2(s), \ldots, \alpha_p(s)] \qquad (2.5)$$

$$b_o(s) = L_{21}^{-R}\left[y^{M}(s) - L_{22}u(s)\right] \qquad (2.6)$$

equation 2.3 becomes:

$$b(s) = b_o(s) + V\alpha(s) \qquad (2.7)$$

The vector $b_o(s)$ can be thought of as a particular solution to equation 2.2. The vector $V\alpha(s)$ on the other hand represents the null space component of the general solution. In other words $V\alpha(s)$ can be viewed as the ambiguity in determining b(s) given the input-output measurement $[u(s), y^{M}(s)]$. The need for multiple test frequencies is to resolve such ambiguity which is intrinsically present in any formulation of the problem. Recall the simple example illustrated by figure 5 at the beginning of Chapter 2, which could not be solved by using a single

test frequency. The above development characterizes this "insolubility" as the null space of the L_{21} matrix.

Since more than one test frequency will usually be required for fault diagnosis, let q be the number of test frequencies required. Denote the test frequencies: $s = s_i$, $i=1,2,\ldots,q$. The inverted output equation (equation 2.7) becomes a family of equations:

$$b(s_i) = b_o(s_i) + V\alpha(s_i) \qquad i = 1,2,\ldots,q \tag{2.8}$$

Next substitute $b(s_i)$ from equation 2.8 into the connection equations, $a(s) = L_{11}b(s) + L_{12}u(s)$, which is part of the tableau in equation 2.1a. This provides

$$a(s_i) = L_{11}\left[b_o(s_i) + V\alpha(s_i)\right] + L_{12}u(s) \tag{2.9a}$$

$$a(s_i) = L_{11}b_o(s_i) + L_{21}u(s_i) + L_{11}V\alpha(s_i) \qquad i = 1,2,\ldots,q \tag{2.9b}$$

Since the first two terms on the right hand side of equation 2.9b are known, $a(s_i)$ can also be written as the sum of a particular solution and an ambiguity component:

$$a(s_i) = a_o(s_i) + L_{11}V\alpha(s_i) \qquad i = 1,2,\ldots,q \tag{2.10}$$

where

$$a_o(s_i) = L_{11}b_o(s_i) + L_{21}u(s_i) \tag{2.11}$$

Now substitute equations 2.8 and 2.10 into the remaining part of the tableau equation (component characteristic $b(s)=Z(s,r)a(s)$).

$$b_o(s_i) + V\alpha(s_i) = Z(s_i,r)\left[a_o(s_i) + L_{11}V\alpha(s_i)\right] \quad i = 1,2,..,q \qquad (2.12)$$

The unknowns in equations 2.12 are r and $\alpha(s_i)$, i=1,2,...,q. Finally rewrite equation 2.12 in the following product form [7]:

$$\left[Z(s_i,r) \mid -V\right] \begin{bmatrix} L_{11}V\alpha(s_i) + a_o(s_i) \\ \hline \alpha(s_i) \end{bmatrix} = b_o(s_i) \quad i = 1,2,..,q \qquad (2.13)$$

The family of equations defined by equation 2.13 constitute the tableau form of the fault diagnosis equations. Notice that this set of equations does not require the computation of the composite transfer function matrix. The nonlinear component of these equations are the terms $Z(s_i,r)L_{11}V\alpha(s_i)$. The order of this nonlinearity does not increase as the size of the system increases. In fact for systems where the components have the form $Z_i(s,r_i) = r_iZ_i(s)$ the equations are quadratic regardless of system size. Further discussion of these points follows in a later chapter.

3. Solution of the Fault Diagnosis Equations

The product form of equation 2.13 lends itself to the following compact characterization of the fault diagnosis equations [7]:

$$F(x) = \begin{bmatrix} f_1(r)g_1(\underline{\alpha}_1)-\beta_1 \\ \vdots \\ f_q(r)g_q(\underline{\alpha}_q)-\beta_q \end{bmatrix} = \theta \qquad (3.1)$$

where (i) $\underline{\alpha}_i = \alpha(s_i)$

(ii) $x = \mathrm{col}(\underline{\alpha}_1, \underline{\alpha}_2, \ldots, \underline{\alpha}_q, r)$

(iii) $f_i(r) = [Z(s_i, r) | -V]$

(iv) $g_i(\underline{\alpha}_i) = \begin{bmatrix} L_{11}V\underline{\alpha}_i + a_o(s_i) \\ \hline \underline{\alpha}_i \end{bmatrix}$

(v) $\beta_i = b_o(s_i)$

The objective is to find the value of x for which $F(x) = \theta$. One method is to apply the Newton-Raphson scheme introduced in the previous chapter. In the case of the tableau form the iteration step is:

$$J_F(x^{(k)})(x^{(k+1)} - x^{(k)}) = - F(x^{(k)}) \tag{3.2}$$

where (i) $x^{(k)}$ is the k-th estimate of the root

and (ii) J_F is the Jacobian of F(.)

As a result of the product structure of equation 3.1 the Jacobian has a sparse elegant structure [7]:

$$J_F(x) = \begin{bmatrix} f_1(r)\frac{\partial g_1}{\partial \underline{\alpha}_1}(\underline{\alpha}_1) & 0 & \cdots & 0 & \frac{\partial f_1}{\partial r}(r) g_1(\underline{\alpha}_1) \\ 0 & f_2(r)\frac{\partial g_2}{\partial \underline{\alpha}_2}(\underline{\alpha}_2) & & \vdots & \vdots \\ \vdots & 0 & \ddots & 0 & \\ & \vdots & & f_q(r)\frac{\partial g_q}{\partial \underline{\alpha}_q}(\underline{\alpha}_q) & \frac{\partial f_q}{\partial r}(r) g_q(\underline{\alpha}_q) \end{bmatrix} \tag{3.3}$$

where

$$f_i(r)\,\frac{\partial g_i}{\partial \underline{\alpha}_i}(\underline{\alpha}_i) = Z(s_i,r)\,L_{11}\,V - V \qquad (3.4a)$$

and

$$\frac{\partial f_i}{\partial r}(r)\,g_i(\underline{\alpha}_i) = \left[\frac{\partial Z}{\partial r_1}(s_i,r)\left[L_{11}\,V\,\underline{\alpha}_i + a_0(s_i)\right]\right| \qquad (3.4b)$$

$$\cdots\left|\frac{\partial Z}{\partial r_N}(s_i,r)\left[L_{11}\,V\,\underline{\alpha}_i + a_0(s_i)\right]\right]$$

Note that $f_i(r)\frac{\partial g_i}{\partial \underline{\alpha}_i}(\underline{\alpha}_i)$ is independent of $\underline{\alpha}_i$. Also notice that when the components have the form $Z_j(s,r_j) = r_j Z_j(s)$ (e.g. RLC circuit elements) then $\frac{\partial f_i}{\partial r}(r)g_i(\underline{\alpha}_i)$ forms a diagonal block of $J_F(.)$ which is independent of r. Thus the Jacobian associated with the tableau fault diagnosis equations has an elegant simple sparse structure which compares favorably with the "ugly" structure of the Jacobian in the composite approach (equation 3.3 in Chapter II).

4. An Example

The example presented below is the same example which was presented in Chapter 2 (figure 7). Besides illustrating the use of the fault diagnosis equations in the CCM context this will provide a basic comparison of the two approaches. Such a comparison will illustrate the relative ease with which the fault diagnosis equations are solved as well as the simplicity in computing the Jacobian necessary for the Newton-Raphson iteration. Also the Jacobian will illustrate the sparse structure shown in equation 3.3. Finally a brief comparison of the performance of algorithms based on each approach will be presented.

Recall, then, the following CCM equations from the example presented in Chapter 2

$$\begin{bmatrix} b_1(s) \\ b_2(s) \\ b_3(s) \\ b_4(s) \end{bmatrix} = \begin{bmatrix} G_1 & & & \\ & \frac{1}{SC_2} & 0 & \\ & 0 & G_3 & \\ & & & G_4 \end{bmatrix} \begin{bmatrix} a_1(s) \\ a_2(s) \\ a_3(s) \\ a_4(s) \end{bmatrix} \tag{4.1a}$$

$$\begin{bmatrix} a_1(s) \\ a_2(s) \\ a_3(s) \\ a_4(s) \end{bmatrix} = \begin{bmatrix} 0 & -1 & 0 & 0 \\ 1 & 0 & -1 & 0 \\ 0 & 1 & 0 & 0 \\ 0 & 0 & 0 & 0 \end{bmatrix} \begin{bmatrix} b_1(s) \\ b_2(s) \\ b_3(s) \\ b_4(s) \end{bmatrix} + \begin{bmatrix} 1 \\ 0 \\ 0 \\ 1 \end{bmatrix} u(s) \tag{4.1b}$$

$$\begin{bmatrix} y_1(s) \\ y_2(s) \end{bmatrix} = \begin{bmatrix} 1 & 0 & 0 & 1 \\ 0 & 1 & 0 & 0 \end{bmatrix} \begin{bmatrix} b_1(s) \\ b_2(s) \\ b_3(s) \\ b_4(s) \end{bmatrix} + \begin{bmatrix} 0 \\ 0 \end{bmatrix} u(s) \tag{4.1c}$$

In addition to the information provided in equation 4.1 the tableau approach requires a right inverse for L_{21} and a basis for the null space of L_{21}. These can be computed very efficiently using singular value decomposition techniques [15] such as those found in IMSL [16] or LINPACK[17]. In this example L_{21} is small enough to compute the following by inspection.

$$L_{21}^{-R} = \begin{bmatrix} 1 & 0 \\ 0 & 1 \\ 0 & 0 \\ 0 & 0 \end{bmatrix} \tag{4.2}$$

$$V = \begin{bmatrix} v_1 & v_2 \end{bmatrix} = \begin{bmatrix} 1 & 0 \\ 0 & 0 \\ 0 & 1 \\ -1 & 0 \end{bmatrix} \tag{4.3}$$

Now suppose the same two real test frequencies are used: $s_1 = 1$ and $s_2 = 2$. Let $u(s_1) = u(s_2) = 1$ and let the output measurements be:

$$y^M(s_1) = \begin{bmatrix} \frac{5}{3} \\ \frac{1}{3} \end{bmatrix} \quad \text{and} \quad y^M(s_2) = \begin{bmatrix} \frac{7}{4} \\ \frac{1}{4} \end{bmatrix} \tag{4.4}$$

If the above information is substituted into the fault diagram equations (equation 3.1) the following set of non-linear simultaneous equations result:

$$\begin{bmatrix} G_1 & & & -1 & 0 \\ & \frac{1}{C_2} & & 0 & 0 \\ & & G_3 & 0 & -1 \\ & & & G_4 & 1 & 0 \end{bmatrix} \begin{bmatrix} \frac{2}{3} \\ \alpha_1(1) - \alpha_2(1) + \frac{5}{3} \\ \frac{1}{3} \\ 1 \\ \alpha_1(1) \\ \alpha_2(1) \end{bmatrix} - \begin{bmatrix} \frac{5}{3} \\ \frac{1}{3} \\ 0 \\ 0 \end{bmatrix} = 0 \tag{4.5a}$$

$$\begin{bmatrix} G_1 & & & -1 & 0 \\ & \frac{1}{2C_2} & & 0 & 0 \\ & & G_3 & 0 & -1 \\ & & G_4 & 1 & 1 \end{bmatrix} \begin{bmatrix} \frac{3}{4} \\ \alpha_1(2)-\alpha_2(2)+\frac{7}{4} \\ \frac{1}{4} \\ 1 \\ \alpha_1(2) \\ \alpha_2(2) \end{bmatrix} - \begin{bmatrix} \frac{7}{4} \\ \frac{1}{4} \\ 0 \\ 0 \end{bmatrix} = 0 \qquad (4.5b)$$

Equations 4.5 consists of eight independent equations in eight unknowns,

$$x = (\alpha_1(1), \alpha_2(1), \alpha_1(2), \alpha_2(2), G_1, \frac{1}{C_2}, G_3, G_4)^t.$$

To solve equation 4.5 using the Newton-Raphson scheme,

$$J_F(x^{(k)})(x^{(k+1)} - x^{(k)}) = - F(x^{(k)}) \qquad (4.6)$$

requires the following Jacobian matrix.

$$J_F(x) = \left[\begin{array}{cccc|c|cc} -1 & 0 & 0 & 0 & \frac{2}{3} & 0 & 0 & 0 \\ \frac{1}{C_2} & -\frac{1}{C_2} & 0 & 0 & 0 & \alpha_1(1)-\alpha_2(1)+\frac{5}{3} & 0 & 0 \\ 0 & -1 & 0 & 0 & 0 & 0 & \frac{1}{3} & 0 \\ 1 & 0 & 0 & 0 & 0 & 0 & 0 & 1 \\ \hline 0 & 0 & -1 & 0 & \frac{3}{4} & 0 & 0 & 0 \\ 0 & 0 & \frac{1}{2C_2} & -\frac{1}{2C_2} & 0 & \frac{\alpha_1(2)-\alpha_2(2)+\frac{7}{4}}{2} & 0 & 0 \\ 0 & 0 & 0 & -1 & 0 & 0 & \frac{1}{4} & 0 \\ 0 & 0 & 1 & 0 & 0 & 0 & 0 & 1 \end{array}\right] \qquad (4.7)$$

The partition on the matrix in equation 4.7 emphasizes the sparse structure for the Jacobian presented in equation 3.3 A potential disadvantage of the sparse matrix tableau formulation should be noted at this point. Although the Jacobian in equation 4.7 is sparse the number of non-zero entries is not small enough to provide any obvious advantage over the transfer function matrix approach in memory requirements to store the Jacobian. It remains to be seen if this short coming is intrinsic to the sparse tableau approach or if it may be circumvented by somehow exploiting the regular structure of the Jacobian (equation 3.3).

Although the sparse tableau formulation produces a set of fault diagnosis equations for this example (equation 4.5) which are equivalent to the equations generated by the composite transfer function matrix approach (equation 5.6 of Chapter 3) there are several important differences which give the tableau approach numerical advantages. First the sparse tableau formulation does not require the computation of a transfer function matrix and hence the equations describing the circuit

are much easier to develop. In particular the inverse of the matrix $(I-Z(s,r)L_{11})^{-1}$ is not needed. Second the polynomial order of the fault diagnosis equations in the sparse tableau formulations does not increase with the size of the system as the equations in the composite transfer function matrix approach do. In many applications (e.g. RLC circuits) the sparse tableau form of the fault diagnosis equations will be quadratic.

One final comparison which should be noted is the performance of the Newton Raphsons iteration scheme as applied to the two different approaches. The basis for the comparison is two FORTRAN programs executed on a VAX 11/780 minicomputer. The first program uses the Transfer Function matrix approach and the second uses the Sparse Tableau approach. Both approaches were applied to the example presented in this and the previous chapter except that a single complex test frequency (s = j1) was used instead of two real test frequencies. (A discussion on the use of complex test frequencies will be presented in the next chapter.) Table 1 is a summary of the comparison which lists the number of iterations required by each scheme to find the given parameter vector using the nominal value (all parameters equal to unity) as a first guess for the Newton Raphson iteration.

The information in Table 1 indicates that for the example used the Tableau equations converge faster. In one case the Transfer Function Matrix equations failed to converge. These results certainly indicate that further study of the numerical properties of the tableau fault diagnosis equations is warranted.

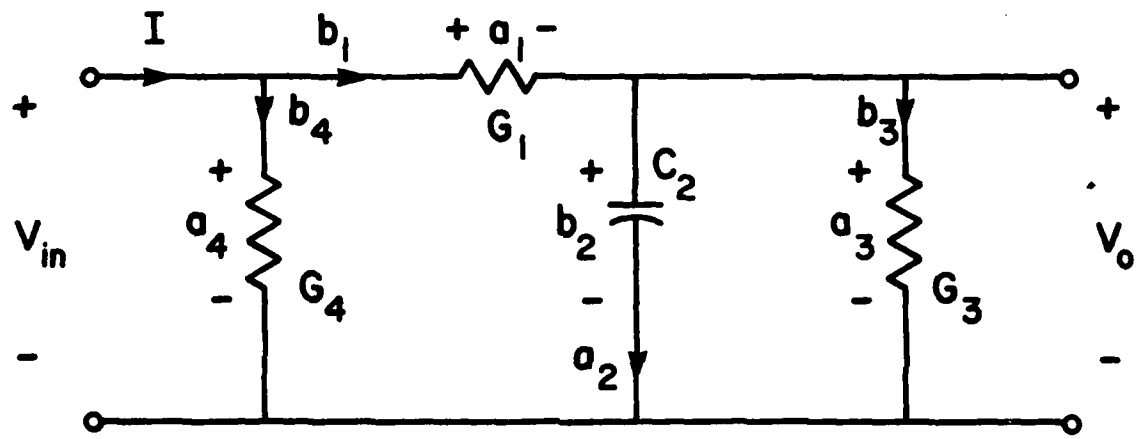

Figure 7. Circuit to illustrate the use of the Fault Diagnosis Equations.

5. Summary and Conclusions

The sparse tableau formulation produces a set of fault diagnosis equations equivalent to those of the composite transfer function matrix approach but they are much easier to compute and potentially easier to solve. The development of the Sparse Tableau approach however is far from complete and before any final conclusions are made on its merits many aspects of the approach remain to be investigated. Among these are:

(1) The extension of the measure of testability from the transfer function matrix approach to the tableau approach;

(2) The investigation of test frequency selection in the sparse tableau context;

(3) The development of a method for test point selection;

(4) A more detailed comparison of the solution algorithms of the two approaches;

(5) The investigation of the modification of the Sparse Tableau Solution Algorithm to exploit the quadratic order which characterizes the tableau equations in many cases;

(6) Application of the sparse tableau equations to the diagnosis of a relatively large example (more than 30 components)

The first item and some aspects of the second form a major part of the next chapter of this report.

Solution Vector	Number of Iterations	
	Sparse Tableau	Transfer Function
(r_1, r_2, r_3, r_4)	Approach	Matrix Approach
(2, 1, 1, 1)	1	4
(3, 1, 1, 1)	1	4
(4, 1, 1, 1)	1	5
(5, 1, 1, 1	1	(solutions diverged)
(1, 2, 1, 1)	3	3
(1, 3, 1, 1)	3	4
(1, 4, 1, 1)	3	5
(1, 5, 1, 1)	3	5
(1, 1, 2, 1)	1	4
(1, 1, 3, 1)	1	4
(1, 1, 4, 1)	1	5
(1, 1, 5, 1)	1	6
(1, 1, 1, 2)	1	1
(1, 1, 1, 3)	1	1
(1, 1, 1, 4)	1	1
(1, 1, 1, 5)	1	1

Table 1

Comparison of Sparse Tableau and Transfer Matrix Approaches

CHAPTER 4

CURRENT RESEARCH IN THE TABLEAU APPROACH

1. Introduction

This chapter contains a collection of results stemming from recent research into the Tableau Approach to fault diagnosis [9]. These include a discussion of the Newton Raphson iteration applied to overspecified equations, a test for diagnosability in the Tableau context, bounds on test frequencies and the presentation of several examples.

2. Newton-Raphson Iterations and the Non-Square Jacobian

In all previous discussions of the solution of the nonlinear equation $F(x) = \theta$ the underlying assumption was that $F(x)$ mapped R^n into R^n. In this case the Newton Raphson iteration step

$$J_F(x^{(k)})(x^{(k+1)} - x^{(k)}) = - F(x^{(k)}) \qquad (2.1)$$

has a unique solution for $(x^{(k+1)} - x^{(k)})$ when the Jacobian $J_F(x^{(k)})$ is non-singular. In many cases the fault diagnosis equation will be a mapping from R^n into R^m where $m \neq n$. To see why this occurs recall the tableau equations from Chapter 3:

$$F(x) = \begin{bmatrix} f_1(r)g_1(\underline{\alpha}_1) - \beta_1 \\ \vdots \\ f_q(rg_q(\underline{\alpha}_q) - \beta_q \end{bmatrix} = \theta \qquad (2.2)$$

where (i) $\underline{\alpha}_i = \alpha(s_i)$

(ii) $x = \text{col}(\underline{\alpha}_1, \underline{\alpha}_2, \ldots, \underline{\alpha}_q, r)$

(iii) $f_i(r) = [Z(s_i, r) \mid -V]$

(iv) $g_i(\underline{\alpha}_i) = \begin{bmatrix} L_{11} V \underline{\alpha}_i + a_0(s_i) \\ \hline \underline{\alpha}_i \end{bmatrix}$

(v) $\beta_i = b_0(s_i)$

In the case of real test frequencies (complex test frequencies are discussed later in the chapter), $F(x)$: $D \subset R^{N+pq} \rightarrow R^{Mq}$ and $J_F(x^k) \in R^{(Mq)x(N+pq)}$

where (i) $N = \dim(r)$

(ii) $p = \dim(\underline{\alpha}_i)$, $i = 1,2,\ldots,q$

(iii) M = row dimension of $Z(s_i, r)$

(iv) q = the number of test frequencies

Since N, p, M and q are all integers it is not necessarily true that:

$$N + pq = Mq \qquad (2.3)$$

If equation 2.3 holds the solution of equation 2.1 proceeds using any of the many accurate numerical techniques available for inverting the square non-singular Jacobian, $J_F(x^{(k)})$.

Under the diagnosability criterion to be developed later in the chapter, a system for which $J_F(\cdot)$ does not have full column rank is not guaranteed to be diagnosable and therefore the usual techniques are not directly applicable. This situation is characteristic of a lack of sufficient measurement data for diagnosis. For the underspecified case it is necessary to augment the available data by adding test frequencies, providing more test outputs, or assigning known or assumed values to a subset of the parameters. Assuming however, that $J_F(x^{(k)})$ has full column rank the only other possible relation for the dimensions of $J_F(x^{(k)})$ is

$$N+pq < Mq \tag{2.4}$$

A simple example will illustrate the nature of the Newton Raphson iteration when inequality 2.4 holds ($J_F(\cdot)$ has more rows than columns).

Suppose $F(x)$: $D \subset R^2 \rightarrow R^3$ is defined as

$$F(x_1,x_2) = \begin{bmatrix} x_1^2 + x_2 - 2 \\ 2x_1 + x_2^2 - 3 \\ x_1^2 + x_2^2 - 2 \end{bmatrix} \tag{2.5}$$

The point $(1,1)^t$ is a solution to the equation $F(x) = \theta$, $x = (x_1,x_2)^t$. The Jacobian, $J_F(x_1,x_2) \in R^{3x2}$ is:

$$J_F(x_1,x_2) = \begin{bmatrix} 2x_1 & 1 \\ 2 & 2x_2 \\ 2x_1 & 2x_2 \end{bmatrix} \tag{2.6}$$

Let the starting point for the Newton Raphson iteration, be $(2,2)^t$. Equation 2.1 evaluated at the first iteration of this example becomes:

$$\begin{bmatrix} 4 & 1 \\ 2 & 4 \\ 4 & 4 \end{bmatrix} \begin{bmatrix} h_1 \\ h_2 \end{bmatrix} = - \begin{bmatrix} 4 \\ 5 \\ 6 \end{bmatrix} \tag{2.7}$$

where

$$\begin{bmatrix} h_1 \\ h_2 \end{bmatrix} = \begin{bmatrix} x_1^{(1)} - 2 \\ x_2^{(1)} - 2 \end{bmatrix}$$

Since the vector $-[4 \;\; 5 \;\; 6]^t$ is not contained in the space spanned by the "column vectors" $[4 \;\; 2 \;\; 4]^t$ and $[1 \;\; 4 \;\; 4]^t$ equation 2.7 is inconsistent.

How then is the Newton-Raphson iteration step solved when the linearized equations are inconsistent? A reasonable approach to provide a solution to equation 2.1 when it is inconsistent is to find $x^{(k+1)} - x^{(k)} \triangleq h$ such that

$$||J_F(x^{(k)})h + F(x^{(k)})||_2 \tag{2.8}$$

is minimized, where $||\cdot||_2$ is the Euclidean norm. This "least squares" problem is readily solved using singular value decomposition techniques [15] available in many computer subroutine libraries such as

LINPACK[17]. To see why such a scheme is reasonable suppose $F(\cdot)$: $D \subset R^n \to R^m$ and $m < n$. Consider the Taylor expansion of $F(x^*)$ about the point x where $F(x^*) = \theta$.

$$F(x^*) = \theta = F(x) + J_F(x)(x^* - x) + \epsilon \tag{2.9}$$

The term ϵ represents the effect all the higher order terms of the expansion. Recall from the derivation of the Newton Raphson scheme (Section 4 of Chapter 2) that ϵ is assumed to be small enough to be disregarded. Before doing that decompose $F(x)$ and ϵ into orthogonal components in the following manner:

$$F(x) = F(x)^C + F(x)^\perp \tag{2.10a}$$

$$\epsilon = \epsilon^C + \epsilon^\perp \tag{2.10b}$$

where the superscript C denotes the projection onto the column space of $J_F(x)$ and the superscript $\perp$ denote the projection onto the orthogonal complement of the column space of $J_F(x)$. Substituting equation 2.10 into 2.9 yields:

$$\theta = F(x)^C + F(x)^\perp + J_F(x^* - x) + \epsilon^C + \epsilon^\perp \tag{2.11}$$

Since those terms which lie in the column space of $J_F(x)$ are orthogonal to those which lie in its orthogonal complement, equation 2.11 can be decomposed into two equations:

$$\theta = F(x)^C + J_F(x^* - x) + \epsilon^C \tag{2.12a}$$

$$\theta = F(x)^{\perp} + \epsilon^{\perp} \tag{2.12b}$$

Since $\epsilon = \epsilon^{C} + \epsilon^{\perp}$ where ϵ^{C} and $\epsilon^{\perp}$ are orthogonal then $||\epsilon||_2^2 = ||\epsilon^{C}||_2^2 + ||\epsilon^{\perp}||_2^2$. If $||\epsilon||_2$ is small then $||\epsilon^{C}||_2$ and $||\epsilon^{\perp}||_2$ must also be small. Neglecting the term ϵ^{C} in equation 2.12a leads to the following iteration step:

$$J_F(x^{(k)})(x^{(k+1)} - x^{(k)}) = - F(x^{(k)})^{C} \tag{2.13}$$

Equation 2.13 is simply the Newton Raphson step used earlier except the right hand consists of only that part of $-F(x^{(k)})$ which lies in the column space of $J_F(x^{(k)})$. Not only is equation 2.13 consistent but it is mathematically equivalent to the "least square" problem of equation 2.8.

One would expect that equation 2.13 has convergence properties similar to the Newton Raphson iteration when $F: D \subset R^n \rightarrow R^n$. To illustrate this a simple "attraction theorem" for equation 2.13 will be presented later in this chapter. Intuitively, however, as the estimate $x^{(k)}$ approaches the solution point the linear term of equation 2.9 becomes more accurate causing $||\epsilon||_2$ to decrease. This implies that $||\epsilon^{\perp}||_2$ and $||\epsilon^{C}||_2$ must also decrease since $\epsilon^{\perp}$ and ϵ^{C} are orthogonal components of ϵ.

3. Diagnosability

The purpose of this section is to develop a test to determine under what conditions it is reasonable to attempt to solve the Tableau fault diagnosis equations (Equation 2.2). Unlike the Matrix Transfer Function Equations the Tableau equations have the ambiguity unknowns, α_i,

$i=1,2,..,q$ in addition to the parameter vector, r. Because the objective is to identify the parameter vector r, computing the $\underline{\alpha}_i$'s may seem unnecessary. The role of the these auxiliary unknowns is to "unfold" the fault diagnosis equations from R^N where r lives (as in other approaches) to the larger dimensional space, R^{N+pq}, where x lives. In R^N the fault diagnosis equations are highly nonlinear. In R^{N+pq} the equations are often quadratic, and the data of the end of Chapter 3 supports the conjecture that solving for the larger dimensional x is preferable to solving for r directly. See Table 1 of Chapter 3, page 49.

Like the fault diagnosis equations in the Transfer Function Matrix Context (equation 2.7 of Chapter 2) the solvability of the tableau equations (equation 2.2) is based on the existence of an isolated solution (Section 3 of Chapter 2). For the tableau equations however the issue is confused by the presence of the auxiliary unknowns, $\underline{\alpha}_i$, $i = 1,2,\ldots,q$. For example suppose $x^* \in R^{N+pq}$, $x^* = (\underline{\alpha}_1^*, \underline{\alpha}_2^*, \ldots, \underline{\alpha}_q^*, r^*)^t$ is a solution to equation 2.2. Suppose furthermore that for every $\delta \in R$, $\delta > 0$, there exists a vector $h \in R^{N+pq}$, with $||h||_2 > 0$, such that $x^* + \delta h$ is also a solution. Clearly in this situation x^* is not an isolated solution. Now suppose the vector h in the above situation always has the form $h = (h_1, h_2, \ldots, h_q, 0)$. In other words even though the solution x^* is not uniquely specified by equation 2.2 the subvector, r, is uniquely specified. If such a situation were possible a criterion of solvability, which required that the solution x^* be isolated in order to completely specify r, might be too restrictive. The objective of the next few paragraphs is to show that such a situation will not occur and

thus permit the criterion of an isolated solution to be used as the basis for a definition of diagnosability.

Recall that the tableau fault diagnosis equations are based on measurements $y^M(s_i)$ in response to inputs $u(s_i)$, $i = 1,2,\ldots,q$. Using the transfer function matrix,

$$S(s,r) = L_{22} + L_{21}\left[I-Z(s,r)L_{11}\right]^{-1} Z(s,r)L_{12} \qquad (3.1)$$

the measurement can be expressed in terms of the parameter vector directly as:

$$y^M(s_i) = \left[L_{22} + L_{21}[I-Z(s_i,r)L_{11}\ ]^{-1} Z(s,r)L_{12}\right] u(s_i) \qquad (3.2)$$

for $i = 1,2,\ldots,q$. The family of equations in equation 3.2 share the same properties as the fault diagnosis equations of the Transfer Function Matrix approach. In fact the input $u(s_i)$ and s_i, $i = 1,2,\ldots,q$ can be chosen so that equations 3.2 correspond exactly to the Transfer Function Matrix fault diagnosis equations (equation 2.6 of Chapter 2).

The concern that basing a criterion for solvability of the Tableau Fault diagnosis equation (equation 2.2) on the existence of an isolated solution can now be dispelled with the following theorem:

Theorem 3.3: The vector r^* is an isolated solution of equations 3.2 if and only if there exist auxiliary vectors $\underline{a}_i^*$, $i = 1,2,\ldots,q$ such that $x^* = (\underline{a}_i^*,\underline{a}_i^*,\ldots,\underline{a}_q^*,r^*)^t$ is an isolated solution of equation 2.2. The proof of theorem 1 requires the following Lemmas.

Lemma 3.4: If r^* is a solution of equation 3.2 then there exist unique $\underline{a}_i^*$, $i = 1,2,\ldots,q$, such that $x^* = (\underline{a}_i^*,\underline{a}_i^*,\ldots,\underline{a}_q^*,r^*)^t$ is a solution to

equation 2.2.

Proof of Lemma 3.4: The proof is by construction. Since r^* is given it may be used in the tableau equation (equation 2.1a of Chapter 3) to simulate the system. Now suppose that the test frequencies, s_i, $i = 1,2,\ldots,q$, are neither circuit/system poles nor component poles. In this case equation 2.1a of Chapter 3 is well defined and can be solved uniquely for $b(s_i)$, $i = 1,2,\ldots,q$. Denote these solutions $b^*(s_i)$, $i = 1,2,\ldots,q$. From equations 2.8 of Chapter 3:

$$V\underline{a}_i = b^*(s_i) - b_0(s_i) \qquad i = 1,2,\ldots,q. \tag{3.5}$$

By construction the right hand side lies only in the column space of V. This implies that

$$\text{Rank}[V] = \text{Rank}\left[V \mid b^*(s_i) - b_0(s_i)\right] \tag{3.6}$$

and therefore solutions $\underline{a}_i$, $i = 1,2,\ldots,q$, of equation 3.5 exist. Since V has full column rank these solutions are unique. Furthermore the construction insures that the vector $x^* = (\underline{a}_1^*, \underline{a}_2^*, \ldots, \underline{a}_q^*, r^*)^t$ satisfies equation 2.2.

Q.E.D.

Lemma 3.7: If $x^* = (\underline{a}_1^*, \underline{a}_2^*, \ldots, \underline{a}_q^*, r^*)^t$ is a solution to equation 2.2 then r^* is a solution to equation 3.2.

Proof of Lemma 3.7:

Since x^* is a solution to equation 2.2, the vectors r^* and $_i$ $i = 1,2,\ldots,q$, satisfy

$$\left[Z(s_i,r^*) \mid -V\right] \left[\begin{array}{c} L_{11}V\underline{\alpha}_i^* + a_0(s_i) \\ \hline \underline{\alpha}_i^* \end{array}\right] - b_0(s_i) = \theta \qquad (3.8)$$

Recall that

$$b_0(s_i) \triangleq L_{21}^{-R}\left[y^M(s_i) - L_{22}u(_i)\right] \qquad (3.9)$$

and

$$a_0(s_i) \triangleq L_{11}b_0(s_i) + L_{12}u(s_i) \qquad (3.10)$$

Multiplying out equation 3.8 and substituting equation 3.10 yields:

$$Z(s_i,r^*)L_{11}\left[b_0(s_i) + V\underline{\alpha}_i^*\right] + Z(s_i,r^*)L_{12}u(s_i) - \left[b_0(s_i) + \underline{\alpha}_i^*\right] = \theta \qquad (3.11)$$

Solve for $b_0(s_i) + V\underline{\alpha}_i$:

$$b_0(s_i) + V\underline{\alpha}_i^* = \left[I - Z(s_i,r^*)L_{11}\right]^{-1}Z(s_i,r^*)L_{12}u(s_i) \qquad (3.12)$$

Multiply on the left by L_{21} and recall that the columns of V span the null space of L_{21}. Hence

$$L_{21}b_0(s_i) = L_{21}\left[I - Z(s_i,r^*)L_{11}\right]^{-1}Z(s_i,r^*)L_{12}u(s_i) \qquad (3.13)$$

Finally substitute equation 3.9 into 3.13 to obtain:

$$y^M(s_i) = \{L_{22} + L_{21}\left[I - Z(s_i,r^*)L_{11}\right]^{-1}Z(s_i,r^*)L_{12}\}\, u(s_i) \qquad (3.14)$$

$i = 1,2,\ldots,q$ for which coincides with equation 3.2.

Q.E.D.

Proof of Theorem 3.3:

Part 1 - "only if"

Suppose $x^* = (\underline{\alpha}_1^*, \underline{\alpha}_2^*, \ldots, \underline{\alpha}_q^*, r^*)t$ is not an isolated solution of equation 2.2 but r^* is an isolated solution of equation 3.2. Since x^* is not isolated, for any arbitrarily small $\delta > 0$ there exists another solution $\hat{x} = (\hat{\underline{\alpha}}_1, \hat{\underline{\alpha}}_2, \ldots, \hat{\underline{\alpha}}_q, \hat{r})^t$ such that $0 < ||x^* - \hat{x}||_2 < \delta$. Now according to Lemma 3.7 $\hat{r}$ must also be a solution to equation 3.2 and furthermore $r^* \neq \hat{r}$ (If $r^* = \hat{r}$ then by Lemma 3.4, $\underline{\alpha}_i^* = \hat{\underline{\alpha}}_i^*$, $i = 1,2,\ldots,q$ which contradicts $x^* \neq \hat{x}$.). Since r^* and $\hat{r}$ are corresponding components of x^* and $\hat{x}$ respectively then $0 < ||x^* - \hat{x}||_2 < \delta$ and $r^* \neq \hat{r}$ imply that $0 < ||r^* - \hat{r}||_2 < \delta$. But δ can be chosen arbitrarity small which implies $\hat{r}$ becomes arbitrarily close to r^* implying r^* is not an isolated solution to equation 3.2. This contradicts the assumption that r^* is isolated.

Part 2 - "if"

Now suppose r^* is not an isolated solution of equation 3.2. Use r^* in Lemma 3.4 to construct a solution to equation 2.2. Denote this solution $x^* = (\underline{\alpha}_i^*, \underline{\alpha}_2^*, \ldots, \underline{\alpha}_q^*, r^*)^t$ and assume that x^* is an isolated solution to equation 2.2. From the construction in Lemma 3.4 the $\underline{\alpha}_i$, $i = 1,2,\ldots,q$ and hence $x = (\underline{\alpha}_1, \underline{\alpha}_2, \ldots, \underline{\alpha}_q, r)$ are continuous functions of r. Now select an $\hat{r}$ and construct the corresponding $\hat{x}$. From the property of continuity for any $\varepsilon > 0$ there exists a $\delta > 0$ such that whenever $||r^* - \hat{r}||_2 < \delta$, $||x^* - \hat{x}||_2 < \varepsilon$. Since r^* is not an isolated solution the $\hat{r}$ can always be chosen to be a solution as well. Consequently from Lemma 3.4 $\hat{x}$ must be a solution to equation 2.2. Since ε is arbitrary, in any open neighborhood of x^* it is possible to find

another solution $\hat{x}$. This contradicts the assumption that x^* is isolated.

Q.E.D.

Lemma 3.4 and 3.7 and Theorem 3.3 clearly establish the equivalence of the Fault Diagnosis equations in the Tableau Form with those in transfer function matrix form and make the following definition possible.

Definition 3.15: A circuit/system modeled by equation 2.1 of Chapter 3 is said to be "DIAGNOSABLE" if and only if there exist real test frequencies, s_i, and corresponding test inputs $u(s_i)$, $i = 1,2,\ldots,q$, with q finite, for which a solution to equation 2.2 exists and is an isolated solution.

With respect to the above definition the terms DIAGNOSABLE and DIAGNOSABILITY will be used in the context of the tableau approach to avoid confusion with the measure of testability defined in the transfer function matrix context. Also the test frequencies, s_i, are not necessarily distinct. For example a system with two inputs could be diagnosable with q=2 where $s_1 = 5$, $u(s_1) = (1,0)^t$ and $s_2 = 5$, $u(s_2) = (0,1)^t$.

The next theorem provides an explicit test for diagnosability.

Theorem 3.16: Suppose a circuit/system is characterized by a parameter vector r. Let x be a solution to equation 2.2 which includes the subvector, r. Then the circuit/system is diagnosable for the parameter vector, r, if there are sufficient test frequencies, s_i, and corresponding inputs, $u(s_i)$, $i = 1,2,\ldots,q$, such that $J_F(x)$ has full column rank.

Proof: Recall that in the tableau fault diagnosis equation, $F(x) = \theta$, the nonlinear function $F: D \subset R^{N+pq} \rightarrow R^{Mq}$ where $Mq \geq N+pq$. Since the $Mq \times (N+pq)$ Jacobian matrix has full column rank it must have an $(N+pq) \times (N+pq)$ submatrix, $J_{\tilde{F}}(s)$, which is non-singular. Define $\tilde{F}$: $D \subset R^{N+pq} \rightarrow R^{N+pq}$ to be a subvector of F whose entries are the entries of F corresponding to the rows of $J_{\tilde{F}}(x)$. Clearly if x satisfies $F(x) = \theta$ it must satisfy $\tilde{F}(x) = \theta$. Since $J_{\tilde{F}}(s)$ is non-singular the Inverse Function Theorem insures that x must be an isolated solution of $\tilde{F}(x) = \theta$. The vector x must likewise be an isolated solution of $F(x) = \theta$ and therefore definition 3.15 is satisfied.

Q.E.D.

To be of any practical use the fact that $J_F(\cdot)$ has full column rank at some specific solution point must infer that it has full column rank elsewhere. This is important for two reasons. First, the Newton-Raphson iteration scheme requires that $J_F(x)$ have full column rank to uniquely solve the Newton-Raphson step for a sequence of estimate x^k. If at any point there is no unique solution the iteration scheme could not proceed. Second, it would be reassuring to know that when a circuit/system is designed to be diagnosable for some nominal parameter vector r, it will still be diagnosable should the parameter vector change due to aging or failure of the components.

In practice the use of the Newton-Raphson iteration scheme requires that $J_F(x)$ have full column rank almost everywhere. In this context almost everywhere means everywhere except in a lower dimensional algebraic variety [9]. If this is true then whenever the algorithm encounters a "bad" value for x an arbitrarily small perturbation of x

will yield a value from which the iteration can proceed. The following theorem shows that this is indeed the case:

Theorem 3.17: Suppose $x^* \in R^{N+pq}$ and $J_F(x^*)$ has full column rank then $J_F(x)$ has full column rank for almost all $x \in R^{N+pq}$.

Proof: If $J_F(x^*)$ has full column rank then there is an N+pq by N+pq submatrix, $M(x^*)$, such that $\det[M(x^*)] \neq 0$. Since every entry of $J_F(x^*)$ is either a constant or a linear combination of the elements of x^*, this *determinant is a polynomial in* x^*. Now consider the polynomial $\det[M(x)]$. It is not zero at $x = x^*$ and therefore is not identically zero. The zero set of this polynomial is an algebraic variety of R^{N+pq} of dimension no larger than N+pq-1 and contains all points where $J_F(x)$ is NOT full column rank.

Q.E.D.

The question still remains: Can the parameter vector change to make a diagnosable circuit non-diagnosable? Diagnosability is defined only for those points $x \in R^{N+pq}$ which are possible solutions to equation 2.2 and according to lemmas 3.4 and 3.7 this is an N dimensional subspace of R^{N+pq}. Clearly measure over R^{N+pq} is not appropriate to this situation. Since the solution space is isomorphic to R^N the measure over R^N is used in the following:

Theorem 3.18: Suppose a circuit/system is known to be diagnosable via Theorem 3.16 for parameter vector r^*. Then it is diagnosable for almost all $r \in R^N$.

Proof: By Theorem 3.16 test frequencies exist such that $J_F(x^*)$ has full column rank. (Note: x^* is determined uniquely from r^* as per Lemma 3.4.) If $J_F(x)$ is evaluated only over the solution space of equation 2.2

it may be considered a function of r only, since the $\underline{a}_i$, $i = 1,2,\ldots,q$, are functions of r. J_F can be expressed explicitly as a function of r by replacing the term $[L_{11}V\underline{a}_i + a_0(s_i)]$ in expression 3.4b of Chapter 3 as follows:

$$\left[L_{11}V\underline{a}_i + a_o(s_i)\right] = \left[I - L_{11}Z(s_i,r)\right]^{-1} L_{12}u(s_i) \tag{3.19}$$

Now all entries of $J_F(r)$ are constants, polynomials in r, or ratios of polynomials in r. Because $J_F(r^*)$ has full column rank, k, there is a k by k minor $M(r^*)$ such that det $M(r^*)$ is defined and is not zero. Now consider the parameter vector $r \neq r^*$. The determinant of M(r) can be written as a ratio of polynomials in r:

$$\text{Det}[M(r)] = \frac{p_1(r)}{p_2(r)} \tag{3.20}$$

Since M(r) is not zero and defined at r^* polynomials $p_1(\cdot)$ and $p_2(\cdot)$ are not identically zero. $J_F(r)$ has full column rank everywhere except possibly over the zero sets of $p_1(\cdot)$ or $p_2(\cdot)$, which are algebraic varieties in R^N and hence so is their union.

Q.E.D.

The discussion thus far has required real test frequencies. The most likely test signal in fault diagnosis testing, however, is a sinusoidal signal which is equivalent to using a complex pair of test frequencies. It is appropriate therefore to illustrate how the fault diagnosis equations are affected by the use of complex test frequencies. When the $s_i = j\omega_i$, $i = 1,2,\ldots,q$ are complex, the fault diagnosis equations simply become complex vector equations but since r is

generally real it is convenient to use real arithmetic. To do this it is necessary to convert the fault diagnosis equation to an equivalent set of real equations. Equation 2.2 becomes:

$$\mathrm{Re}[F(x_{Re})] = 0$$
$$\mathrm{Im}[F(x_{Re})] = 0$$

where Re[ ] and Im[ ] denote real and imaginary parts respectively. The unknown vector $x_{Re} \in R^{N+2pq}$ is defined:

$$x_{Re} = \begin{vmatrix} \mathrm{Re}[\alpha] \\ \mathrm{Im}[\alpha] \\ r \end{vmatrix} \text{ where } \alpha = \begin{bmatrix} \alpha_1 \\ \alpha_2 \\ \vdots \\ \alpha_q \end{bmatrix}. \tag{3.21}$$

The Jacobian $J_F(x_{Re})$ has the form:

$$J_F(x_{Re}) = \begin{bmatrix} \frac{\partial \mathrm{Re}[F]}{\partial \mathrm{Re}[\alpha]} & \frac{\partial \mathrm{Re}[F]}{\partial \mathrm{Im}[\alpha]} & \frac{\partial \mathrm{Re}[F]}{\partial r} \\ \frac{\partial \mathrm{Im}[F]}{\partial \mathrm{Re}[\alpha]} & \frac{\partial \mathrm{Im}[F]}{\partial \mathrm{Im}[\alpha]} & \frac{\partial \mathrm{Im}[F]}{\partial r} \end{bmatrix} \tag{3.22}$$

Like the Jacobian in the real test frequency case, $J_F(x_{Re})$ is sparse and each block has a diagonal or block diagonal structure. In light of the above discussion it is possible to state the following test:

Corollary 3.23: (to Theorem 3.16): A circuit characterized by parameter vector, r, is diagnosable if there are complex test frequencies, $s_i = j\omega_i$ and corresponding inputs, $u(s_i)$, $i = 1,2,\ldots,q$, such that $J_F(x_{Re})$ has full column rank.

Q.E.D.

Proof: Special case of Theorem 3.16.

This last test is significant because a single sinusoidal input embodies two test frequencies, $\pm j\omega$, and thus fewer input-output measurements are required.

4. Test Frequencies

The use of Theorem 3.16 or corollary 3.23 requires the selection of appropriate test frequencies. Presently no method is known to make this selection in an optimal manner. Nevertheless it is possible to place some simple bounds of the number of test input/frequency combinations necessary to satisfy the conditions of Theorem 3.16 and its corollary. The bounds developed here are applicable to complex test frequencies and greatly simplify the use of corollary 3.23 in determining diagnosability.

Theorem 4.1 (lower bound): Suppose a circuit/system has the following characteristics:

i) N real parameters

ii) $\text{Dim}\{\text{null}[L_{21}]\} = p$,

iii) The test frequencies are s_i and test inputs are $u(s_i)$, and $i = 1,2,\ldots,q$.

iv) The row dimension of $Z(\cdot,\cdot)$ is M

The minimum number of test inputs/frequencies, q, required to make the circuit/system diagnosable is

$$\beta = \left\lceil \frac{N}{2(M-p)} \right\rceil \tag{4.2}$$

where the square bracket indicates "least upper-bounding integer."

Proof: For complex frequencies it is convenient to consider a set of equivalent real scalar equations since the parameter vector r is real. Thus q complex test frequencies result in 2Mq equations in N+2pq unknowns (the $\underline{\alpha}_i$ may be complex but r is not). In the best case all equations are independent. Hence $2Mq \geq N+2pq$ which implies

$$q \geq \frac{N}{2(M-p)} = \beta.$$

Q.E.D.

Note: Implicit in the above proof is the fact that M must be greater than p in order for q to be positive and finite. Intuitively, if the dimension of ambiguity at any single test frequency is not strictly less than the number of scalar equations generated by each test frequency, no choice of test frequencies could possibly resolve it.

Theorem 4.3 (upper bound): Consider the same circuit/system as Theorem 4.1. If it is diagnosable the maximum number of test inputs/frequencies necessary is N.

Proof: Each of the terms $f_i(r)g_i(\underline{\alpha}_i) - \beta_i = 0$ in equation 2.2 consists of M complex scalar equations in N+p unknowns. N unknowns corresponding to the parameter subvector r are common to each set. Converting to an equivalent set of real equations this yields 2M equations in N+2p unknowns (again r is real). Therefore the first test input/frequency produces N+2p unknowns and each subsequent measurement introduces 2p more. Clearly if each such set of 2M equations contributes 2p independent equations to the entire set there could be no locally unique solution, whereas if each contributes 2p+1, a locally unique solution is possible. Since the circuit/system is diagnosable by hypothesis then

the worst case (requiring the most test frequencies) is 2p+1 independent equations per test frequency. In this case q must satisfy: $q(2p+1) \leq N+2pq$ and $q \leq N$. Since q=N is the minimum integer which satisfies the worst case this must be the most test frequencies necessary.

Q.E.D.

For a given circuit is now possible to choose test frequencies and determine if the choice renders the circuit diagnosable for some nominal set of parameters. After a circuit is found to be diagnosable the Newton-Raphson iteration scheme can be used to solve for the actual values for those parameters from measurements taken at the selected test frequencies.

5. Nonlinearity of the Fault Diagnosis Equations

An extremely important special case form of the component transfer function matrix arises when

$$Z_i(s,r_i) = r_i\, Z_i(s) \qquad (5.1)$$

In this case each of the product terms of the Tableau form of the fault diagnosis equations is affine [21] and the components of F(x) are always quadratic polynomials in x, regardless of the number of components in the system. This is not the case with the Transfer Function Matrix form of the Fault diagnosis equations (equation 2.6 of Chapter 2). Each entry of equation 2.6 of Chapter 2 has the form:

$$m_k - \frac{p_{kn}(r)}{p_{kd}(r)} = 0 \qquad (5.$$

where m_k is the measurement of one entry of the transfer function matrix and $p_{kn}(r)$ and $p_{kd}(r)$ are polynomials in r. The ratio $p_{kn}(r)/p_{kd}(r)$ is a scalar transfer function from the system input to the system output associated with the entry of the transfer function matrix to which the measurement, m_k, corresponds.

As the size of the system/circuit increases the degree of the polynomials, $p_{kn}(r)$ and $p_{kd}(r)$, will generally increase. A simple approach to see why this occurs is to form the directed graph which is equivalent to the CCM equations and then use Mason's gain formula [20] to make some general observations about the nature of $p_{kn}(r)$ and $p_{kd}(r)$ as the number of components of the circuit in question increases.

A directed graph is easily constructed from the CCM equations by assigning to each component a directed branch with weight $r_i Z_i(s)$, $i = 1,2,\ldots,N$. Thus each branch weight is a first degree polynomial in r. The vertices of each of these branches represent the component's input and output. The graph is completed by connecting the component inputs and outputs and vertices representing the system inputs and outputs with directed branches whose weights correspond to the non zero entries of the L_{ij} (connection matrices) in such a way that the appropriate conservation laws are satisfied. Figure 8 is an illustration of a graph constructed in such a manner. The graph is based on the CCM equations for the example circuit from Chapter 2 (equations 5.1, 5.2 and 5.3 of Chapter 2).

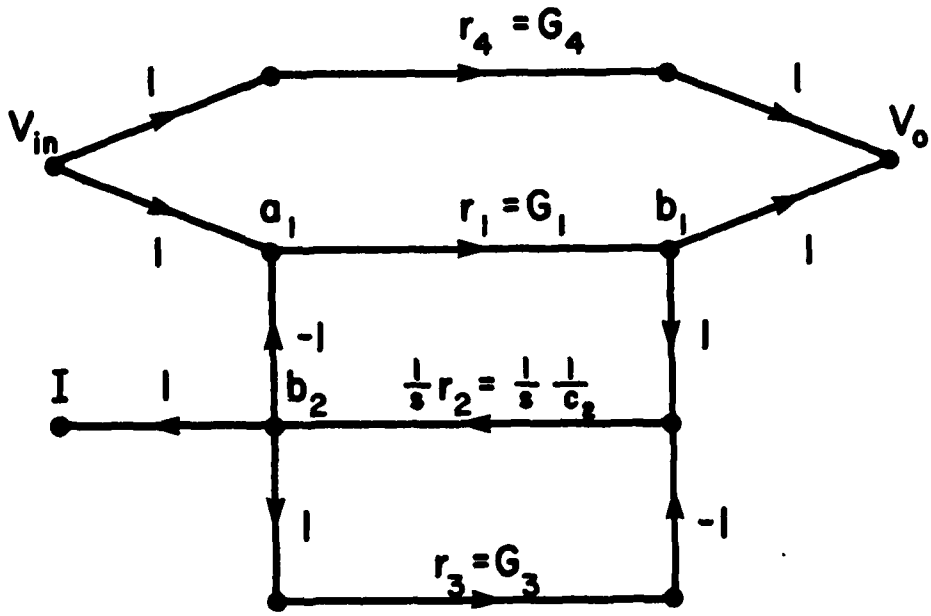

Figure 8. Graph of example circuit.

Before starting Mason's gain formula the following definitions associated with the use of graphs are necessary [20]:

Path gain - The product of the weights of the branches of a directed path in the graph.

Cycle gain - The product of the weights of all branches in a directed circuit of the graph.

Let

t_1 = sum of cycle gains of all directed circuits in the graph;

t_2 = sum of products of all vertex-disjoint (non-touching) directed circuits taken two at a time;

t_k = sum of products of all vertex-disjoint directed circuits taken k at a time;

$\Delta = 1 - t_1 + t_2 - t_3 + \cdots + (-1)^q t_q$

where q is the maximum number of vertex-disjoint directed circuits in the graph;

P_k = path gain of the kth directed path from output to input vertex for which the transfer function is to be computed;

Δ_k = the value of Δ for that part of the directed graph having no vertices in common with the path associated with P_k.

Notice that the expressions for Δ, Δ_k and P_k are all polynomials in r. The scalar transfer function can now be computed using Mason's gain formula [20] as:

$$\frac{p_{kn}(r)}{p_d(r)} = \frac{\sum_k P_k \Delta_k}{\Delta} \qquad (5.3)$$

Consider each of the terms Δ, Δ_k and P_k as the circuit/system and hence its graph increase in size. The paths from input vertices to output vertices will tend to get longer and the number and size of the directed circuits will likewise increase. Thus the polynomial degree of Δ, Δ_k and P_k and consequently of $p_{kn}(r)$ and $p_{kd}(r)$ will increase in proportion to the size of the circuit/system.

The degree of the components of the Tableau Equation on the other hand remains fixed (quadratic) as the system/circuit size increases. Therefore each term has a constant second derivative with respect to r and higher derivatives vanish. A solution algorithm which exploits this easily computed second derivative information should offer greatly improved performance over the Newton-Raphson scheme discussed earlier.

6. Convergence of the Newton Raphson Iteration

At the beginning of the Chapter a form of the Newton-Raphson iteration step (equation 2.13) was derived to solve $F(x) = 0$, where the nonlinear function $F: D \subset R^n \rightarrow R^m$ and $m > n$. The objective of this section is to show that the iteration of equation 2.13 is locally convergent. An iteration is said to be locally convergent if the iteration will converge to the solution point, x^*, whenever the initial estimate, $x^{(0)}$, is sufficiently close to x^*. The following definition and theorem from [19] are the basis for achieving this objective.

Definition [19]: Let $G: D \subset R^n \rightarrow R^n$. Then x^* is a point of attraction of the iteration, $x^{(k+1)} = G(x^{(k)})$, $k = 0,1,\ldots$, if there is an open neighborhood S of x^* such that $S \subset D$ and, for any $x_0 \in S$, the iterates $\{x^{(k)}\}$ all lie in D and converge to x^*.

Ostrowski Theorem [19]: Suppose that $G: D \subset R^n \to R^n$ has a fixed point $x^* \in \text{int}(D)$ and is Frechet differentiable at x^*. If $\rho(G'(x^*)) < 1$ then x^* is a point of attraction of the iteration $x^{(k+1)} = G(x^{(k)})$. Where

(i) x^* is a fixed point of G if $x^* = G(x^*)$

(ii) G' is the Frechet derivative of G.

(iii) $\rho(A)$ is the magnitude of the largest eigenvalue of A (known as the spectral radius).

To establish the local convergence of equation 2.13, use the following:

Theorem 6.1: Suppose there is a point $x^* \in R^n$, such that $F(x^*) = \theta$, where $F: D \subset R^n \to R^m$ and $m > n$. Suppose also that in a neighborhood of x^* the function, F, has a continuous Frechet derivative, J_F, and J_F has full column rank. Then x^* is a point of attraction for the iteration

$$x^{(k+1)} = x^{(k)} - \left[J_F^T(x^{(k)})J_F(x^{(k)})\right]^{-1} J_F^T(x^{(k)})F(x^{(k)}) \qquad (6.2)$$

Proof: Define $G: D \subset R^n \to R^n$ as

$$G(x) = x - \left[J_F^T(x)J_F(x)\right]^{-1} J_F^T(x)F(x) \qquad (6.3)$$

Notice that x^* is a fixed point of G - i.e.

$$x^* = G(x^*) \qquad (6.4)$$

For convenience note that a left inverse of $J_F(x)$ denoted $[J_F(x)]^{-L}$ [14] has the form,

$$\left[J_F(x)\right]^{-L} = \left[J_F^T(x)J_F(x)\right]^{-1} J_F^T(x) \qquad (6.5)$$

and notice that

$$\left[J_F(x)\right]^{-L} J_F(x) = I \tag{6.6}$$

To apply the Ostrowski Theorem it is sufficient to prove that $G'(x^*) = \theta$ in which case the spectral radius is zero. Equivalently show that

$$\lim_{x-x^* \to \theta} \frac{1}{||x-x^*||_2} ||G(x) - G(x^*)||_2 = 0 \tag{6.7}$$

To prove equation 6.7 holds, evaluate the argument of the limit operation using equation 6.3 and note that $F(x^*) = \theta$. In particular

$$\frac{1}{||x-x^*||_2} ||G(x)-G(x^*)||_2 = \frac{1}{||x-x^*||_2} ||I(x-x^*) - \left[J_F(x)\right]^{-L} F(x)||_2 \tag{6.8}$$

Next use equation 6.6 and the fact that, $F(x) = F(x) - F(x^*)$ which produces

$$\frac{1}{||x-x^*||_2} ||G(x) - G(x^*)||_2 =$$

$$\frac{1}{||x-x^*||_2} \left|\left|\left[J_F(x)\right]^{-L} \left[J_F(x)(x-x^*) - \left[F(x) - F(x^*)\right]\right]\right|\right|_2 \tag{6.9}$$

and

$$\frac{1}{||x-x^*||_2} ||G(x) - G(x^*)||_2 \leq$$

$$\left|\left|\left[J_F(x)\right]^{-L}\right|\right| \left|\left|J_F(x)(x-x^*) - \left[F(x) - F(x^*)\right]\right|\right|_2 \tag{6.10}$$

where

$$\left|\left|\left[J_F(x)\right]^{-L}\right|\right| = \max_{||h||_2=1} \left|\left|J_F(x)^{-L}h\right|\right|_2 \qquad (6.11)$$

is the spectral norm of the matrix $J_F(x)^{-L}$. Add and subtract $J_F(x^*)(x-x^*)$ from the last term of equation 6.10 and use the triangle inequality to obtain:

$$\frac{1}{||x-x^*||_2} \left|\left|G(x) - G(x^*)\right|\right|_2 \leq$$

$$\left|\left|\left[J_F(x)\right]^{-L}\right|\right| \left\{\frac{1}{||x-x^*||_2} \left|\left|(J_F(x) - J_F(x^*))(x-x^*)\right|\right|_2 + \right.$$

$$\left. \frac{1}{||x-x^*||_2} \left|\left|J_F(x^*)(x-x^*) - (F(x)-F(x^*)\right|\right|_2 \right\} \qquad (6.12)$$

Since $J_F(x)$ is continuous

$$\lim_{x-x^* \to \theta} \frac{1}{||x-x^*||_2} \left|\left|[J_F(x) - J_F(x^*)](x-x^*)\right|\right|_2 = 0 \qquad (6.13)$$

and by definition of the Frechet derivative

$$\lim_{x-x^* \to \theta} \frac{1}{||x-x^*||_2} \left|\left|J_F(x^*)(x-x^*) - F(x) - F(x^*)\right|\right|_2 = 0 \qquad (6.14)$$

Hence $G'(x^*) = 0$.

Q.E.D.

This establishes the validity of the least squares solution for the Newton Raphson iteration.

This section concludes the theoretical development of the tableau approach to date. The next section will demonstrate the application of this theory to several examples.

7. Fault Diagnosis Examples

The purpose of this section is to illustrate the use of the fault diagnosis equations by applying them to several example problems. Each example includes its CCM characterization as well as nominal and actual parameter values. Currently no method exists in the context of the tableau approach for optimal test point selection. In each example the selection of test points took place via the trial and error procedure below:

(1) Model the circuit/system in terms of the CCM.

Note: This includes the use of frequency and impedance scaling. As in the simulation process the scaling enhances the numerical variations in the nominal values of the parameters from component to component. Such scaling is always possible and requires only that actual measurements undergo a reverse scaling before their entry into the solution program.

(2) Select candidate test outputs (usually functional outputs).

(3) Select a minimum set of test input/frequency combinations (via Theorem 4.1).

Note: All the examples presented here are single input circuits/systems. Selecting test input/frequency combinations amounts to selecting distinct test frequencies. In all cases $u(s_i)=1+j0$, $i=1,2,\ldots,q$.

(4) Test the rank of $J_F(x^0)$ (see Theorem 3.16) to determine if the circuit/system is diagnosable, where x^0 is the nominal parameter vector.

(5) If the diagnosability test fails, include an additional test input/frequency combination, if the test succeeds go to step 8.

(6) Repeat steps 4 and 5 until N input/frequency combinations are used (see Theorem 4.3).

(7) Select additional test outputs and return to step 3.

(8) Use the resulting test outputs and test input/frequency combinations to generate the tableau fault diagnosis equations (equation 2.2).

The solution of the resulting equations proceeds via a computer implementation of the Newton-Raphson iteration step with the nominal parameter values and corresponding ambiguity vectors ($\underline{\alpha}_i$, i=1,...,q) serving as the first estimate of the solution. This "diagnosis program", written in FORTRAN uses the subroutine LLSQF from IMSL[16] to determine the least squares solution to the Newton-Raphson iteration (equation 2.1). Sparse matrix techniques were not utilized. The program executed on a VAX 11/780 computer. Each example concludes with a summary of the performance of this solution algorithm. The next chapter introduces a modification to the solution algorithm which exploits the quadratic form of the tableau fault diagnosis equations and several of the examples presented here will also demonstrate the performance of the modified algorithm.

Example 7.1: The first example is based on the AC equivalent circuit of the single stage transistor amplifier in figure 9 selected from reference [6]. The component connection equations are shown below: (Note: The input voltage for the dependent source is defined differently than it was in [6] making Z(s,r) diagonal and changing one entry in L_{11}.)

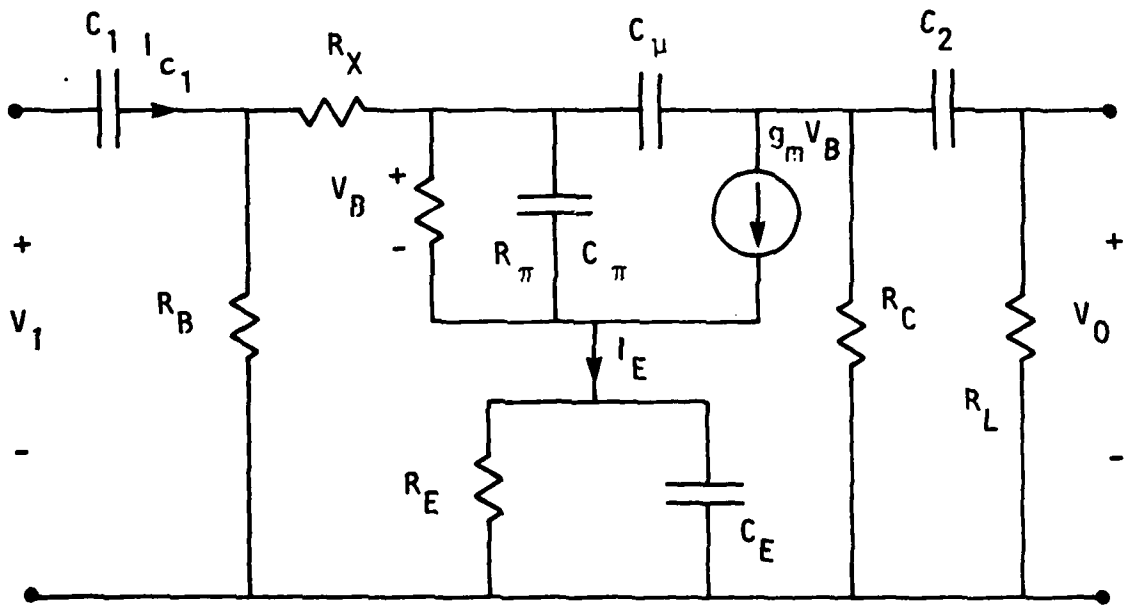

Figure 9. Amplifier model for example 7.1.

$$
\begin{bmatrix} V_{C_1} \\ V_{R_x} \\ V_{R_\pi} \\ V_{C_\mu} \\ V_{C_2} \\ I_{R_B} \\ I_{R_E} \\ I_{C_\pi} \\ I_{C_E} \\ I_{g_m} \\ I_{R_C} \\ I_{R_L} \end{bmatrix} = \begin{bmatrix} 1/sC_1 & R_x & & & & & & & & & & \\ & R_\pi & & & & & & & & & & \\ & & 1/sC_\mu & & & & & & & & & \\ & & & 1/sC_2 & & & & & & & & \\ & & & & 1/R_B & & & & & & & \\ & & & & & 1/R_E & & & & & & \\ & & & & & & sC_\pi & & & & & \\ & & & & & & & sC_E & & & & \\ & & & & & & & & g_m & & & \\ & & & & & & & & & 1/R_C & & \\ & & & & & & & & & & 1/R_L & \end{bmatrix} \begin{bmatrix} I_{C_1} \\ I_{R_x} \\ I_{R_\pi} \\ I_{C_\mu} \\ I_{C_2} \\ V_{R_B} \\ V_{R_E} \\ V_{C_\pi} \\ V_{C_E} \\ V_B \\ V_{R_C} \\ V_{R_L} \end{bmatrix} \tag{7.2}
$$

$$
\begin{bmatrix} I_{C_1} \\ I_{R_x} \\ I_{R_\pi} \\ I_{C_\mu} \\ I_{C_2} \\ V_{R_B} \\ V_{R_E} \\ V_{C_\pi} \\ V_{C_E} \\ V_{R_B} \\ V_{R_c} \\ V_{R_L} \\ V_0 \\ I_{C_1} \\ I_E \end{bmatrix} = \begin{bmatrix} 0 & 0 & 0 & 0 & 0 & 1 & 1 & 0 & 1 & 0 & 1 & 1 & 0 \\ 0 & 0 & 0 & 0 & 0 & 0 & 1 & 0 & 1 & 0 & 1 & 1 & 0 \\ 0 & 0 & 0 & 0 & 0 & 0 & 1 & -1 & 1 & -1 & 0 & 0 & 0 \\ 0 & 0 & 0 & 0 & 0 & 0 & 0 & 0 & 0 & 1 & 1 & 1 & 0 \\ 0 & 0 & 0 & 0 & 0 & 0 & 0 & 0 & 0 & 0 & 0 & 1 & 0 \\ -1 & 0 & 0 & 0 & 0 & 0 & 0 & 0 & 0 & 0 & 0 & 0 & 1 \\ -1 & -1 & -1 & 0 & 0 & 0 & 0 & 0 & 0 & 0 & 0 & 0 & 1 \\ 0 & 0 & 1 & 0 & 0 & 0 & 0 & 0 & 0 & 0 & 0 & 0 & 0 \\ -1 & -1 & -1 & 0 & 0 & 0 & 0 & 0 & 0 & 0 & 0 & 0 & 1 \\ 0 & 0 & 1 & 0 & 0 & 0 & 0 & 0 & 0 & 0 & 0 & 0 & 0 \\ -1 & -1 & 0 & -1 & 0 & 0 & 0 & 0 & 0 & 0 & 0 & 0 & 1 \\ -1 & -1 & 0 & -1 & -1 & 0 & 0 & 0 & 0 & 0 & 0 & 0 & 1 \\ -1 & -1 & 0 & -1 & -1 & 0 & 0 & 0 & 0 & 0 & 0 & 0 & 1 \\ 0 & 0 & 0 & 0 & 0 & 1 & 1 & 0 & 1 & 0 & 1 & 1 & 0 \\ 0 & 0 & 0 & 0 & 0 & 0 & 1 & 0 & 1 & 0 & 0 & 0 & 0 \end{bmatrix} \begin{bmatrix} V_{C_1} \\ V_{R_x} \\ V_{R_\pi} \\ V_{C_\mu} \\ V_{C_2} \\ I_{R_B} \\ I_{R_E} \\ I_{C_\pi} \\ I_{C_E} \\ I_{g_m} \\ I_{R_c} \\ I_{R_L} \\ V_I \\ \\ \end{bmatrix} \tag{7.3}
$$

The right inverse for L_{21} computed using the LINPACK [17] routine SSVDC is:

$$L_{21}^{-R} = \begin{bmatrix} -.25 & 0 & 0 \\ -.25 & 0 & 0 \\ 0 & 0 & 0 \\ -.25 & 0 & 0 \\ -.25 & 0 & 0 \\ 0 & .333 & -.333 \\ 0 & 0 & .5 \\ 0 & 0 & 0 \\ 0 & 0 & .5 \\ 0 & 0 & 0 \\ 0 & .333 & -.333 \\ 0 & .333 & -.333 \end{bmatrix} \qquad (7.4)$$

A basis for the null space of L_{21} in matrix form is:

$$V = \begin{bmatrix} 1 & 1 & 0 & 0 & 0 & 0 & 0 & 0 & 0 \\ -1 & 0 & 0 & 0 & 0 & 0 & 0 & 0 & 0 \\ 0 & 0 & 1 & 0 & 0 & 0 & 0 & 0 & 0 \\ 0 & -1 & 0 & 1 & 0 & 0 & 0 & 0 & 0 \\ 0 & 0 & 0 & -1 & 0 & 0 & 0 & 0 & 0 \\ 0 & 0 & 0 & 0 & 0 & 0 & 0 & 0 & 1 \\ 0 & 0 & 0 & 0 & 0 & 1 & 0 & 0 & 0 \\ 0 & 0 & 0 & 0 & 1 & 0 & 0 & 0 & 0 \\ 0 & 0 & 0 & 0 & 0 & -1 & 0 & 0 & 0 \\ 0 & 0 & 0 & 0 & 0 & 0 & 1 & 0 & 0 \\ 0 & 0 & 0 & 0 & 0 & 0 & 0 & 1 & -1 \\ 0 & 0 & 0 & 0 & 0 & 0 & 0 & -1 & 0 \end{bmatrix} \qquad (7.5)$$

For this circuit M=N=12 , p=9 and q=2. All parameters have nominal values of unity. For test frequencies $s_1 = j1.4$ and $s_2 = j2$ the nominal values for the ambiguity vectors, $\underline{\alpha}_1$ and $\underline{\alpha}_2$, are:

$$\underline{a}_1 = \begin{bmatrix} .72545E-01 \\ .26209E+00 \\ .92251E-01 \\ .18192E+00 \\ -.39387E-01 \\ .64166E-01 \\ .92251E-01 \\ .16710E+00 \\ .26166E+00 \end{bmatrix} + j \begin{bmatrix} -.42669E+00 \\ .28641E-01 \\ .28133E-01 \\ -.38153E-01 \\ .12915E+00 \\ -.98703E-01 \\ .28133E-01 \\ .11155E+00 \\ .21033E+00 \end{bmatrix} \tag{7.6a}$$

$$\underline{a}_2 = \begin{bmatrix} -.86316E-01 \\ .29425E+00 \\ .10092E+00 \\ .17635E+00 \\ -.21282E-01 \\ .35081E-01 \\ .10092E+00 \\ .19156E+00 \\ .31972E+00 \end{bmatrix} + j \begin{bmatrix} -.48784E+00 \\ .80346E-01 \\ .10641E-01 \\ -.11167E-01 \\ .20184E+00 \\ -.13916E+00 \\ .10641E-01 \\ .97295E-01 \\ .21512E+00 \end{bmatrix} \tag{7.6b}$$

Next the parameter vector r was changed to:

$$r = (2. \quad 1.2 \quad .9 \quad .9 \quad 1.1 \quad .8 \quad 1. \quad 1.1 \quad 2. \quad .9 \quad 1.2 \quad 1.1)^t \tag{7.7}$$

The small variations from unity represent normal production variations for "good" components while the larger variations for the first and ninth components represent failures. This perturbed parameter vector r (representing an actual circuit under test) was used to compute the following test outputs:

$$y^M(s_1) = \begin{bmatrix} -.18299E-01 \\ .24554E+00 \\ .73848E-01 \end{bmatrix} + j \begin{bmatrix} .44648E-01 \\ .55346E+00 \\ .15117E+00 \end{bmatrix} \tag{7.8a}$$

$$y^M(s_2) = \begin{bmatrix} .62142E\text{-}02 \\ .41992E{+}00 \\ .10101E{+}00 \end{bmatrix} + j \begin{bmatrix} .67445E\text{-}01 \\ .68044E{+}00 \\ .19389E{+}00 \end{bmatrix} \qquad (7.8b)$$

These test outputs and the nominal data were the input to the diagnosis program for determination of the actual parameter values. The program used twelve Newton-Raphson iterations and 31.5 seconds on the VAX 11/780 to compute the estimates of the circuit parameters, all within .11% of the actual values.

Example 7.9: This example consists of the op-amp circuit shown in Figure 10. The op-amp/feedback resistor combination forms a "voltage-follower" which is extremely insensitive to changes in the actual value of the feedback resistor. Intuitively, the individual diagnosis of this resistor's value will be numerically unstable. It is therefore reasonable to combine the op-amp and feedback resistor as a single component for the purposes of fault diagnosis and model them as a voltage controlled voltage source. The resulting circuit with parameters scaled, appears in Figure 11. The test points for this example are a result of the trial and error process discussed at the beginning of the section. The CCM equations as well as L_{21}^{-R} and V are given below:

$$\begin{bmatrix} b_1 \\ b_2 \\ b_3 \\ b_4 \\ b_5 \end{bmatrix} = \begin{bmatrix} r_1 & & & & \\ & r_2 s & & 0 & \\ & & r_3 & & \\ & 0 & & r_4/s & \\ & & & & r_5 \end{bmatrix} \begin{bmatrix} a_1 \\ a_2 \\ a_3 \\ a_4 \\ a_5 \end{bmatrix} \qquad (7.10)$$

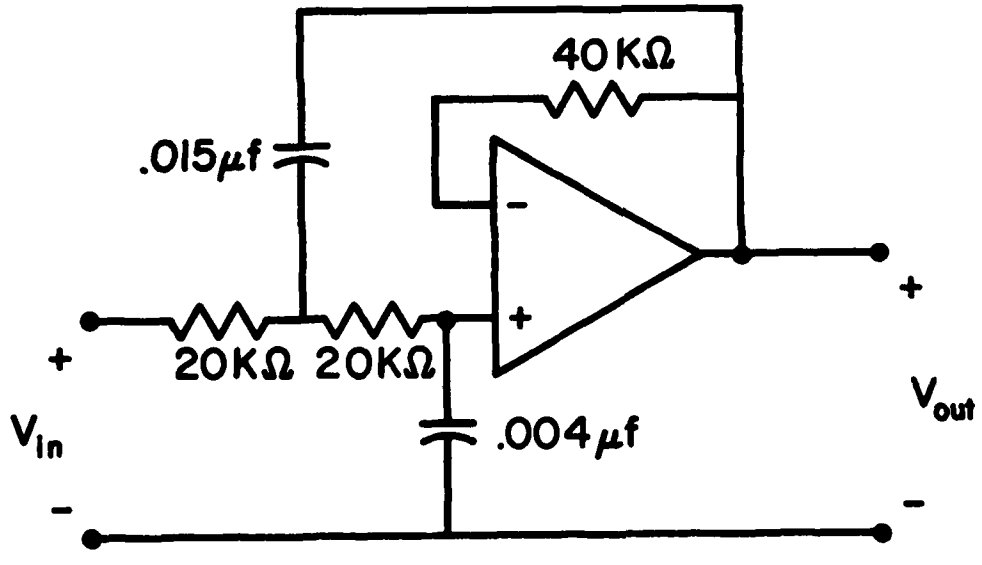

Figure 10. Op-amp circuit for example 7.9.

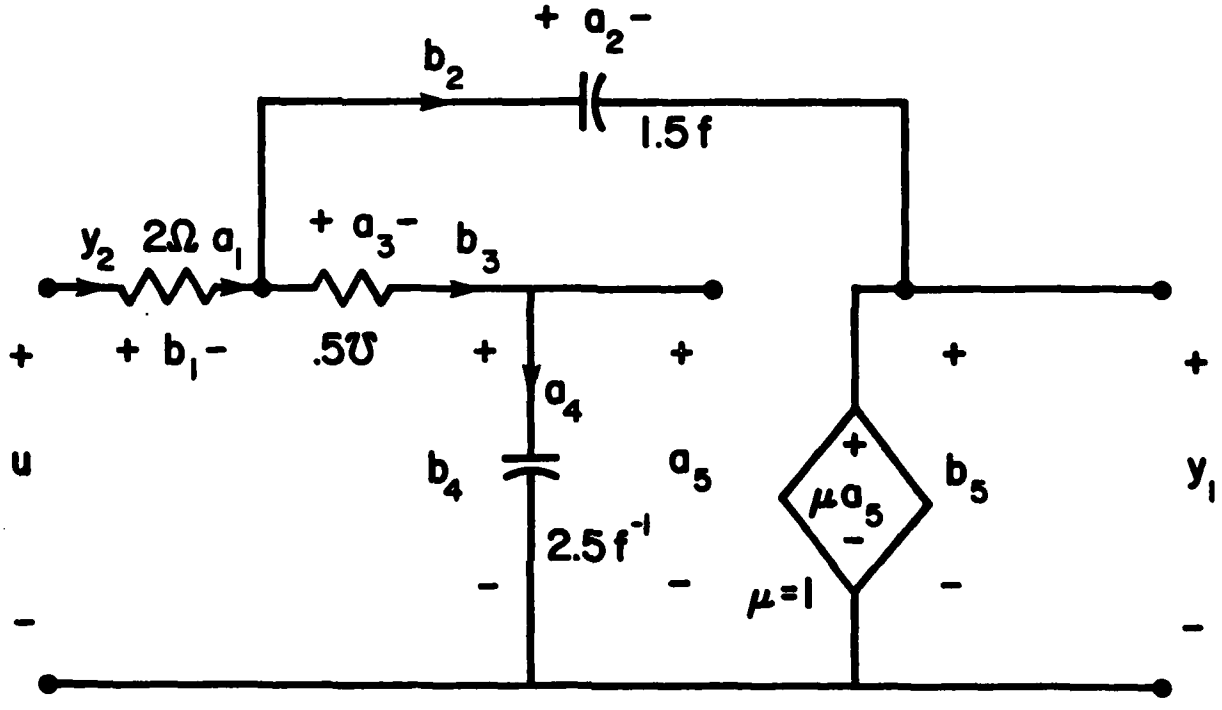

Figure 11. Model of op-amp circuit for example 7.9.

$$\begin{bmatrix} a_1 \\ a_2 \\ a_3 \\ a_4 \\ a_5 \\ y_1 \\ y_2 \end{bmatrix} = \begin{bmatrix} 0 & 1 & 1 & 0 & 0 \\ -1 & 0 & 0 & 0 & -1 \\ -1 & 0 & 0 & -1 & 0 \\ 0 & 0 & 1 & 0 & 0 \\ 0 & 0 & 0 & 1 & 1 \\ 0 & 0 & 0 & 0 & 1 \\ 0 & 1 & 1 & 0 & 0 \end{bmatrix} \begin{bmatrix} b_1 \\ b_2 \\ b_3 \\ b_4 \\ b_5 \end{bmatrix} + \begin{bmatrix} 0 \\ 1 \\ 1 \\ 0 \\ 0 \\ 0 \\ 0 \end{bmatrix} u \qquad (7.11)$$

$$L_{21}^{-R} = \begin{bmatrix} 0 & 0 \\ 0 & .5 \\ 0 & .5 \\ 0 & 0 \\ 1 & 0 \end{bmatrix} \qquad (7.12)$$

$$V = \begin{bmatrix} 1 & 0 & 0 \\ 0 & -1 & 0 \\ 0 & -1 & 0 \\ 0 & 0 & 1 \\ 0 & 0 & 0 \end{bmatrix} \qquad (7.13)$$

For this example M=N=5, p=3 and q=2. The test frequencies are $s_1 = j\ .5$ and $s_2 = j\ 1.5$. As in the previous example the parameter vector, r^*, used to compute test outputs was a perturbation of the nominal, r_o. The values used for r^* and r_o are

$$r_o = (1 \quad 1.5 \quad .5 \quad 2.5 \quad 1)^t \qquad (7.14)$$

$$r^* = (2.2 \quad .75 \quad .90 \quad 2.2 \quad 1)^t \tag{7.15}$$

The nominal values for the ambiguity vectors are:

$$\underline{a}_1 = \begin{bmatrix} -.10588E+00 \\ -.19412E+00 \\ .82353E+00 \end{bmatrix} + j \begin{bmatrix} .37647E+00 \\ .23529E-01 \\ -.70588E+00 \end{bmatrix} \tag{7.16a}$$

$$\underline{a}_2 = \begin{bmatrix} .92496E+00 \\ .28630E+00 \\ -.27732E+00 \end{bmatrix} + j \begin{bmatrix} .62643E+00 \\ .47961E+00 \\ -.29364E+00 \end{bmatrix} \tag{7.16b}$$

The measurements corresponding to actual parameter values are:

$$y^M(s_1) = \begin{bmatrix} .66358E+00 \\ .80518E-01 \end{bmatrix} + j \begin{bmatrix} -.63077E+00 \\ .21054E+00 \end{bmatrix} \tag{7.17a}$$

$$y^M(s_2) = \begin{bmatrix} -.14926E+00 \\ .38978E+00 \end{bmatrix} + j \begin{bmatrix} -.38510E+00 \\ .22644E+00 \end{bmatrix} \tag{7.17b}$$

The Jacobian for this problem has dimension 20 x 17 and therefore the solution algorithm requires the use of the modified Newton-Raphson iteration discussed at the beginning of this chapter. This is accomplished by the IMSL[16] routine LLSQF. The diagnosis program required five iterations and 1.73 seconds on the VAX 11/780 to find r^* to .1% accuracy.

Example 7.18: Suppose the circuit of Example 7.9 is cascaded to form the multistage filter shown in Figure 12. Diagnosis of this circuit required test points between stages of the amplifiers. The reason is that the individual stages are isolated so that using output measurements only, the

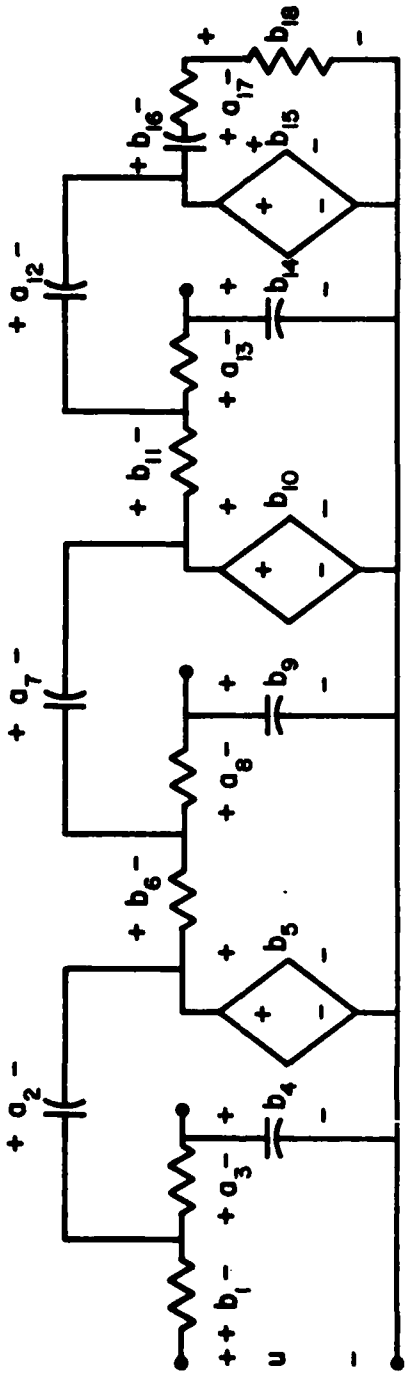

Figure 12. Multistage filter for example 7.18.

changes in a component in one stage are indistinguishable from similar changes in the corresponding component in another stage. The CCM equations, L_{21}^{-R}, and V for the circuit of Figure 12 are given below. They present an excellent example of the sparseness typical of the matrices of the CCM.

$$a(s) = \begin{bmatrix}
0 & 1 & 1 & 0 & 0 & 0 & 0 & 0 & 0 & 0 & 0 & 0 & 0 & 0 & 0 & 0 & 0 & 0 \\
-1 & 0 & 0 & 0 & -1 & 0 & 0 & 0 & 0 & 0 & 0 & 0 & 0 & 0 & 0 & 0 & 0 & 0 \\
-1 & 0 & 0 & -1 & 0 & 0 & 0 & 0 & 0 & 0 & 0 & 0 & 0 & 0 & 0 & 0 & 0 & 0 \\
0 & 0 & 1 & 0 & 0 & 0 & 0 & 0 & 0 & 0 & 0 & 0 & 0 & 0 & 0 & 0 & 0 & 0 \\
0 & 0 & 0 & 1 & 0 & 0 & 0 & 0 & 0 & 0 & 0 & 0 & 0 & 0 & 0 & 0 & 0 & 0 \\
0 & 0 & 0 & 0 & 0 & 0 & 1 & 1 & 0 & 0 & 0 & 0 & 0 & 0 & 0 & 0 & 0 & 0 \\
0 & 0 & 0 & 0 & 1 & -1 & 0 & 0 & 0 & -1 & 0 & 0 & 0 & 0 & 0 & 0 & 0 & 0 \\
0 & 0 & 0 & 0 & 1 & -1 & 0 & 0 & -1 & 0 & 0 & 0 & 0 & 0 & 0 & 0 & 0 & 0 \\
0 & 0 & 0 & 0 & 0 & 0 & 0 & 1 & 0 & 0 & 0 & 0 & 0 & 0 & 0 & 0 & 0 & 0 \\
0 & 0 & 0 & 0 & 0 & 0 & 0 & 0 & 1 & 0 & 0 & 0 & 0 & 0 & 0 & 0 & 0 & 0 \\
0 & 0 & 0 & 0 & 0 & 0 & 0 & 0 & 0 & 0 & 0 & 1 & 1 & 0 & 0 & 0 & 0 & 0 \\
0 & 0 & 0 & 0 & 0 & 0 & 0 & 0 & 0 & 1 & -1 & 0 & 0 & 0 & -1 & 0 & 0 & 0 \\
0 & 0 & 0 & 0 & 0 & 0 & 0 & 0 & 0 & 1 & -1 & 0 & 0 & -1 & 0 & 0 & 0 & 0 \\
0 & 0 & 0 & 0 & 0 & 0 & 0 & 0 & 0 & 0 & 0 & 0 & 1 & 0 & 0 & 0 & 0 & 0 \\
0 & 0 & 0 & 0 & 0 & 0 & 0 & 0 & 0 & 0 & 0 & 0 & 0 & 1 & 0 & 0 & 0 & 0 \\
0 & 0 & 0 & 0 & 0 & 0 & 0 & 0 & 0 & 0 & 0 & 0 & 0 & 0 & 0 & 1 & 0 & 0 \\
0 & 0 & 0 & 0 & 0 & 0 & 0 & 0 & 0 & 0 & 0 & 0 & 0 & 0 & 1 & 0 & 1 & 0 \\
0 & 0 & 0 & 0 & 0 & 0 & 0 & 0 & 0 & 0 & 0 & 0 & 0 & 0 & 0 & 1 & 0 & 1
\end{bmatrix} b(s) + \begin{bmatrix} 0 \\ 1 \\ 1 \\ 0 \\ 0 \\ 0 \\ 0 \\ 0 \\ 0 \\ 0 \\ 0 \\ 0 \\ 0 \\ 0 \\ 0 \\ 0 \\ 0 \\ 0 \end{bmatrix} u(s)$$

(7.19)

$$y(s) = \begin{bmatrix}
0 & 1 & 1 & 0 & 0 & 0 & 0 & 0 & 0 & 0 & 0 & 0 & 0 & 0 & 0 & 0 & 0 & 0 \\
0 & 0 & 0 & 0 & 1 & 0 & 0 & 0 & 0 & 0 & 0 & 0 & 0 & 0 & 0 & 0 & 0 & 0 \\
0 & 0 & 0 & 0 & 0 & 0 & 1 & 1 & 0 & 0 & 0 & 0 & 0 & 0 & 0 & 0 & 0 & 0 \\
0 & 0 & 0 & 0 & 0 & 0 & 0 & 0 & 0 & 1 & 0 & 0 & 0 & 0 & 0 & 0 & 0 & 0 \\
0 & 0 & 0 & 0 & 0 & 0 & 0 & 0 & 0 & 0 & 0 & 1 & 1 & 0 & 0 & 0 & 0 & 0 \\
0 & 0 & 0 & 0 & 0 & 0 & 0 & 0 & 0 & 0 & 0 & 0 & 0 & 0 & 1 & 0 & 0 & 0 \\
0 & 0 & 0 & 0 & 0 & 0 & 0 & 0 & 0 & 0 & 0 & 0 & 0 & 0 & 0 & 0 & 1 & 0 \\
0 & 0 & 0 & 0 & 0 & 0 & 0 & 0 & 0 & 0 & 0 & 0 & 0 & 0 & 0 & 0 & 0 & 1
\end{bmatrix} b(s) + \begin{bmatrix} 0 \\ 0 \\ 0 \\ 0 \\ 0 \\ 0 \\ 0 \\ 0 \end{bmatrix} u(s)$$

(7.20)

AD-A117 568 PURDUE UNIV LAFAYETTE IN SCHOOL OF ELECTRICAL ENGINEERING F/G 9/5
FAULT DIAGNOSIS OF NONLINEAR ANALOG CIRCUITS. VOLUME II. A MULT--ETC(U)
JUL 82 L RAPISARADA, R DECARLO N00014-81-K-0323
UNCLASSIFIED TR-EE-82-22 NL

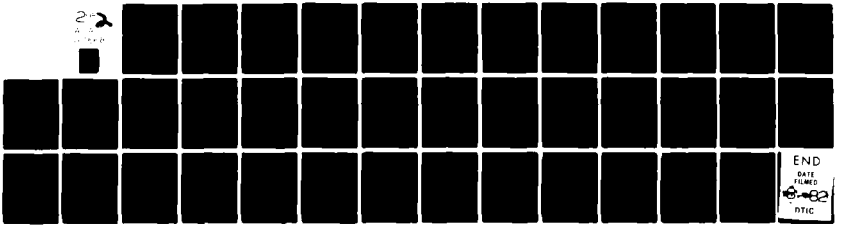

END
DATE FILMED
8-82
DTIC

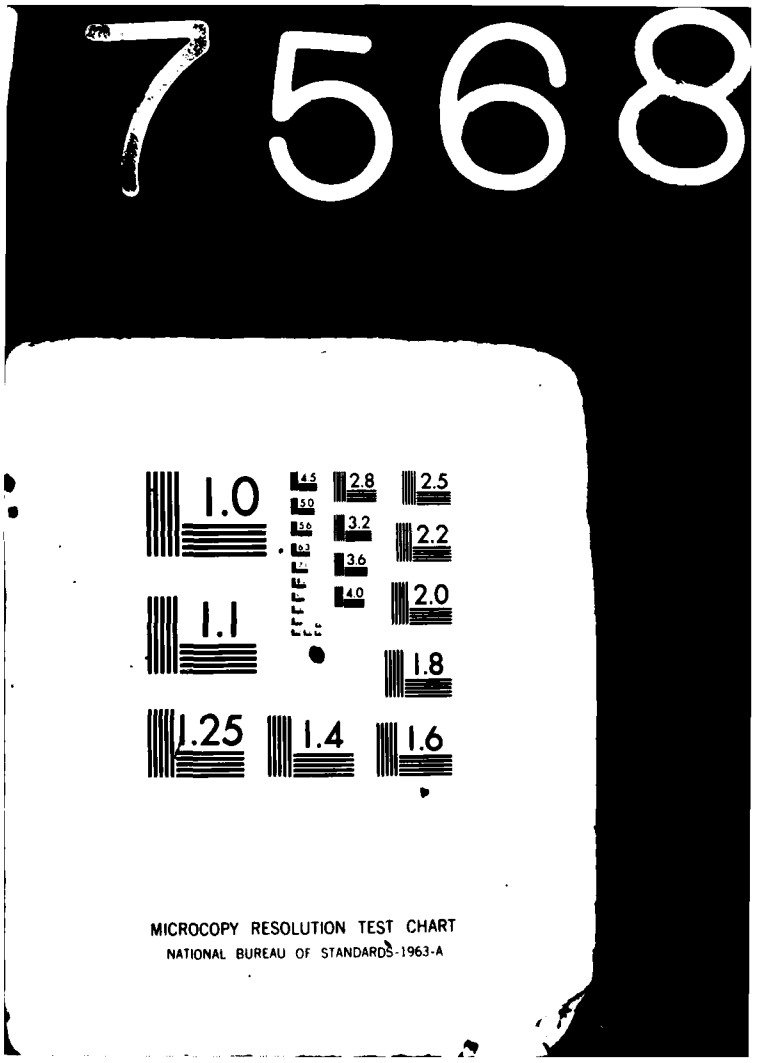
7568
1.0
1.1
1.25
1.4
1.6
1.8
2.0
2.2
2.5
2.8
3.2
3.6
4.0
4.5
5.0
5.6
6.3
MICROCOPY RESOLUTION TEST CHART
NATIONAL BUREAU OF STANDARDS-1963-A

$$b(s) = \begin{bmatrix} r_1 & & & & & & & & & & & & & & & & & \\ & r_2 s & & & & & & & & & & & & & & & & \\ & & r_3 & & & & & & & & & & & & & & & \\ & & & r_4/s & & & & & & & & & & & & & & \\ & & & & r_5 & & & & & & & & & & & & & \\ & & & & & r_6 & & & & & & & & & & & & \\ & & & & & & r_7 s & & & & & & & & & & & \\ & & & & & & & r_8 & & & & & & & & & & \\ & & & & & & & & r_9/s & & & & & & & & & \\ & & & & & & & & & r_{10} & & & & & & & & \\ & & & & & & & & & & r_{11} & & & & & & & \\ & & & & & & & & & & & r_{12} s & & & & & & \\ & & & & & & & & & & & & r_{13} & & & & & \\ & & & & & & & & & & & & & r_{14}/s & & & & \\ & & & & & & & & & & & & & & r_{15} & & & \\ & & & & & & & & & & & & & & & r_{16}/s & & \\ & & & & & & & & & & & & & & & & r_{17} & \\ & & & & & & & & & & & & & & & & & r_{18} \end{bmatrix} a(s)$$

(7.21)

$$L_{21}^{-R} = \begin{bmatrix} 0 & 0 & 0 & 0 & 0 & 0 & 0 & 0 \\ .5 & 0 & 0 & 0 & 0 & 0 & 0 & 0 \\ .5 & 0 & 0 & 0 & 0 & 0 & 0 & 0 \\ 0 & 0 & 0 & 0 & 0 & 0 & 0 & 0 \\ 0 & 1 & 0 & 0 & 0 & 0 & 0 & 0 \\ 0 & 0 & 0 & 0 & 0 & 0 & 0 & 0 \\ 0 & 0 & .5 & 0 & 0 & 0 & 0 & 0 \\ 0 & 0 & .5 & 0 & 0 & 0 & 0 & 0 \\ 0 & 0 & 0 & 0 & 0 & 0 & 0 & 0 \\ 0 & 0 & 0 & 1 & 0 & 0 & 0 & 0 \\ 0 & 0 & 0 & 0 & 0 & 0 & 0 & 0 \\ 0 & 0 & 0 & 0 & .5 & 0 & 0 & 0 \\ 0 & 0 & 0 & 0 & .5 & 0 & 0 & 0 \\ 0 & 0 & 0 & 0 & 0 & 0 & 0 & 0 \\ 0 & 0 & 0 & 0 & 0 & 1 & 0 & 0 \\ 0 & 0 & 0 & 0 & 0 & 0 & 0 & 0 \\ 0 & 0 & 0 & 0 & 0 & 0 & 1 & 0 \\ 0 & 0 & 0 & 0 & 0 & 0 & 0 & 1 \end{bmatrix}$$

(7.22)

$$V = \begin{bmatrix} 1 & 0 & 0 & 0 & 0 & 0 & 0 & 0 & 0 & 0 \\ 0 & 1 & 0 & 0 & 0 & 0 & 0 & 0 & 0 & 0 \\ 0 & -1 & 0 & 0 & 0 & 0 & 0 & 0 & 0 & 0 \\ 0 & 0 & 1 & 0 & 0 & 0 & 0 & 0 & 0 & 0 \\ 0 & 0 & 0 & 0 & 0 & 0 & 0 & 0 & 0 & 0 \\ 0 & 0 & 0 & 1 & 0 & 0 & 0 & 0 & 0 & 0 \\ 0 & 0 & 0 & 0 & 1 & 0 & 0 & 0 & 0 & 0 \\ 0 & 0 & 0 & 0 & -1 & 0 & 0 & 0 & 0 & 0 \\ 0 & 0 & 0 & 0 & 0 & 1 & 0 & 0 & 0 & 0 \\ 0 & 0 & 0 & 0 & 0 & 0 & 0 & 0 & 0 & 0 \\ 0 & 0 & 0 & 0 & 0 & 0 & 1 & 0 & 0 & 0 \\ 0 & 0 & 0 & 0 & 0 & 0 & 0 & 1 & 0 & 0 \\ 0 & 0 & 0 & 0 & 0 & 0 & 0 & -1 & 0 & 0 \\ 0 & 0 & 0 & 0 & 0 & 0 & 0 & 0 & 1 & 0 \\ 0 & 0 & 0 & 0 & 0 & 0 & 0 & 0 & 0 & 0 \\ 0 & 0 & 0 & 0 & 0 & 0 & 0 & 0 & 0 & 1 \\ 0 & 0 & 0 & 0 & 0 & 0 & 0 & 0 & 0 & 0 \\ 0 & 0 & 0 & 0 & 0 & 0 & 0 & 0 & 0 & 0 \end{bmatrix} \tag{7.23}$$

For this example test frequencies are $s_1 = j1$ and $s_2 = j2$. The nominal and solution parameter vectors are:

$$r_0 = (2.\ 1.5\ .5\ 2.5\ 1.\ 2.\ 1.5\ .5\ 2.5\ 1.\ 2.\ 1.5\ .5\ 2.5\ 1.\ .7\ 1.\ 2.)^t \tag{7.24}$$

$$r^* = (2.1\ 1.4\ .5\ 2.5\ 1.\ 1.4\ 1.\ .5\ 2.4\ 1.\ 1.8\ 1.6\ .45\ 2.6\ 1.\ .8\ 1.2\ 1.8)^t \tag{7.25}$$

The nominal values for the ambiguity vectors are:

$$\underline{a}_1 = \begin{bmatrix} .10265E+01 \\ .11504E+00 \\ -.30973E+00 \\ -.10494E+00 \\ .61477E-01 \\ -.29368E-01 \\ -.16210E+00 \\ -.63535E-01 \\ .86718E-01 \\ -.82515E-02 \end{bmatrix} + j \begin{bmatrix} .60177E+00 \\ .27434E+00 \\ -.35398E+00 \\ -.54977E+00 \\ -.12570E+00 \\ .21928E+00 \\ .20743E+00 \\ .17170E-01 \\ -.57523E-01 \\ -.22160E-01 \end{bmatrix} \qquad (7.26a)$$

$$\underline{a}_2 = \begin{bmatrix} .10413E+01 \\ .22993E+00 \\ -.10214E+00 \\ -.98704E-01 \\ -.18465E-01 \\ .89878E-02 \\ .77955E-02 \\ .10413E-02 \\ -.62294E-03 \\ -.13895E-03 \end{bmatrix} + j \begin{bmatrix} .20143E+00 \\ .13207E+00 \\ -.38005E-01 \\ -.60149E-01 \\ -.22227E-01 \\ .77634E-02 \\ .98947E-02 \\ .29720E-02 \\ -.11345E-02 \\ .56466E-04 \end{bmatrix} \qquad (7.26b)$$

The measured outputs corresponding to the actual parameter values are:

$$y^M(s_1) = \begin{bmatrix} .48041E+00 \\ -.29928E+00 \\ .90992E-01 \\ -.22825E+00 \\ -.21237E+00 \\ .15498E+00 \\ .53761E-01 \\ .96770E-01 \end{bmatrix} + j \begin{bmatrix} .28688E+00 \\ -.36303E+00 \\ -.29353E+00 \\ .23811E+00 \\ .58070E-01 \\ .11242E-02 \\ .16759E-01 \\ .30167E-01 \end{bmatrix} \qquad (7.27a)$$

$$y^M(s_2) = \begin{bmatrix} .49466E+00 \\ -.10323E+00 \\ -.58126E-01 \\ .12314E-01 \\ .47561E-02 \\ -.51815E-03 \\ -.51469E-04 \\ -.92643E-04 \end{bmatrix} + j \begin{bmatrix} .97823E-01 \\ -.40269E-01 \\ -.58063E-01 \\ .20497E-01 \\ .13267E-01 \\ -.24983E-02 \\ -.95655E-03 \\ -.17218E-02 \end{bmatrix} \qquad (7.27b)$$

The diagnosis program determined all components of r^* to .02% accuracy. This required six iterations and 31.2 seconds on the VAX 11/780.

Example 7.18 illustrates the fact that it may be extremely costly in terms of test points (8 required by that example) to determine the value of every individual component. In many instances individual components will be part of a functional block which is replaceable as a unit. In this situation it is merely necessary to determine if the functional block is operating properly. The next two examples illustrate this type of tradeoff.

Example 7.28: Figure 13 depicts a twelve component system. Suppose y_1 is a functional output which makes it a natural choice as a test output as well. From the trial and error procedure described at the beginning of the section one finds that the identification of all the parameter values requires four additional test points, y_2 through y_5. The CCM equations, L_{21}^{-R} and V below reflect this choice of test points:

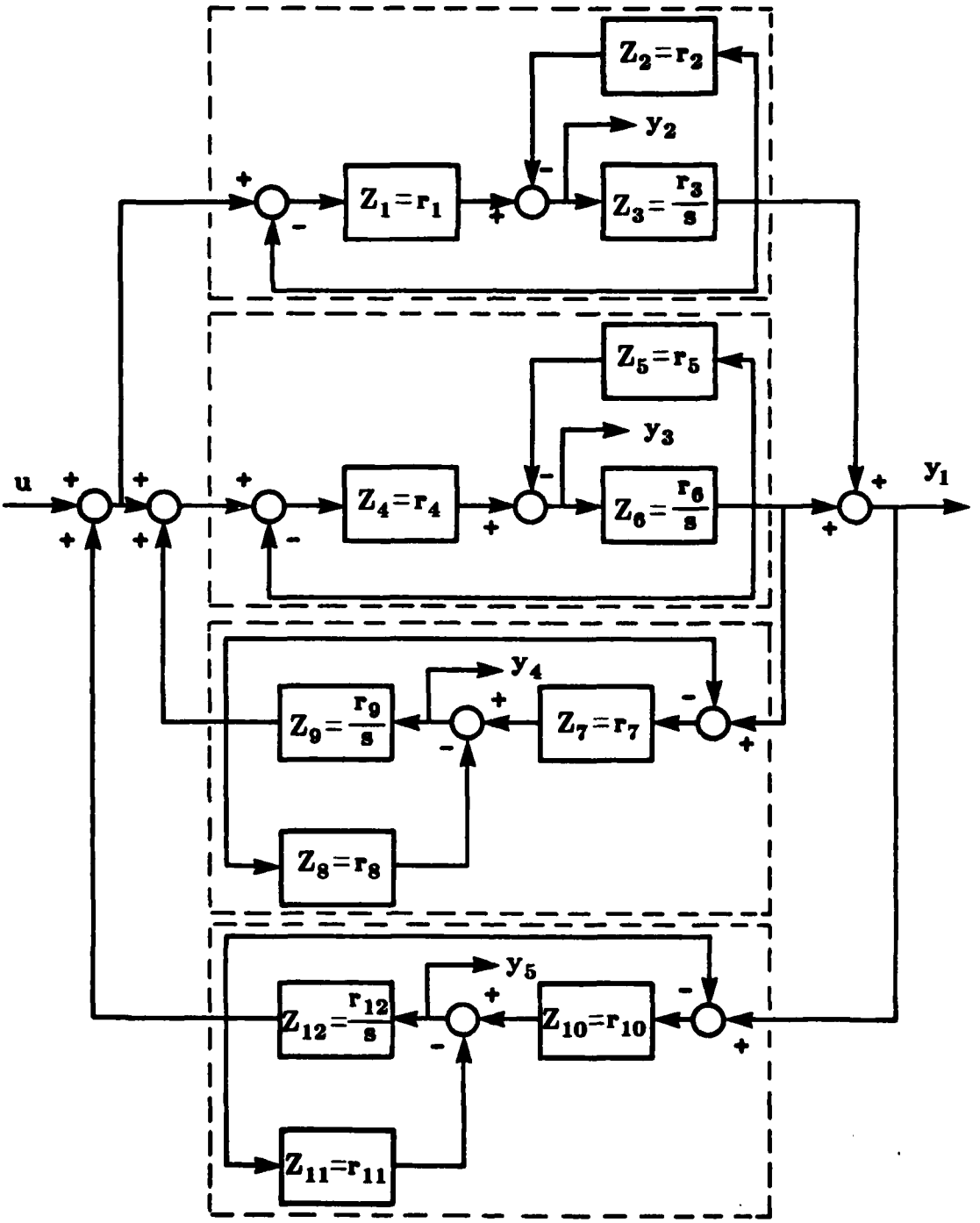

Figure 13. System for example 7.28.

$$a(s) = \begin{bmatrix} 0 & 0 & -1 & 0 & 0 & 0 & 0 & 0 & 0 & 0 & 0 & 1 \\ 0 & 0 & 1 & 0 & 0 & 0 & 0 & 0 & 0 & 0 & 0 & 0 \\ 1 & -1 & 0 & 0 & 0 & 0 & 0 & 0 & 0 & 0 & 0 & 0 \\ 0 & 0 & 0 & 0 & 0 & -1 & 0 & 0 & 1 & 0 & 0 & 1 \\ 0 & 0 & 0 & 0 & 0 & 1 & 0 & 0 & 0 & 0 & 0 & 0 \\ 0 & 0 & 0 & 1 & -1 & 0 & 0 & 0 & 0 & 0 & 0 & 0 \\ 0 & 0 & 0 & 0 & 0 & 1 & 0 & 0 & -1 & 0 & 0 & 0 \\ 0 & 0 & 0 & 0 & 0 & 0 & 0 & 0 & 1 & 0 & 0 & 0 \\ 0 & 0 & 0 & 0 & 0 & 0 & 1 & -1 & 0 & 0 & 0 & 0 \\ 0 & 0 & 1 & 0 & 0 & 1 & 0 & 0 & 0 & 0 & 0 & -1 \\ 0 & 0 & 0 & 0 & 0 & 0 & 0 & 0 & 0 & 0 & 0 & 1 \\ 0 & 0 & 0 & 0 & 0 & 0 & 0 & 0 & 0 & 1 & -1 & 0 \end{bmatrix} b(s) + \begin{bmatrix} 1 \\ 0 \\ 0 \\ 1 \\ 0 \\ 0 \\ 0 \\ 0 \\ 0 \\ 0 \\ 0 \\ 0 \end{bmatrix} u(s) \tag{7.29}$$

$$y(s) = \begin{bmatrix} 0 & 0 & 1 & 0 & 0 & 1 & 0 & 0 & 0 & 0 & 0 & 0 \\ 1 & -1 & 0 & 0 & 0 & 0 & 0 & 0 & 0 & 0 & 0 & 0 \\ 0 & 0 & 0 & 1 & -1 & 0 & 0 & 0 & 0 & 0 & 0 & 0 \\ 0 & 0 & 0 & 0 & 0 & 0 & 1 & -1 & 0 & 0 & 0 & 0 \\ 0 & 0 & 0 & 0 & 0 & 0 & 0 & 0 & 0 & 1 & -1 & 0 \end{bmatrix} b(s) + \begin{bmatrix} 0 \\ 0 \\ 0 \\ 0 \\ 0 \end{bmatrix} u(s) \tag{7.30}$$

$$b(s) = \begin{bmatrix} r_1 & & & & & & & & & & & \\ & r_2 & & & & & & & & & & \\ & & r_3/s & & & & & & & & & \\ & & & r_4 & & & & & & & & \\ & & & & r_5 & & & & & & & \\ & & & & & r_6/s & & & & & & \\ & & & & & & r_7 & & & & & \\ & & & & & & & r_8 & & & & \\ & & & & & & & & r_9/s & & & \\ & & & & & & & & & r_{10} & & \\ & & & & & & & & & & r_{11} & \\ & & & & & & & & & & & r_{12}/s \end{bmatrix} a(s) \tag{7.31}$$

$$L_{21}^{-R} = \begin{bmatrix} 0 & .5 & 0 & 0 & 0 \\ 0 & -.5 & 0 & 0 & 0 \\ .5 & 0 & 0 & 0 & 0 \\ 0 & 0 & .5 & 0 & 0 \\ 0 & 0 & -.5 & 0 & 0 \\ .5 & 0 & 0 & 0 & 0 \\ 0 & 0 & 0 & .5 & 0 \\ 0 & 0 & 0 & -.5 & 0 \\ 0 & 0 & 0 & 0 & 0 \\ 0 & 0 & 0 & 0 & .5 \\ 0 & 0 & 0 & 0 & -.5 \\ 0 & 0 & 0 & 0 & 0 \end{bmatrix} \tag{7.32}$$

$$V = \begin{bmatrix} 1 & 0 & 0 & 0 & 0 & 0 & 0 \\ 1 & 0 & 0 & 0 & 0 & 0 & 0 \\ 0 & 0 & 0 & 0 & 0 & 1 & 0 \\ 0 & 1 & 0 & 0 & 0 & 0 & 0 \\ 0 & 1 & 0 & 0 & 0 & 0 & 0 \\ 0 & 0 & 0 & 0 & 0 & -1 & 0 \\ 0 & 0 & 1 & 0 & 0 & 0 & 0 \\ 0 & 0 & 1 & 0 & 0 & 0 & 0 \\ 0 & 0 & 0 & 0 & 1 & 0 & 0 \\ 0 & 0 & 0 & 1 & 0 & 0 & 0 \\ 0 & 0 & 0 & 1 & 0 & 0 & 0 \\ 0 & 0 & 0 & 0 & 0 & 0 & 1 \end{bmatrix} \tag{7.33}$$

Let the nominal and actual parameter vectors, r_o and r^* respectively, be the following:

$$r_o = (1 \quad 0 \quad 1.25 \quad 2 \quad -1 \quad .67 \quad .9 \quad .1 \quad 2 \quad 1.1 \quad -.1 \quad 1)^t \tag{7.34}$$

$$r^* = (.9 \quad .1 \quad 1.11 \quad 1.8 \quad -.8 \quad .71 \quad 1 \quad 0 \quad 1.33 \quad 1.05 \quad -.05 \quad 1.05)^t \tag{7.35}$$

The nominal values for the ambiguity vectors are:

$$\underline{a}_1 = \begin{bmatrix} .16508E+00 \\ .60717E+00 \\ -.52401E-02 \\ .20590E+00 \\ -.37403E+00 \\ .23949E+00 \\ -.53498E+00 \end{bmatrix} + j \begin{bmatrix} .53947E-01 \\ .92653E-01 \\ -.10637E+00 \\ -.23701E+00 \\ -.12865E+00 \\ -.30979E-01 \\ -.30480E+00 \end{bmatrix} \tag{7.36a}$$

$$\underline{a}_2 = \begin{bmatrix} .28803E+00 \\ .61570E+00 \\ .42695E-01 \\ .20456E+00 \\ -.19671E+00 \\ .98183E-01 \\ -.30755E+00 \end{bmatrix} + j \begin{bmatrix} .93115E-01 \\ .23719E+00 \\ -.11083E+00 \\ -.29017E+00 \\ -.12473E+00 \\ -.14411E-02 \\ -.17381E+00 \end{bmatrix} \tag{7.36b}$$

The measurements corresponding to actual parameter values are:

$$y^M(s_1) = \begin{bmatrix} -.18201E+00 \\ .34693E+00 \\ .52903E+00 \\ .78978E-01 \\ .30958E+00 \end{bmatrix} + j \begin{bmatrix} -.76336E+00 \\ .92198E-01 \\ -.39824E+00 \\ -.27258E+00 \\ -.47566E+00 \end{bmatrix} \tag{7.37a}$$

$$y^M(s_2) = \begin{bmatrix} .45295E-01 \\ .56059E+00 \\ .10124E+01 \\ .13830E+00 \\ .32849E+00 \end{bmatrix} + j \begin{bmatrix} -.67300E+00 \\ .15584E+00 \\ -.11559E+00 \\ -.26937E+00 \\ -.53376E+00 \end{bmatrix} \tag{7.37b}$$

The diagnosis program required only three iterations and 7.2 seconds on the VAX 11/780 to determine the elements of r^* to three significant digits. The cost in terms of the number of test points is relatively high (five test outputs). In the next example the requirement for complete identification is relaxed causing a dramatic reduction in test points.

Example 7.38: Now suppose the components of Example 7.28 permit functional grouping as indicated by the dashed lines in figure 13. If the requirement to isolate faults to a specific component is relaxed to the identification of a faulty group it becomes possible to eliminate test points by

transforming each group of three components into individual components. For example the components, Z_1, Z_2, and Z_3, combine to form the single component, $\hat{Z}_1$ where:

$$\hat{Z}_1(K_1,\tau_1) = \frac{K_1}{\tau_1 s+1} \tag{7.39}$$

and

$$K_1 = \frac{r_1}{r_1+r_2} \tag{7.40a}$$

$$\tau_1 = \frac{1}{r_1 r_3+r_2 r_3} \tag{7.40b}$$

If the remaining components have similar transformations the twelve parameter system of figure 13 becomes the eight parameter (4 component) system of figure 14. For the system of figure 14 the system output y_1 at four distinct sinusoidal test frequencies is sufficient to identify the parameters, K_i and τ_i, i=1,..,4 and hence isolate the fault to a component group. The CCM equations for the system are:

$$\begin{bmatrix} a_1 \\ a_2 \\ a_3 \\ a_4 \\ y \end{bmatrix} = \begin{bmatrix} 0 & 0 & 0 & -1 \\ 0 & 0 & 1 & 1 \\ 0 & 1 & 0 & 0 \\ 1 & 1 & 0 & 0 \\ 1 & 1 & 0 & 0 \end{bmatrix} \begin{bmatrix} b_1 \\ b_2 \\ b_3 \\ b_4 \end{bmatrix} + \begin{bmatrix} 1 \\ 1 \\ 0 \\ 0 \end{bmatrix} u \tag{7.41}$$

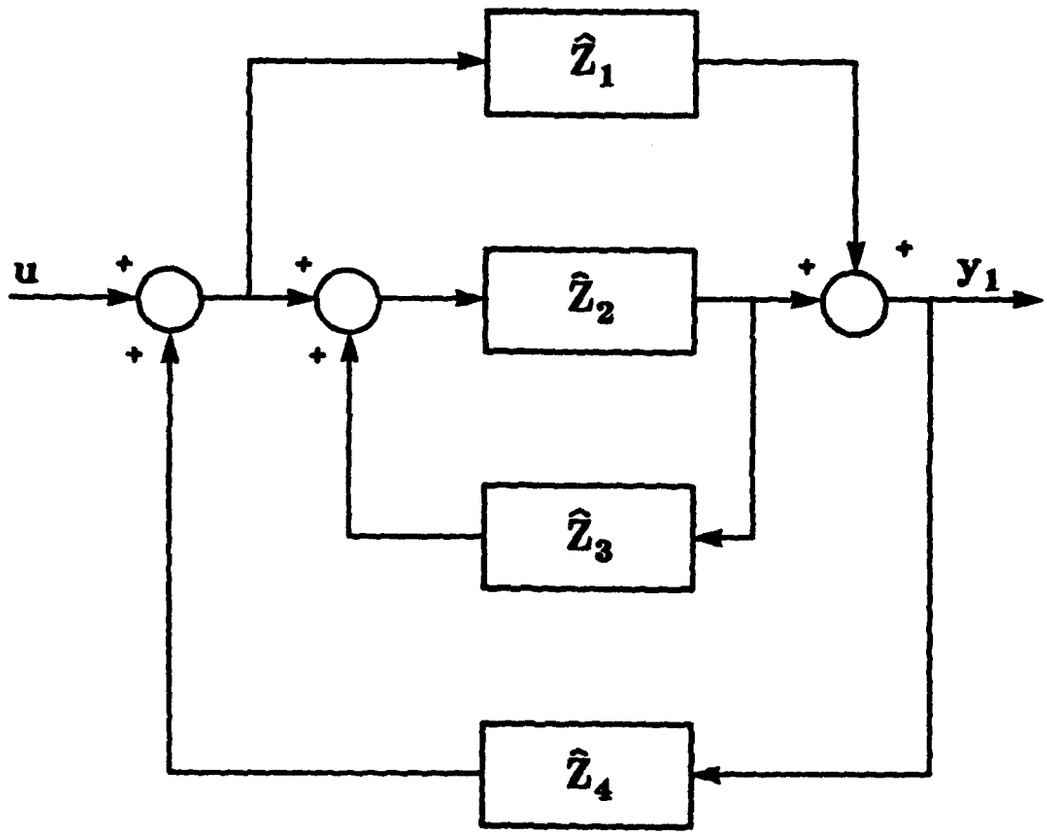

Figure 14. Interconnected functional units for example 7.38.

$$\begin{bmatrix} b_1 \\ b_2 \\ b_2 \\ b_4 \end{bmatrix} = \begin{bmatrix} \frac{K_1}{\tau_1 s+1} & 0 & 0 & 0 \\ 0 & \frac{K_2}{\tau_2 s+1} & 0 & 0 \\ 0 & 0 & \frac{K_3}{\tau_2 s+1} & 0 \\ 0 & 0 & 0 & \frac{K_4}{\tau_4 s+1} \end{bmatrix} \begin{bmatrix} a_1 \\ a_2 \\ a_3 \\ a_4 \end{bmatrix} \tag{7.42}$$

The parameter vector to be identified is:

$$r = (K_1, K_2, K_3, K_4, \tau_1, \tau_2, \tau_3, \tau_4)^t \tag{7.43}$$

The test frequencies are $s_1 = j1$, $s_2 = j3$, $s_3 = j6$ and $s_4 = j10$. The nominal and actual parameter vectors are:

$$r_0 = (1 \quad 2 \quad .9 \quad 1.1 \quad .8 \quad 1.5 \quad .5 \quad 1)^t \tag{7.44}$$

$$r^* = (.9 \quad 1.8 \quad 1 \quad 1.05 \quad .9 \quad 1.4 \quad .75 \quad .95)^t \tag{7.45}$$

The nominal values for the ambiguity vectors are:

$$\underline{a}_1 = \begin{bmatrix} .4789805E+00 \\ -.3740277E+00 \\ -.5349754E+00 \end{bmatrix} + j \begin{bmatrix} -.6195888E-01 \\ -.1286507E+00 \\ -.3048038E+00 \end{bmatrix} \tag{7.46a}$$

$$\underline{a}_2 = \begin{bmatrix} .9605259E-01 \\ -.1289079E+00 \\ -.1911152E+00 \end{bmatrix} + j \begin{bmatrix} .3421843E-02 \\ -.8045628E-01 \\ -.9222372E-01 \end{bmatrix} \tag{7.46b}$$

$$\underline{\alpha}_3 = \begin{bmatrix} .2229586E\text{-}01 \\ -.5140581E\text{-}01 \\ -.6668712E\text{-}01 \end{bmatrix} + j\begin{bmatrix} .7406399E\text{-}02 \\ -.2090679E\text{-}01 \\ -.1981173E\text{-}01 \end{bmatrix} \qquad (7.46c)$$

$$\underline{\alpha}_4 = \begin{bmatrix} .7343345E\text{-}02 \\ -.2164005E\text{-}01 \\ -.2659364E\text{-}01 \end{bmatrix} + j\begin{bmatrix} .6553531E\text{-}02 \\ -.5590791E\text{-}02 \\ -.5010533E\text{-}02 \end{bmatrix} \qquad (7.46d)$$

The measurements corresponding to actual parameter values are:

$$y^M(s_1) = -.1820130E\text{-}00 + j.7633615e+00 \qquad (7.47a)$$

$$y^M(s_2) = .7491249E\text{-}01 - j.5557519E+00 \qquad (7.47b)$$

$$y^M(s_3) = .4131773E\text{-}01 - j.3430093E+00 \qquad (7.47c)$$

$$y^M(s_4) = .1806347E\text{-}01 - j.2193868E+00 \qquad (7.47d)$$

The program to solve this example was executed on the VAX 11/780 and required 9 iterations to determine r^* to approximately 1%. The larger number of iterations necessary for this example versus the previous is most likely a result of (1) the greater nonlinearity in the tableau equations due to the form of the component (equation 7.39) and (2) from the drastic reduction in test points making the extraction of parameters more difficult.

8. Concluding Remarks

This completes the presentation of the preliminary development of the tableau approach which, as pointed out earlier, offers superior convergence and conditioning properties over the equivalent composite formulation. The five examples demonstrate the successful application of the results introduced thus far, including the determination of diagnosability of a circuit/system, the calculation of the number of required test frequencies and the actual solution of the fault diagnosis equations. Additional advantage for the tableau formulation remains to be gleaned from the knowledge of the quadratic form of its fault diagnosis equations. Details of the exploitation of this information as well as a demonstration of the resulting improvement in convergence follow in the next chapter.

CHAPTER 5

EXPLOITATION OF THE QUADRATIC FORM

1. Introduction

This chapter introduces some improvements to the Newton algorithm for solving the Tableau Fault Diagnosis Equations (equation 2.2 of Chapter 4) which apply when these equations are quadratic. Recall that the Tableau Fault Diagnosis Equations have a quadratic form whenever $Z_i(s,r_i) = r_i Z_i(s)$. In the case of electrical networks this form of component transfer function suffices for modelling resistors, inductors, capacitors, and dependent sources. This means that the quadratic form of the Tableau Fault Diagnosis Equations is valid for any circuit modelled by an interconnection of the above components. This is an extremely large category of possible circuits.

The significance of this special form is that it represents specific information about Tableau Fault Diagnosis Equations which, under appropriate circumstances, is useful in determining their solution. This chapter addresses two ways of exploiting this information. First the quadratic form of the Tableau Fault Diagnosis Equations allows an exact characterization of their behavior along a search direction. In particular this characterization provides a simple means of precisely establishing the point along the search direction at which the norm of the nonlinear function, $F(x)$, is a minimum. Use of this "minimum point" as the next estimate of the solution is designed to guarantee and streamline the convergence of the Newton-Raphson iteration. Second, this special form may permit the

determination of a better search direction by allowing a two term approximation of the Hessian of the function, $||F(x)||_2^2$.

2. Multidimensional Quadratic Functions

Before proceeding with a simple example of a set of quadratic equations, it will be useful to draw an analogy between the problem of solving $F(x) = \theta$ and a functional minimization problem. Recall the square of the Euclicean norm, $||\ ||_2^2$, is a functional which has a unique global minimum at θ so the problem of finding x^* such that $F(x^*) = \theta$ is equivalent to finding x^* such that [13]

$$||F(x_2^*)||_2^2 \leq ||F(x)||_2^2 \quad \text{for all } x \in R^n \tag{2.1}$$

For circumstances which cause the Newton-Raphson algorithm to diverge, this new perspective suggests a modification which results in a nondiverging algorithm [13]. Namely, choose λ such that

$$||F(x^{k+1})||_2^2 = ||F(x^k + \lambda d^k)||_2^2 \leq ||F(x^k)||_2^2 \tag{2.2}$$

where d^k satisfies:

$$J_F(x^k)d^k = -F(x^k) \tag{2.3}$$

The vector d^k is called the "search direction". This modification is based on the "Global Convergence Theorem" which appears in Chapter 2. The following example will illustrate how knowledge of the quadratic form assists in the selection of λ.

Consider the following problem in two dimensions:

$$F(x,y) = \begin{bmatrix} F_1(x,y) \\ F_2(x,y) \end{bmatrix} = \begin{bmatrix} xy-2x-2y+3 \\ xy-2y+1 \end{bmatrix} = \theta \qquad (2.4)$$

where $\begin{bmatrix} x \\ y \end{bmatrix} \epsilon R^2$. The nonlinearity of the function, F, is the second order term, xy. Such second order terms likewise characterize the nonlinearity of the Tableau Fault Diagnosis Equations.

Now solve $F(x,y) = \theta$ via the Newton-Raphson iteration method. The Jacobian of F(x,y) is

$$J_F(x,y) = \begin{bmatrix} y-2 & x-2 \\ y & x-2 \end{bmatrix} \qquad (2.5)$$

Assume an initial guess: $\begin{bmatrix} x^0 \\ y^0 \end{bmatrix} = \begin{bmatrix} 2.1 \\ 3 \end{bmatrix}$. The next estimate of the desired solution, $\begin{bmatrix} x^1 \\ y^1 \end{bmatrix}$, is the solution of:

$$J_F(x^0,y^0) \begin{bmatrix} x-2.1 \\ y-3 \end{bmatrix} = -F(x^0,y^0) \qquad (2.6)$$

which is equivalent to solving the pair of linear simultaneous equations:

$$x + .1y = 3.3 \qquad (2.7a)$$

$$3x + .1y = 5.3 \qquad (2.7b)$$

To develop an understanding of the nature of the solution process consider the following physical interpretation: Let the first component of F define a surface as

$$z = F_1(x,y) \qquad (2.8)$$

Figure 15 is a graph of this surface with the point $z^o = F_1(x^o,y^o) = F_1(2.1,3)$ annotated. Consider next the plane which is tangent to the surface at the point $\begin{bmatrix} x^o \\ y^o \end{bmatrix}$, depicted in figure 16. Equation 2.7a is the equation of the line in the xy plane which is the intersection of the tangent plane with the plane z=0. In other words, equation 2.7a is the linear approximation of the zero set of the nonlinear function, $F_1(x,y)$ determined as the zero set of the tangent plane of the surface $z = F_1(x,y)$ at the point $\begin{bmatrix} x^o \\ y^o \end{bmatrix}$. Of course a similar interpretation holds for the second equation. Thus the intersection of the two tangent planes is the approximate intersection of the two nonlinear equations.

The solution to equation 2.7 is the point $\begin{bmatrix} x \\ y \end{bmatrix} = \begin{bmatrix} 1 \\ 23 \end{bmatrix}$. To determine if the algorithm may be diverging, test the condition in 2.2, i.e. determine if $||F(1,23)||_2^2 < ||F(2.1,3)||_2^2$. Evaluating $||F||_2^2$ at these points yields:

$$||F(2.1,3)||_2^2 = 2.5 \qquad ||F(1,23)||_2^2 = 968 \tag{2.9}$$

This indicates that the Newton-Raphson iteration is diverging. For this simple example it is very possible that subsequent iterations may recover from this divergent step but in general, adjustment of the algorithm to insure that the condition in 2.2 holds will be necessary.

This adjustment consists of finding a value for λ such that

$$||F(x^k+\lambda d^k)||_2^2 \leq ||F(x^k)||_2^2 \tag{2.10}$$

For this example the search direction, $d^o = \begin{bmatrix} 1 \\ 23 \end{bmatrix} - \begin{bmatrix} 2.1 \\ 3 \end{bmatrix} = \begin{bmatrix} -1.1 \\ 20 \end{bmatrix}$. The desired value for the next estimate of the solution is now

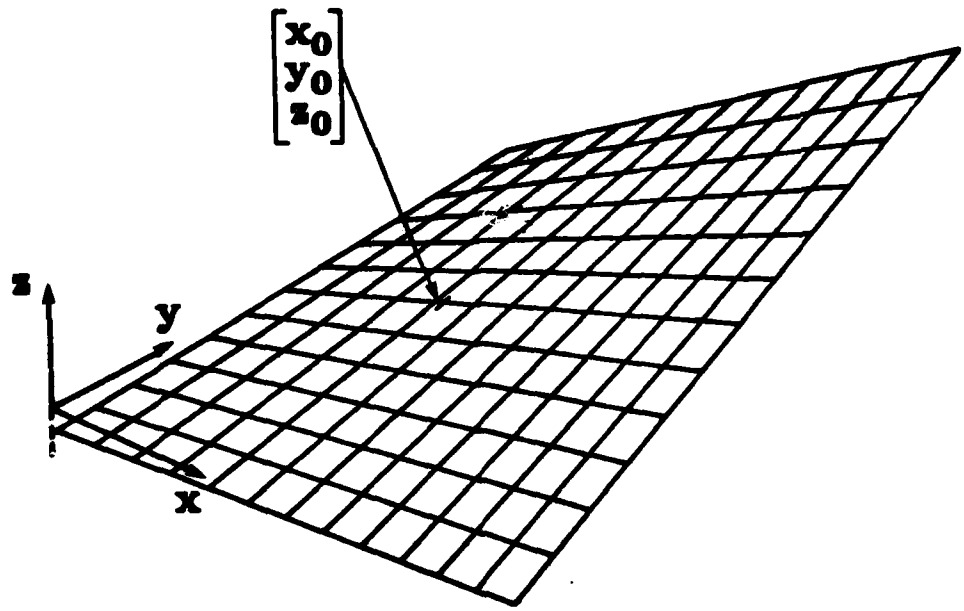

Figure 15. Graph of z=f,(x,y).

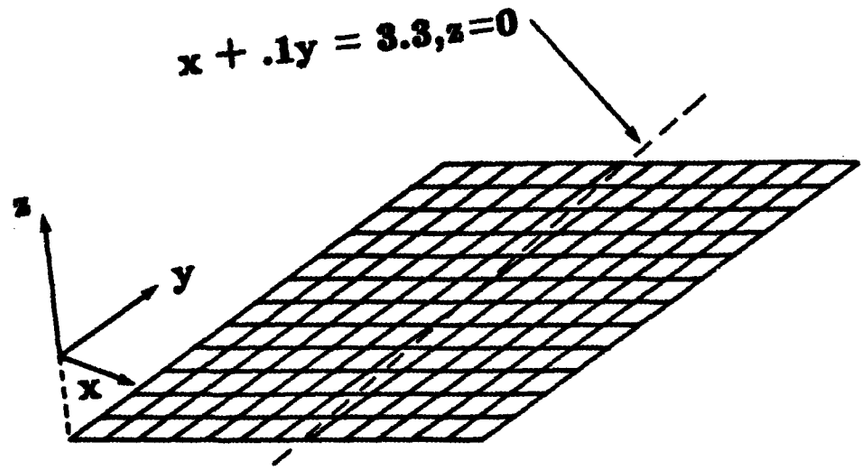

Figure 16. Tangent Plane.

$$\begin{bmatrix} x^1 \\ y^1 \end{bmatrix} = \begin{bmatrix} x^o \\ y^o \end{bmatrix} + \lambda \begin{bmatrix} d_x^o \\ d_y^o \end{bmatrix} \qquad (2.11)$$

Notice that when $\lambda = 0$ the next estimate equals the previous and when $\lambda = 1$ the next estimate is the Newton-Raphson estimate. The set of possible values for $\begin{bmatrix} x^1 \\ y^1 \end{bmatrix}$ corresponds to a line parallel to the search direction and passing through $\begin{bmatrix} x^o \\ y^o \end{bmatrix}$. Figure 17 illustrates this set of points for the current example. In the Navid and Willson application of the "Global Convergence Theorem" λ has an initial value of 1 (the Newton-Raphson iterate). If the condition in 2.2 does not hold then λ decreases by half until it does [13]. Points corresponding to $\lambda = 1, .5$ and .25 appear in figure 17. Table 2 displays the results of the computation of $||F||_2^2$ for the sequence of $\lambda = 2^{-j}$ for j=0,1,2 and 3.

λ	$\|\|F\|\|_2^2$
1	968
.5	58.93
.25	4.363
.125	1.910

Table 2

Evaluation of $||F||_2^2$ at selected points.

The data in table 2 indicates that $\lambda = .125$ will satisfy the condition in 2.2. Although this value for λ satisfies the condition, it is not optimal in the sense that $||F||_2^2$ is not minimized along the search direction. Knowledge of the quadratic nature of the Tableau Fault Diagnosis Equations and hence the fourth order behavior of $||F||_2^2$ offers an easily implemented scheme for choosing this optimal value as seen in the next section.

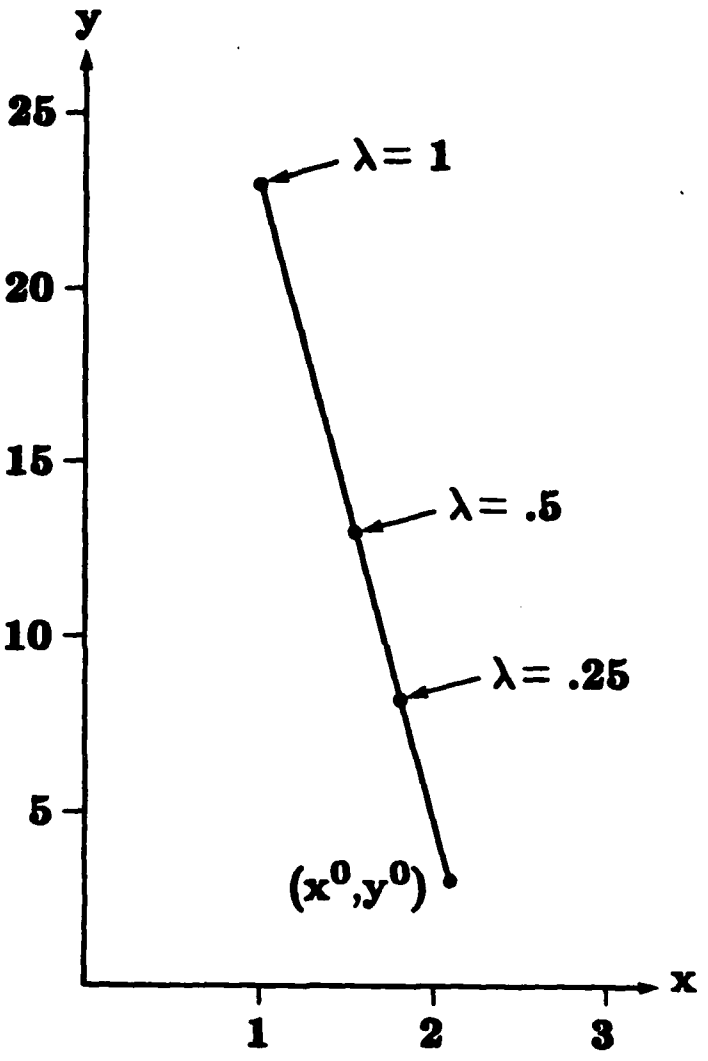

Figure 17. Set of Points Along the Search Direction.

3. An Algorithm for Selecting λ

To illustrate an optimal scheme for choosing λ, return to the example in the previous section. Evaluate $F(x^1,y^1)$ as a function of λ by substituting equation 2.11 into the expression for $F(x,y)$ given in equation 2.4. This produces:

$$F(2.1-1.1\lambda,3+20\lambda) = \begin{bmatrix} -22\lambda^2+.9\lambda-.9 \\ -22\lambda^2-1.3\lambda+1.3 \end{bmatrix} \tag{3.1}$$

Note that F is a vector whose entries are quadratic functions of λ. Now find λ such that $||F(2.1-1.1\lambda,3.+20.\lambda)||_2^2$ is a minimum. Computing the square of the norm of F yields the following fourth degree polynomial in λ:

$$||F(x^1,y^1)||_2^2 = (-22\lambda^2+.9\lambda-.9)^2 + (-22\lambda^2-1.3\lambda+1.3)^2$$

$$= 968\lambda^4+17.6\lambda^3-15.1\lambda^2-5\lambda+2.5 \tag{3.2}$$

Since equation 3.2 is a fourth degree polynomial the minimum point is the result of solving:

$$\frac{d||F(x^1,y^1)||_2^2}{d\lambda} = 3872\lambda^3+52.8\lambda^2-30.2\lambda-5 = 0 \tag{3.3}$$

Equation 3.3 has a single real root at $\lambda = .12731$. Thus the point

$$\begin{bmatrix} x^1 \\ y^1 \end{bmatrix} = \begin{bmatrix} 2.1 \\ 3. \end{bmatrix} + .12731 \begin{bmatrix} -1.1 \\ 20. \end{bmatrix} = \begin{bmatrix} 1.9600 \\ 5.5462 \end{bmatrix} \tag{3.4}$$

is the point along the search direction for which $||F||_2^2$ is a minimum. Evaluating F at this point gives

$$||F(1.96,5.5462)||_2^2 = 1.909 \tag{3.5}$$

This process has produced a new estimate for the solution of $F(x,y) = 0$ void of the divergence problem.

The procedure for finding the optimum value for λ worked very well for the simple example. The next step in this development is to show explicitly that it applies to the Tableau Fault Diagnosis Equations. Recall the fault diagnosis equations presented in equation 3.1 of chapter 3, namely:

$$F(x) = \begin{bmatrix} f_1(r)g_1(\underline{\alpha}_1)-\beta_1 \\ \vdots \\ f_q(r)g_q(\underline{\alpha}_q)-\beta_q \end{bmatrix} = 0 \tag{3.6}$$

where

(i) $x = \text{col}(\underline{\alpha}_1,\underline{\alpha}_2,\ldots,\underline{\alpha}_q,r)$;

(ii) $f_i(r) = [Z(s_i,r)|-V]$;

(iii) $g_i(\underline{\alpha}_i) = \begin{bmatrix} L_{11}V\underline{\alpha}_i+a_o(s_i) \\ \hline \underline{\alpha}_i \end{bmatrix}$; and

(iv) $\beta_i = b_o(s_i)$.

Furthermore recall the assumption that $Z_j(s,r_j) = r_jZ_j(s)$.

To explicitly see that the procedure used in the simple example applies to these equations as well, take a closer look at the individual entries of the nonlinear vector function, F. Let $\phi_{ij}(x)$ denote the [N(i-1)+j]th component of F(x), (i.e. $F_{N(i-1)+j}(x)$) where i=1,2,...,q and j=1,2,...,N. Then

$$\phi_{ij}(x) = Z_j(s_i)r_j \sum_{k=1}^{p} (L_{11}V)_{jk}\alpha_{ik}$$

$$+ Z_j(s_i)r_j a_{oj}(s_i) - \sum_{k=1}^{p} V_{jk}\alpha_{ik} - b_{oj}(s_i) \qquad (3.7)$$

where

(i) $(L_{11}V)_{jk}$ denotes the (j,k) entry of the matrix product $L_{11}V$;

(ii) α_{ik} is the k-th entry of $\underline{\alpha}_i$;

(iii) V_{jk} denotes the (j,k) entry of the matrix V; and

(iv) $a_{oj}(s_i)$ and $b_{oj}(s_i)$ denote the j-th entry of $a_o(s_i)$ and $b_o(s_i)$ respectively.

The nonlinear terms are those with the products: $r_j\alpha_{ik}$ where i=1,2,...,q, j=1,2,...,n, and k=1,2,...,p. Clearly then the nonlinearity in the Tableau Fault Diagnosis Equations consists of sums of pairwise products of r_j with α_{ik}, strictly quadratic.

Now apply the modified Newton-Raphson iteration to the Tableau Fault Diagnosis Equations in the same manner as in the earlier simple illustrative example. As before the objective is to select the value of λ such that $||F(x^k+\lambda d^k)||_2^2$ is a minimum and then compute $x^{k+1} = x^k+\lambda d^k$. From equation 3.7 it is apparent that with x^k and d^k fixed (known)

(i) $\phi_{ij}(x^k+\lambda d^k)$ is a quadratic function of λ, and

(ii) $||F(x^k+\lambda d^k)||_2^2$ is a fourth degree polynomial in λ.

Furthermore the above is true regardless of the size of the Tableau Fault Diagnosis Equations as long as $Z_j(s,r_j) = r_j Z_j(s)$.

This means that the following algorithm will assign the optimum value to λ:

Step 1- Evaluate $||F(x^k+\lambda d^k)||_2^2$ at five values of λ.

Remark: Because of the form of the Tableau Fault Diagnosis Equations, this requires matrix addition and multiplication only. No matrix inverses are necessary.

Step 2- Generate a fourth order interpolant, $h(\lambda)$, for the data from Step 1.

Remark: Although it is possible to generate the coefficients of $||F(x^k+\lambda d^k)||_2^2$ by substituting $x^k+\lambda d^k$ into the expression for F as in the example above it is far simpler in a computer implementation to use steps 1 and 2 for the following reasons. First, any computer implementation of the Newton-Raphson algorithm (e.g. the program used to solve the examples in chapter 5) must already have a routine for evaluating the value of F. Second, since the $||F||_2^2$ is a fourth degree polynomial in λ then

$$h(\lambda) = ||F(x^k+\lambda d^k)||_2^2 \tag{3.9}$$

for all λ (i.e. the interpolant is exact).

Step 3- Find the roots of the equation:

$$\frac{dh(\lambda)}{d\lambda} = 0 \tag{3.10}$$

Remark: The solution to equation 3.10 is easily computed since $\frac{dh(\lambda)}{d\lambda}$ is a third degree polynomial.

Step 4- Set λ_k equal that root of equation 3.10 for which 3.9 is minimum.

The result of this procedure is a value for $\lambda=\lambda_k$ which minimizes $||F(x^k-\lambda d^k)||_2^2$ along the search direction, d^k. This is the optimum choice for λ made possible by the quadratic nature of the Tableau Fault Diagnosis

Equations.

Before proceeding to an example some details of the implementation of steps 1 and 2 deserve mention. If infinite precision were available on the computer any five distinct points along the search direction would suffice to uniquely determine the desired interpolant, $h(\lambda)$. With limited precision some choices will produce more accurate results than others. Since the solution to equation 3.10 will normally lie in the interval [0,1] a reasonable choice of five interpolation points is λ = -.5,0.,.5,1., and 1.5.

The polynomial $h(\lambda)$ has the form:

$$h(\lambda) = \gamma_4\lambda^4 + \gamma_3\lambda^3 + \gamma_2\lambda^2 + \gamma_1\lambda + \gamma_0 \tag{3.11}$$

Evaluation of $h(\lambda) = ||F(x^k-\lambda d^k)||_2^2$ at the five points mentioned above results in the following matrix equation whose solution is the coefficients γ_i, i=0,1,..,4, which uniquely specify $h(\lambda)$.

$$\begin{bmatrix} 5.0625 & 3.375 & 2.25 & 1.5 & 1. \\ 1. & 1. & 1. & 1. & 1. \\ 0.0625 & 0.125 & 0.25 & 0.5 & 1. \\ 0. & 0. & 0. & 0. & 1. \\ 0.0625 & -0.125 & 0.25 & -0.5 & 1. \end{bmatrix} \begin{bmatrix} \gamma_4 \\ \gamma_3 \\ \gamma_2 \\ \gamma_1 \\ \gamma_0 \end{bmatrix} = \begin{bmatrix} h(1.5) \\ h(1.0) \\ h(0.5) \\ h(0.0) \\ h(-.5) \end{bmatrix} \tag{3.12}$$

The matrix in equation 3.12 is a 5 x 5 Vandermonde matrix[14] which is nonsingular. Since this matrix is always the same as long as the interpolation points are fixed the solution algorithm computes its inverse once and then uses the inverse at each iteration to determine the coefficients of $h(\lambda)$.

4. Quadratic Form Examples

This section will illustrate the modified Newton-Raphson algorithm (selection of λ) detailed in the previous section via an example circuit (Figure 9) presented in chapter 4.

Example 4.1: The first example is example 7.1 from chapter 4. All the data used in this example is exactly the same as in example 7.1 except that this time the solution to the Tableau Fault Diagnosis Equations proceeds according to the modified Newton-Raphson Algorithm. Recall that for this example M=N=12, p=9 and q=2. The test frequencies are s_1=j1.4 and s_2=j2.0. Determination of the solution point with an accuracy of .11% required 8 iterations and 23.3 seconds on the VAX-11/780. The solution routine is a FORTRAN language program using single precision arithmetic (approximately six decimal places on the VAX). This is a substantial improvement over the Newton-Raphson iteration (λ=1) described in chapter 4, example 7.1, which required 12 iterations and 31.5 seconds on the VAX-11/780 to produce the same results.

Example 4.2: This example also uses the same circuit (Figure 9) as the previous example with the exception of the actual parameter vector and corresponding measurement outputs. For this example the actual parameter vector is:

$$r = (2 \quad 1.4 \quad .9 \quad .7 \quad 1.5 \quad .8 \quad 1.5 \quad 1.4 \quad 2 \quad .9 \quad 1.2 \quad 1.6)^t \qquad (4.23)$$

and the test outputs corresponding to this parameter vector are

$$y^M(j1.4) = \begin{bmatrix} -.14522E-01 \\ .25990E+00 \\ .65868E-01 \end{bmatrix} + j \begin{bmatrix} .29083E-01 \\ .54699E+00 \\ .13866E+00 \end{bmatrix} \qquad (4.4a)$$

for input u(j1.4) = 1, and

$$y^M(j2.0) = \begin{bmatrix} .12406E-02 \\ .43757E+00 \\ .94981E-01 \end{bmatrix} + j \begin{bmatrix} .47175E-01 \\ .66102E+00 \\ .18066E+00 \end{bmatrix} \qquad (4.4b)$$

for input u(j2.0) = 1.

The variations from unity for each of the parameter values are sufficiently large that the usual Newton-Raphson iteration diverges. Consequently this problem solution required the modified algorithm discussed in section 3. Determination of the solution point with an accuracy of 2% required 6 iterations and 17.0 seconds on the VAX-11/780.

The examples illustrate that the modified algorithm will converge under circumstances in which the Newton-Raphson algorithm will not. Furthermore it is possible for the modified algorithm to result in convergence in fewer iterations due to the optimum choice of λ. Of course these conclusions are consistent with the "Global Convergence Theorem" of Navid and Willson [13].

5. Modification of the Search Direction

The algorithm for solving the quadratic form of the Tableau Fault Diagnosis Equations uses this quadratic information at each iteration to determine the optimum point along the search direction for the next estimate of the solution. The search direction used however is exactly the same as the Newton-Raphson algorithm. In both cases the search direction for the k-th iteration, d^k, satisfies:

$$J_F(x^k)d^k = -F(x^k) \qquad (5.1)$$

The purpose of this section is to investigate the use of quadratic information to determine of a new possibly better search direction.

In section 2 the problem of solving the nonlinear vector problem, $F(x) = \theta$, appears recast as a the minimization of a scalar function $||F(x)||_2^2$, where $x \in R^n$. Let the function, $h(x)$, be a scalar multiple of $||F(x)||_2^2$, expressed in terms of vector multiplication as:

$$h(x) = .5\ F(x)^t F(x) \tag{5.2}$$

where $F: D \subset R^n \rightarrow R^m$ with $m \geq n$ and t denotes the matrix transpose. The scale factor .5 has no affect on the minimization problem but its inclusion eliminates the factor two from the derivatives of $h(x)$. Recall that finding the solution to $F(x) = \theta$ is equivalent to finding the value of x which minimizes $h(x)$. Furthermore, finding the minimum of $h(x)$ is equivalent to solving the nonlinear vector problem:

$$\nabla h(x) = \theta \tag{5.3}$$

where ∇ denotes the gradient operator, i.e.

$$\nabla = \begin{bmatrix} \frac{\partial}{\partial x_1} \\ \frac{\partial}{\partial x_2} \\ \vdots \\ \frac{\partial}{\partial x_n} \end{bmatrix} \tag{5.4}$$

Define the function $G(x)$ as:

$$G(x) = \nabla h(x) \tag{5.5}$$

The Newton-Raphson and modified Newton-Raphson algorithms are valid methods for finding the solution to $G(x) = 0$. In both cases the search direction at the k-th iteration is the solution to:

$$J_G(x^k)d^k = -G(x^k) \tag{5.6}$$

Expressing equation 5.6 in terms of the original nonlinear function, $F(x)$, produces an interesting variation on the Newton-Raphson search direction. In order to see this take a closer look at the Jacobian of G. If the vector function

$$G(x) = \text{col}[G_1(x), G_2(x), \ldots, G_n(x)] \tag{5.7}$$

$$= \text{col}\left[\frac{\partial h(x)}{\partial x_1}, \frac{\partial h(x)}{\partial x_2}, \ldots, \frac{\partial h(x)}{\partial x_n}\right]$$

then $J_G(x)$ is

$$J_G(x) = \begin{bmatrix} \frac{\partial G_1}{\partial x_1} & \frac{\partial G_1}{\partial x_2} & \cdots & \frac{\partial G_1}{\partial x_n} \\ \frac{\partial G_2}{\partial x_1} & \frac{\partial G_2}{\partial x_2} & \cdots & \frac{\partial G_2}{\partial x_n} \\ \vdots & \vdots & \vdots & \vdots \\ \frac{\partial G_n}{\partial x_1} & \frac{\partial G_n}{\partial x_2} & \cdots & \frac{\partial G_n}{\partial x_n} \end{bmatrix} \tag{5.8}$$

$$= \begin{bmatrix} \frac{\partial^2 h(x)}{\partial x_1 \partial x_1} & \frac{\partial^2 h(x)}{\partial x_2 \partial x_1} & \cdots & \frac{\partial^2 h(x)}{\partial x_n \partial x_1} \\ \frac{\partial^2 h(x)}{\partial x_1 \partial x_2} & \frac{\partial^2 h(x)}{\partial x_2 \partial x_2} & \cdots & \frac{\partial^2 h(x)}{\partial x_n \partial x_2} \\ \vdots & \vdots & \ddots & \vdots \\ \frac{\partial^2 h(x)}{\partial x_1 \partial x_n} & \frac{\partial^2 h(x)}{\partial x_2 \partial x_n} & \cdots & \frac{\partial^2 h(x)}{\partial x_n \partial x_n} \end{bmatrix} = \nabla^2 h(x)$$

The ∇^2 operator denotes the Hessian matrix (the matrix of second partial derivatives.

Both the gradient, $G(x) = \nabla h(x)$, and the Hessian matrix, $\nabla^2 h(x)$, have expressions in terms of $F(x)$ based on the definition of $h(x)$ given in equation 5.2. These are [22]:

$$G(x) = \nabla h(x) = \left[J_F(x)\right]^t F(x) \tag{5.9}$$

$$\nabla^2 h(x) = \left[J_F(x)\right]^t J_F(x) + \sum_{k=1}^{m} F_k(x) H_k(x) \tag{5.10}$$

where $F_k(x)$ is the k-th entry of $F(x)$ and $H_k(x)$ is the Hessian matrix of $F_k(x)$ i.e.

$$H_k(x) = \nabla^2 F_k(x) \tag{5.11}$$

The substitution of the identities of equations 5.9 and 5.10 into equation 5.6 produces the following equation for the search direction:

$$\left[\left[J_F(x)\right]^t J_F(x) + \sum_{k=1}^{m} F_k(x)H_k(x)\right]d^k = -\left[J_F(x)\right]^t F(x) \qquad (5.12)$$

Omitting the term $\sum_{k=1}^{m} F_k(x)H_k(x)$ from equation 5.12 yields

$$\left[\left[J_F(x)\right]^t J_F(x)\right]d^k = -\left[J_F(x)\right]^t F(x) \qquad (5.13)$$

Solving equation 5.13 is mathematically equivalent to finding the least squares solution to equation 5.1 which produces the Newton-Raphson search direction. Equation 5.12 on the other hand produces a search direction based on a complete expression of the Hessian matrix of h(x). An algorithm based on the use of equation 5.12 might therefore produce an improved solution scheme for solving $F(x) = \theta$. As will be seen from the examples of the next section, the procedure does not in fact produce an improved search direction.

In general information to permit the computation of $\sum_{k=1}^{m} F_k(x)H_k(x)$ (i.e. the H_k) is not available and a great variety of schemes exist which attempt to approximate it in some manner [22]. In the case of the quadratic form of the Tableau Fault Diagnosis Equations the matrices $H_k(x) = \nabla^2 F_k(x)$, $k=1,2,\ldots,m$ are constant. Furthermore they are sparse which permit efficient storage for use in computing

$$\left[\left[J_F(x)\right]^t J_F(x) + \sum_{k=1}^{m} F_k(x)H_k(x)\right]$$

at each iteration. The sparseness is due to the fact that the only nonlinear terms in F_k are the products of a single component parameter, r_j and the components of a single ambiguity vector, $\underline{a}_i$, $i=1,2,\ldots,q$ and $j=1,2,\ldots N$.

Specifically, each $H_{N(i-1)+j}$ is a (pq+N)(mu(pq+N) symmetric matrix which has all zero entries except for the (pq+i)-th row and column. If $\Gamma_{pq+j,i}$ denotes the non-zero column of $H_{N(i-1)+j}$ then the non-zero row is $\Gamma^t_{pq+j,i}$. $\Gamma_{pq+j,i}$ has the form:

$$\Gamma_{pq+j,i} = \begin{bmatrix} \Lambda_1 \\ \Lambda_2 \\ \cdot \\ \cdot \\ \Lambda_q \\ \theta_N \end{bmatrix} \tag{5.14}$$

where

(i) Λ_k equals the p dimensional zero vector if $k \neq i$ and $\Lambda_k = Z_j(s_i)\ (L_{11}V)^j$, if $K = i$;

(ii) $(L_{11}V)^j$ is the transpose of the j-th row of $L_{11}V$; and

(iii) θ_N is the N dimensional zero vector.

The results of the implementation of this modified search direction method are discussed in the next section.

6. Examples Using Modified Search Direction

As with the other solution algorithms discussed, the implementation of the solution algorithm utilizing the modification of the search direction is a FORTRAN program compiled and executed on the VAX 11/780. The program also employs the interpolation procedure to determine the optimum point along the search direction.

Example 6.1: Since example 4.1 has already served as a basis for comparison between the Newton-Raphson algorithm and the modified Newton-Raphson algorithm discussed in section 3 it is appropriate to attempt to solve this example utilizing the modified search direction. Unfortunately

the results were discouraging. After 250 iterations, the program utilizing the modified search direction failed to converge to a solution point. The following conjecture may serve as an explanation of this unsatisfactory performance. Recall that the modified search direction algorithm is actually a procedure to solve $\nabla h(x) = 0$. This condition is satisfied not only at the desired solution point but at all local maxima and minima and at saddle points. In fact it is possible that some of the points satisfying $\nabla h(x) = 0$ are not even isolated. By construction the modified search direction is influenced by all such points on the surface described by $\begin{bmatrix} h(x) \\ x \end{bmatrix}$. The existence of non-isolated solutions or even clustered isolated solutions to $\nabla h(x) = 0$ would explain the program's inability to converge to a solution point, even an incorrect one.

There is perhaps a very limited set of situations in which use of the modified search direction is appropriate as the next example illustrates.

Example 6.2: Like examples 4.1, 4.2, and 6.1, this example employees the circuit of example 7.1 of chapter 4. All of the necessary data appears there except for the following changes:

(i) The number of test frequencies,q, is three, and these are

$s_1 = j.4$, $s_1 = j1.2$, and $s_1 = j2.$;

Remark: This example uses one more test frequency than actually required. The additional measurement data serves to improve the condition of the problem.

(ii) The actual parameter vector is:

$$r^* = \text{col}(2.1\ 1.5\ .4\ 1.2\ 2\ .7\ .8\ 1.1\ .95\ 1.2\ .95\ 1.3) \quad (6.3)$$

(iii) The nominal values for the ambiguity vectors are:

$$\underline{a}(s_1) = \begin{bmatrix} .26648E+00 \\ .37331E+00 \\ .35839E-01 \\ .28384E+00 \\ -.17221E-01 \\ .54351E-01 \\ .35839E-01 \\ .31641E-01 \\ .92483E-01 \end{bmatrix} + j \begin{bmatrix} -.12054E+00 \\ -.11670E+00 \\ .43052E-01 \\ -.43458E-01 \\ .14336E-01 \\ .17588E-01 \\ .43052E-01 \\ .97458E-01 \\ .14854E+00 \end{bmatrix} \qquad (6.4a)$$

$$\underline{a}(s_2) = \begin{bmatrix} .12731E+00 \\ .25786E+00 \\ .86319E-01 \\ .18968E+00 \\ -.41018E-01 \\ .72697E-01 \\ .86319E-01 \\ .15326E+00 \\ .23754E+00 \end{bmatrix} + j \begin{bmatrix} -.38703E+00 \\ .14630E-02 \\ .34182E-01 \\ -.49547E-01 \\ .10358E+00 \\ -.80235E-01 \\ .34182E-01 \\ .11745E+00 \\ .20604E+00 \end{bmatrix} \qquad (6.4b)$$

$$\underline{a}(s_3) = \begin{bmatrix} -.86316E-01 \\ .29425E+00 \\ .10092E+00 \\ .17635E+00 \\ -.21282E-01 \\ .35081E-01 \\ .10092E+00 \\ .19156E+00 \\ .31972E+00 \end{bmatrix} + j \begin{bmatrix} -.48784E+00 \\ .80346E-01 \\ .10641E-01 \\ -.11167E-01 \\ .20184E+00 \\ -.13916E+00 \\ .10641E-01 \\ .97295E-01 \\ .21512E+00 \end{bmatrix} \qquad (6.4c)$$

and

(iv) The outputs corresponding to the actual parameter vector are:

$$y^M(s_1) = \begin{bmatrix} -.26178E-02 \\ .31077E-01 \\ .21118E-01 \end{bmatrix} + j \begin{bmatrix} -.31569E-02 \\ .18086E+00 \\ .57588E-01 \end{bmatrix} \qquad (6.5a)$$

$$y^M(s_2) = \begin{bmatrix} -.20198E-01 \\ .20012E+00 \\ .64193E-01 \end{bmatrix} + j \begin{bmatrix} .17205E-01 \\ .45228E+00 \\ .12685E+00 \end{bmatrix} \qquad (6.5b)$$

$$y^M(s_3) = \begin{bmatrix} -.78967E-02 \\ .41679E+00 \\ .11324E+00 \end{bmatrix} + j \begin{bmatrix} .48328E-01 \\ .59643E+00 \\ .17160E+00 \end{bmatrix} \qquad (6.5c)$$

The solution of the resulting fault diagnosis equations was computed twice. The first solution program used the modified Newton-Raphson algorithm developed in section 3. This program required 11 iterations and 66.13 seconds on the VAX 11/780 to compute the solution to .07% accuracy. The second solution program was identical to the first except that the first iteration used the modified search direction discussed in section 5. This solution, computed to .07% accuracy, required 8 iterations and 58.07 seconds on the VAX 11/780. In this case a modest improvement resulted from the use of the modification to the Newton-Raphson search direction. Experience indicates that such improvement does not occur in general.

7. Summary

Clearly a notable distinction of the use of the Tableau Fault Diagnosis Equations is the ability to exploit their special structure in the solution process. The most significant observation about this structure is that the equations are quadratic when $Z_i(s,r_i) = r_i Z_i(s)$. This means that it is possible to completely characterize the behavior of $||F||_2^2$ in a search direction with a simple interpolation scheme. The interpolation scheme combined with the Newton-Raphson search direction produces a solution algorithm which converges under conditions in which the Newton-Raphson algorithm does not or is faster under conditions when it does.

Although the attempt to develop an improved search direction based on the use of a complete expression for the Hessian of $||F||_2^2$ was unsuccessful it does provide additional information into the nature of the Tableau Fault Diagnosis Equations. In general the presence of extrema and other points for which $\nabla h(x) = \theta$ precludes the use of this method. In fact this should serve as a caution to the application of this method to the solution of any set of simultaneous nonlinear equations.

REFERENCES

[1] M. N. Ransom and R. Saeks, "Fault isolation via term expansion," Proc. 3rd Pittsburgh Symp. Modeling and Simulation, (Univ. of Pittsburgh), Vol. 4, pp. 224-228, 1973.

[2] R. Saeks, S. P. Singh, and R. W. Liu, "Fault Isolation via component simulation," IEEE Trans. Circuit Theory, Vol. CT-19, pp. 634-640, Nov. 1972.

[3] S. P. Singh and R. W. Liu, "Existence of state equation representation of linear large-scale dynamical systems," IEEE Trans. Circuit Theory, Vol. CT-20, pp. 239-246, May 1973.

[4] Sparse Matrices and Their Applications, edited by D. J. Rose and R. A. Willoughby, (Proceedings of a Symposium on Sparse Matrices and Their Applications, Sept. 9-10, 1971, IBM Thomas J. Watson Research Center, Yorktown heights, N.Y.) New York: Plenum Press 1972.

[5] H. Trauboth and W. McCallum, "MARSYAS Users Manual," Tech. Report A1-34812, Computation Lab, NASA/MSFC, 1973.

[6] N. Sen and R. Saeks, "Fault diagnosis for linear system via multifrequency measurements," IEEE Trans. on Circuits and Systems, Vol. CAS-26, 490-496, July 1979.

[7] R. DeCarlo and C. Gordan, "Tableau Approach to AC-multifrequency Fault Diagnosis," Proceedings of IEEE International Symposium of Circuit and Systems, May 1981.

[8] H. Neudecker, "Some theorems on matrix differentiation with special reference to Kronecker matrix products," J. Amer. Stat. Assoc., Vol. 64, pp. 953-963, 1969.

[9] R. Saeks and R. A. DeCarlo, Interconnected Dynamical Systems, New York: Marcel Dekker, 1981.

[10] John W. Brewer, "Kronecker Products and Matrix Calculus in System Theory," IEEE Trans. on Circuits and Systems, Vol. CAS-25, pp 772-781, Sept. 1978.

[11] R. Bellman, Introduction to Matrix Analysis, New York: McGraw-Hill, 1960.

[12] J. Stoer and R. Bulirsh, Introduction to Numerical Analysis, New York: Springer-Verlag, 1980.

[13] N. Navid and A. N. Willson, "A Theory and an Algorithm for Analog Circuit Fault Diagnosis," IEEE Trans. on circuits and System, Vol. CAS-26, pp. 440-457, July 1979.

[14] Gilbert Strang, Linear Algebra and Its Application, New York: Academic Press, 1976.

[15] Virginia C. Klema and A. J. Laub, "The Singular Value Decomposition and Some Applications," IEEE Trans. Automatic Control, Vol. AC-25, no. 2, April 1980.

[16] IMSL - International Mathematical and Statistical Libraries, IMSL Inc., Houston.

[17] LINPACK - Simultaneous Linear Algebraic Equation Package, Argonne National Laboratories.

[18] W. Fleming, Functions of Several Variables, Reading: Addison-Wesley, 1965.

[19] J. M Ortega and W. C. Rheinboldt, Iterative Solution of Nonlinear Equations in Several Variables, New York: Academic Press, 1970.

[20] D. Deo, Graph Theory with Applications to Engineering and Computer Science, Englewood Cliff, N.J., Prentice-Hall, Inc. 1974.

[21] G. Birkhoff and S. MacLane, A Survey of Modern Algebra, New York: Macmillan, 1965.

[22] L. Nazareth, "Some recent approaches to solving large residual nonlinear least squares problems," SIAM Review, Vol. 22, pp.1-11, Jan. 1980.

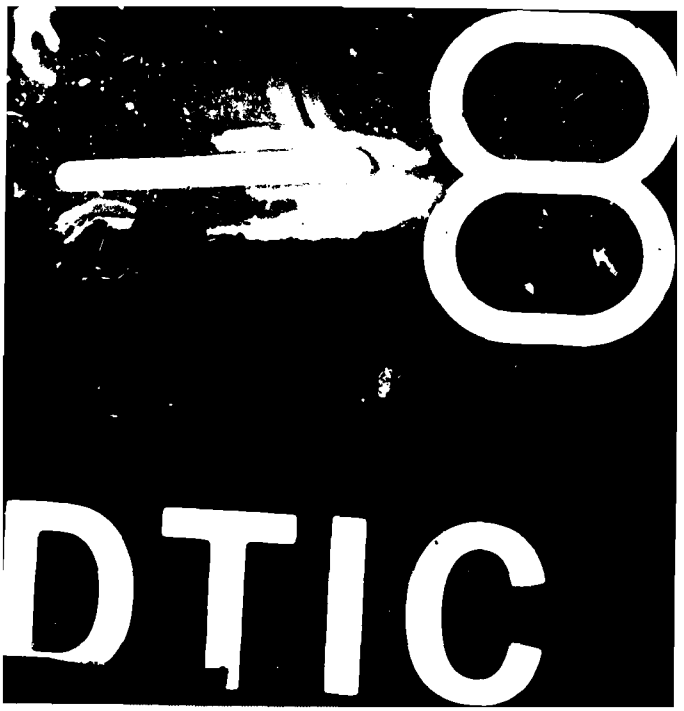
8
DTIC